

University of Alberta

**The Role of Phosphoinositide 3-Kinase in the Regulation of Cardiac
Morphology and Function**

by

Danny Guo

A thesis submitted to the Faculty of Graduate Studies and Research
in partial fulfillment of the requirements for the degree of

Master of Science
in
Experimental Medicine

Department of Medicine

©Danny Guo
Spring 2011
Edmonton, Alberta

Permission is hereby granted to the University of Alberta Libraries to reproduce single copies of this thesis and to lend or sell such copies for private, scholarly or scientific research purposes only. Where the thesis is converted to, or otherwise made available in digital form, the University of Alberta will advise potential users of the thesis of these terms.

The author reserves all other publication and other rights in association with the copyright in the thesis and, except as herein before provided, neither the thesis nor any substantial portion thereof may be printed or otherwise reproduced in any material form whatsoever without the author's prior written permission.

ABSTRACT

PI3K is an evolutionarily conserved lipid kinase whose signaling pathway mediates cellular processes such as growth, survival, and proliferation in response to physiological and pathological, biochemical and biomechanical stimuli. The traditional PI3K pathway relies on agonist mediated stimulation of PI3K α through receptor tyrosine kinases and PI3K γ through G-Protein coupled receptors (GPCRs), both of which phosphorylate PIP₂ into PIP₃, stimulating a plethora of downstream oncogenic enzymes such as Akt, GSK-3 β , and ERK. This pathway has been found to be important in cardiomyocytes and cardiofibroblasts for regulating cardiac morphology and function. However, evidence has suggested that this traditional pathway does not fully represent the complexity of the PI3K signaling cascade. For instance, we demonstrated that PI3K γ regulates calcium cycling through kinase independent interaction with phosphodiesterase. Despite PI3K γ KO hearts' hyper-contractile baseline phenotype and protection from isoproterenol mediated heart failure, these hearts rapidly develop systolic dysfunction and dilated cardiomyopathy (DCM) in response to pressure overload due to excess matrix metalloproteinase mediated degradation of N-cadherin adhesion complexes. Our data also suggests a novel connection between the PI3K/PTEN signaling cascade and Casein Kinase 2 (CK2), an enzyme that deactivates PTEN in the absence of both PI3K α and PI3K γ . This is likely a compensatory mechanism by which the cell replaces the loss of PI3K mediated pro-survival signals with activation of the CK2 pathway. Finally, our results demonstrate crosstalk between GPCRs and PI3K α via transactivation of growth factor receptors such as the epidermal growth factor receptor (EGFR) challenging the traditional pathway's perspective of

GPCR agonist mediated PI3K signaling. It is possible that physiological stressor agonists such as angiotensin II and catecholamines mediate ventricular hypertrophy and fibrosis via PI3K α instead of PI3K γ . Taken together, our results provide insight into the regulation and the complexity of the PI3K/PTEN pathway.

ACKNOWLEDGEMENTS

I would like to thank my supervisor Dr. Gavin Oudit for the support that he has provided during my graduate studies. Without his intellectual guidance, the content of this thesis would not have been possible to accomplish.

I would also like to thank my co-supervisor, Dr. Gary Lopaschuk, and committee members, Dr. Jason Dyck and Dr. Joe Casey, for their willing and eager support of my research experience. Dr. Lopaschuk and Dr. Dyck have also provided great support in my personal development outside of academics.

My sincere gratitude is given to Vijay Kandalam, Ratnadeep Basu and Jennifer Lo for their continued peer support and friendship during my time in the lab through thick and thin.

Last but not least, I would like to thank my fiancée Belle Zou for her continued and unrelenting support. Having her by my side has made it possible for me to surpass my own limitations, overcome all trials, and persevere even during the greatest hardships.

TABLE OF CONTENTS

1	Introduction	1
1.1	Phosphoinositide 3-Kinase	2
1.2	Class Ia PI3K	2
1.3	Class Ib PI3K	5
1.4	PI3K Signaling Cascade	6
1.5	PTEN	10
1.6	PI3K Mutants and Stress	11
1.6.1	Mutant Models	11
1.6.2	Mutant Models and Stress	12
1.7	PI3K and Intercellular Transmission of Mechanical Force	14
1.8	Pharmacological Inhibitors of PI3K	15
1.9	Cardiac Hypertrophy	16
1.10	Hypothesis	18
1.10.1	Chapter 3	18
1.10.2	Chapter 4	19
1.10.3	Chapter 5	19
1.11	References	20
2	Materials and Methods	30
2.1	Animal Care	31
2.2	Heart tissue collection and gravitometry	31
2.3	Isolation and culture of adult mouse cardiomyocytes and cardiofibroblasts	31
2.4	Preparation of cell lysates	34
2.5	Preparation of protein extract from tissue samples	34
2.6	Membrane fractionation	35
2.7	Determination of protein concentrations	35
2.8	Western blot analysis	37
2.9	Stripping western blot membranes	39
2.10	Measurement of cAMP levels	39

2.11	RNA Extraction and cDNA Preparation	40
2.12	TaqMan Real-time PCR	41
2.13	Echocardiography	41
2.14	Hemodynamic Measurements	42
2.15	Statistical analysis	43
2.16	References	44
3	PI3K γ KO and Pressure Overload	45
3.1	Introduction	46
3.2	Methods	48
3.2.1	Experimental animals	48
3.2.2	Aortic Banding	48
3.2.3	Hydroxyproline Assay	49
3.2.4	Tissue fixation, histology, and TUNEL assay	50
3.2.5	Isolated cardiomyocyte contractility	51
3.2.6	Cell Adhesion Assay	51
3.2.7	Gelatin Zymography	52
3.2.8	Collagenase Activity Assay	54
3.2.9	Confocal Fluorescence Microscopy	54
3.2.10	MMP/N-cadherin cleavage assay	54
3.3	Results	55
3.3.1	Accelerated Development of Ventricular Dilation and Pathological Hypertrophy in PI3K γ KO Mice in Response to Biomechanical Stress	55
3.3.2	Uncoupling Between In Vivo Myocardial Contractility and Single-Cardiomyocyte Contractility in Pressure Overloaded PI3K γ KO Mice	56
3.3.3	Selective Upregulation of MMP2 and MT1-MMP and MMP Inhibition Mediated Rescue of Pressure Overloaded PI3K γ KO Mice	58
3.3.4	Specific Loss of N-Cadherin from Adhesion Complexes While β -Adrenergic Blocker Prevents Upregulation of	61

	MMP and Loss of N-Cadherin in Banded PI3K γ KO Mice	
	3.3.5 Beta-Blocker Therapy Prevents the Adverse Remodeling in Response to Chronic Pressure Overload	63
	3.4 Discussion	65
	3.5 References	96
4	PI3K γ KO/ α DN Double Mutant Hearts	104
	4.1 Introduction	105
	4.2 Methods	106
	4.2.1 Heart tissue collection	106
	4.2.2 Western blot analysis	106
	4.2.3 Immunoprecipitation assay	106
	4.2.4 Phosphatase Activity Assay	107
	4.3 Results	108
	4.3.1 Left Ventricular mass in WT, PI3K γ KO, PI3K α DN, and PI3K γ KO/PI3K α DN (DM) mice at 3 and 6 months	108
	4.3.2 Augmented activation of Akt and MAPK signaling cascades and expression of hypertrophy markers in DM LV as compared to WT, PI3K γ KO, and PI3K α DN	108
	4.3.3 Increased phosphorylation and deactivation of PTEN in DM mice as compared to WT, PI3K γ KO, and PI3K α DN	109
	4.3.4 Increased CK2 α ' protein level in DM mice as compared to WT, PI3K γ KO, and PI3K α DN	110
	4.3.5 Partial enhancement of systolic function in DM hearts as compared to WT and PI3K α DN hearts	110
	4.3.6 Increased baseline cAMP levels and phosphorylation of PLN in PI3K γ KO and DM mice compared to WT and PI3K α DN	111
	4.4 Discussion	112
	4.5 References	131
5	Transactivation of PI3K α	134
	5.1 Introduction	135

5.2	Methods	137
	5.2.1 Cell culture	137
5.3	Results	138
	5.3.1 Isoproterenol mediated activation of Akt signaling requires PI3K α but not PI3K γ	138
	5.3.2 Gefitinib blocks angiotensin II but not isoproterenol mediated activation of Akt	138
5.4	Discussion	140
5.5	References	148
6	Discussion, limitation, future directions, and conclusion	150
	6.1 General Discussion	151
	6.1.1 Kinase independent role of PI3K γ in the response to pressure overload induced heart failure	152
	6.1.2 Regulation of PI3K signaling cascade by CK2 activity	154
	6.1.3 Transactivation of PI3K α by GPCR stressor agonists	155
6.2	Limitations	156
6.3	Future directions	158
6.4	Conclusion	159
6.5	References	161

LIST OF TABLES

Table 2.1	Stock Perfusion Buffer	32
Table 2.2	Perfusion Buffer	33
Table 2.3	Digestion Buffer	33
Table 2.4	Stopping Buffer	33
Table 2.5	Plating Buffer	33
Table 2.6	Culture Buffer	33
Table 2.7	Fibroblast Culture Buffer	34
Table 2.8	PBS – pH 7.4	34
Table 2.9	RIPA Buffer	35
Table 2.10	Protein concentration quantification solution from BioRad (per sample)	36
Table 2.11	Protein Standards	36
Table 2.12	Loading Gel (5%)	37
Table 2.13	Separating Gel	38
Table 2.14	Running Buffer (10x) pH 8.3	38
Table 2.15	Running Buffer (1x)	38
Table 2.16	Transfer Buffer (10x) pH 8.3	38
Table 2.17	Transfer Buffer (1x)	39
Table 2.18	Loading Buffer (5x)	39
Table 2.19	Stripping Buffer	39
Table 2.20	cDNA PCR Solution (per sample)	40
Table 2.21	TaqMan cDNA Standards	41
Table 2.22	TaqMan reaction mix (per sample)	41
Table 3.1	Chloramine T (per sample)	49
Table 3.2	Acetate-citrate Buffer	50
Table 3.3	Hydroxyproline Standards	50
Table 3.4	Separating Gel for Zymography (8% with gelatine type-A)	52
Table 3.5	Incubation Buffer	53
Table 3.6	Staining Solution	53

Table 3.7	Destaining Solution	53
Table 3.8	RIPA Buffer without EDTA	53
Table 3.9	Cytobuster extraction buffer	54
Table 3.10	RT-PCR primers and probes (chapter 3)	93
Table 3.11	Functional parameters	95
Table 4.1	Phosphate standard for phosphatase activity assay	107
Table 4.2	RT-PCR primers and probes (chapter 4)	129

LIST OF FIGURES

Figure 1.1	Canonical PI3K signaling cascade	8
Figure 3.1	Development of early-onset dilated cardiomyopathy in response to biomechanical stress in PI3K γ KO mice	69
Figure 3.2	Alterations in signaling are observed in response to biomechanical stress in PI3K γ KO mice	71
Figure 3.3	Uncoupling between <i>in vivo</i> myocardial contractility and isolated single cardiomyocyte contractility in PI3K γ KO mice in response to early biomechanical stress	73
Figure 3.4	Upregulation of myocardial matrix metalloproteinase expression in banded PI3K γ KO mice with beta-adrenergic receptor stimulation of MMPs expression in isolated adult cardiomyocytes and cardiofibroblasts	75
Figure 3.5	Increased collagenase activity and MMP2 activation with prevention of the dilated cardiomyopathy by broad spectrum MMP inhibition was observed in banded PI3K γ KO mice	77
Figure 3.6	Selective loss of N-cadherin from myocardial membrane fraction and the cell-adhesion complexes in the myocardium from banded PI3K γ KO mice	79
Figure 3.7	The non-specific beta-receptor blocker, propranolol (15 mg/kg/day), prevents the molecular, biochemical and functional deterioration in response to biomechanical stress in PI3K γ KO mice	81
Figure 3.8	Chronic beta-blocker prevents pressure-overload induced adverse remodeling and preserves systolic function in WT mice	83
Figure 3.9	Purity of membrane fractionation	85
Figure 3.10	MMP2, but not MT1-MMP, cleaves human recombinant N-cadherin Fc Chimera	87
Figure 3.11	MMP9 protein levels in WT and PI3K γ KO hearts	89

Figure 3.12	β 1D and α 7B integrin protein levels in WT and PI3K γ KO hearts	91
Figure 4.1	DM hearts have reduced LV weight at 3 months but not at 6 months	115
Figure 4.2	DM hearts demonstrated enhanced baseline expression of ANF, BNP, and β MHC	117
Figure 4.3	Western blot analysis shows that DM hearts have enhanced baseline phosphorylation of PI3K signaling cascade	119
Figure 4.4	DM hearts have reduced baseline PTEN phosphatase activity without changes in PTEN protein levels due to enhanced phosphorylation of PTEN	121
Figure 4.5	DM hearts have increased protein levels of CK2 α' but not CK2 α than WT, PI3K γ KO, and PI3K α DN	123
Figure 4.6	Echocardiographic and hemodynamic measurements of LV function demonstrated that DM and PI3K γ KO hearts have enhanced contractile function than WT or PI3K α DN	125
Figure 4.7	A schematic of PTEN phosphorylation and deactivation	127
Figure 5.1	PI-103, but not TGX-221 or AS604850, reduces baseline Akt phosphorylation in WT adult cardiomyocytes	142
Figure 5.2	Isoproterenol mediated Akt phosphorylation can be blocked by PI-103 and AS604850	144
Figure 5.3	Pre-treatment with gefitinib inhibits angiotensin II mediated activation and partially inhibits isoproterenol mediated activation of Akt signaling	146

LIST OF ABBREVIATIONS

A – absorbance

AB – aortic banding

ACi – Adenylate cyclase inhibitor

α MHC – alpha myosin heavy chain

ANOVA – analysis of variance

ANF – atrial natriuretic factor

ATP – adenosine triphosphate

β MHC – beta myosin heavy chain

BNP – B-type natriuretic factor

cAMP – cyclic adenosine monophosphate

CK2 – casein kinase 2

Col I – collagen 1

Col IV – collagen 4

CREB – cAMP response element binding protein

DCM – dilated cardiomyopathy

ddH₂O – double distilled water

DIDA – 2',5'-dideoxyadenosine

DM – PI3K γ KO/ α DN

DMEM – Dulbecco's minimum essential media

ECM – extracellular matrix

EGF – epidermal growth factor

EGFR – epidermal growth factor receptor

ERK 1/2 – extracellular-signal regulated kinase 1 and 2

FAK – focal adhesion kinase

FAM – 6-carboxyfluorescein

FN – fibronectin

GPCR – G-Protein coupled receptor

GSK-3 – glycogen synthase kinase 3

IGF-1 – insulin-like growth factor 1

I.P. - intraperitoneal

LN - laminin

LV – left ventricle

LVEDD – left ventricular end diastolic diameter

LVEDP – left ventricular end diastolic pressure

MAPK – mitogen activated protein kinase

MMP – matrix metalloproteinase

MT1-MMP – membrane-type 1 matrix metalloproteinase

mTORC2 – mammalian target of rapamycin complex 2

OD – optical density

PBS – phosphate buffer saline

PDE – phosphodiesterase

PDK-1 – phosphoinositide dependent kinase 1

PI3K – phosphoinositide 3-kinase

PI3K α CA – phosphoinositide 3-kinase alpha constitutively active

PI3K α DN – phosphoinositide 3-kinase alpha dominant negative

PI3K γ KD – phosphoinositide 3-kinase gamma kinase dead

PI3K γ KO – phosphoinositide 3-kinase gamma knockout

PIP₂ – phosphoinositide 4,5 phosphate

PIP₃ – phosphoinositide 3,4,5 phosphate

PLN – phospholamban

PTEN – phosphatase and tensin homolog

RIPA – radioimmunoprecipitation assay

RTK – receptor tyrosine kinase

SDS – sodium dodecyl sulfate

SERCA2a – sarco-endoplasmic reticulum calcium ATPase 2a

Sh - Sham

SH2 – src homology 2

TAMRA - tetramethylrhodamine

TBST – tris buffered saline tween

TIMP – tissue inhibitor of metalloproteinase

TUNEL - Terminal deoxynucleotidyl transferase dUTP nick end labeling

VcFc – velocity of circumferential fractional shortening

WT - wildtype

Chapter 1

INTRODUCTION

1.1 Phosphoinositide 3-Kinase

Phosphoinositide 3-Kinase (PI3K) is an evolutionarily conserved family of lipid kinases that is found in almost all cell types. It was originally discovered and described by Lewis Cantley's research group [1] and later found to regulate organ size in *Drosophila* by Leever et al. [2]. In 2000, Shioi et al showed that even in vertebrates, PI3K regulates heart size [3]. Shioi's study was one of the first to define a PI3K isoform specific function in a vertebrate species. Since then, a variety of studies in different organisms have described PI3K's isoform specific functions.

The PI3K family of enzymes are separated into three classes, named Class I, Class II, and Class III PI3K, and each class has a distinct modulation of cellular activity [4]. Class I PI3Ks are heterodimeric enzymes that mediate acute cellular responses to biochemical agonists and biomechanical stress. Class I PI3Ks are unique enzymes because unlike Class II and Class III PI3Ks, Class I PI3Ks are able to generate phosphoinositide 3,4,5 triphosphate (PIP₃) [5]. The latter two classes are involved in a variety of other cellular mechanisms such as vesicle trafficking for Class II and autophagy for Class III [6, 7]. The focus of this thesis will be on Class I PI3Ks, which are further subdivided into Class Ia and Class Ib.

1.2 Class Ia PI3K

Class Ia PI3Ks consist of three members, PI3K α , PI3K β , and PI3K δ . These enzymes are heterodimers that consist of a p110 catalytic subunit (p110 α , p110 β , and p110 δ), which interacts with an adaptor subunit (p85 α , p85 β , and p55 γ) [8]. Cardiomyocytes only express PI3K α and PI3K β , which primarily interact with p85 α and

p85 β [9, 10]. The catalytic p110 subunits of PI3K α and PI3K β have similar kinase activity of phosphorylating the 3'-OH position of phosphoinositide 4,5 biphosphate (PIP₂), converting it into PIP₃, thereby generating a second messenger to activate a variety of downstream signaling cascades. The p85 α and p85 β adaptor subunits are both expressed in the heart and have redundant functions [10]. In general, both p85s bind to the Class Ia catalytic p110 subunits and recruit them to the phospho-tyrosine residues of activated receptor tyrosine kinases (RTKs) at the cell membrane via p85's Src Homology 2 (SH2) interaction domain [4, 11]. Simultaneously, the interaction of the p85 subunit with RTKs induces structural changes in the PI3K holo-enzyme and activates the p110 subunit by exposing its catalytic site, which is normally flanked by components of p85 [12]. This recruitment also places PI3K within proximity with PIP₂, its primary cellular substrate. Class Ia PI3Ks have the potential to phosphorylate not only PI(4,5)P₂, but also PI(4)P and PI into PI(3,4)P₂ and PI(3)P, *in vitro* [13]. However, the physiological importance of these reactions is unknown.

Class Ia PI3Ks can be activated by both biochemical and biomechanical stressors. One of the classical agonists for PI3K α activation is insulin. Insulin receptors are RTKs and stimulate PI3K α to modulate the activity of several downstream enzymes such as glycogen synthase and glycogen synthase kinase [14, 15]. Insulin-like Growth Factor 1 (IGF-1) also activates PI3K α in a similar fashion and like many other growth factors that activate PI3K α , IGF-1 has been found to be important in regulating cellular hypertrophy and survival [15, 16]. Recent evidence has suggested that non-growth factor pro-hypertrophic agonists, such as angiotensin II, can also activate PI3K α through

an atypical pathway called transactivation [17]. This concept will be explored in more detail in Chapter 5.

Both PI3K α and PI3K β have been found to be expressed in cardiomyocytes but only the physiological and cellular functions of PI3K α have been explored in the heart while PI3K β 's role remains unclear. PI3K α is necessary for embryonic activation of pro-survival and growth pathways and is necessary for development as a PI3K α KO mutation leads to embryonic lethality [3]. In order to study PI3K α 's role in the adult cardiomyocytes, Izumo's group generated PI3K α Dominant Negative (PI3K α DN) transgenic mutants, which over-express a dominant negative mutant p110 α , a truncated form that lacks kinase activity and strongly competes for interaction with p85 adaptor subunits [3]. This gene was connected to the promoter region of α MHC so that the mutant p110 α is expressed in large quantities. This also allows for the inherent bypass of embryonic development as cardiomyocyte expression of α MHC is postnatal.

While the physiological role of PI3K β is unclear, the study of PI3K α DN and PI3K α constitutively active (PI3K α CA) mutants in mice has made clear indications that PI3K α is a direct determinant of organ and cell size [3]. This is consistent with previous studies that have shown similar results in drosophila, illustrating the conservation of PI3K through both vertebrate and invertebrate species [2]. These two mutant strains also demonstrated a direct correlation between PI3K α activity and basal Akt phosphorylation, which regulates cardiac growth, metabolism, and survival [3, 18]. Recent studies have also suggested that PI3K α may regulate myocardial contractility to some degree but the evidence to this is limited and more research is needed before conclusions can be drawn [17].

1.3 Class Ib PI3K

The only member of Class Ib PI3K is PI3K γ . PI3K γ has identical catalytic functions as Class Ia with the catalytic subunit p110 γ , but instead of interacting to p85 adaptors, it interacts with p101, an adaptor subunit that does not contain the SH2 domain necessary for phospho-tyrosine interaction [19]. PI3K γ is not regulated by RTKs like PI3K α and PI3K β but by G-Protein coupled receptors (GPCRs). Specifically, when GPCRs are activated by appropriate agonists, the heterotrimeric G-protein dissociates into G α and G $\beta\gamma$. The G $\beta\gamma$ subunits can interact with both the p110 γ and p101 domains to activate and recruit PI3K γ to the membrane. Once activated, PI3K γ phosphorylates PIP₂ into PIP₃, leading to the same downstream signaling cascade as Class Ia PI3Ks [19, 20]. Interestingly, G $\beta\gamma$ has also been shown to interact with PI3K β suggesting potential crosstalk between GPCRs and Class Ia PI3Ks [21].

PI3K γ 's role in the heart was first explored by Joseph Penninger's group, which generated the whole body knockout mutant called PI3K γ KO [22]. This group found that unlike PI3K α , PI3K γ was not necessary for embryonic development or baseline Akt activity. In accordance, PI3K γ KO mice did not demonstrate any changes in baseline cardiac and cardiomyocyte size, suggesting that PI3K γ KO does not play a role in physiological cardiac development [9, 23]. However, PI3K γ was necessary for agonist induced pathological myocardial remodeling, indicating that PI3K γ still participates in the cellular response to extracellular agonists [24]. PI3K γ may also regulate Extracellular signal-Regulated Kinase 1/2 (ERK 1/2) signaling as PI3K γ KO hearts demonstrated reduced baseline ERK 1/2 phosphorylation [22, 23].

Unlike PI3K α , PI3K γ is not activated by growth factors. Instead, it responds primarily to stressor agonists such as catecholamines and angiotensin II. For instance, it was demonstrated that PI3K γ is necessary for isoproterenol induced pathological remodeling in the heart [24]. Because of this inherent response to stressor agonists, PI3K γ activity has been classically labelled as pathological and maladaptive.

Despite not regulating baseline cardiac morphology, PI3K γ plays a critical role in the regulation of cyclic adenosine monophosphate (cAMP) in cardiomyocytes [23, 24]. Interestingly, PI3K γ KO hearts have enhanced baseline contractility due to the lack of p110 γ 's protein interaction with phosphodiesterase [23], which upregulates the latter's activity resulting in enhanced sarco-endoplasmic reticulum calcium ATPase 2a (SERCA2a) activity and increased calcium cycling (explored in chapter 3).

1.4 PI3K Signaling Cascade

The conserved PI3K catalytic activity generates PIP₃ from PIP₂, which acts as a second messenger to activate a variety of downstream signaling cascades (Figure 1.1). Perhaps the most well known of these cascades is the Akt/PKB pathway, which is a key regulator of cellular growth, survival and proliferation [25]. The generation of PIP₃ recruits Akt to the membrane via PIP₃'s interaction with Akt's pleckstrin homology (PH) domain, which is required for phosphoinositide mediated plasma membrane docking [26, 27]. Phosphoinositide-Dependent Kinase 1 (PDK-1) then phosphorylates the Thr 308 residue of Akt [28]. Similarly, mammalian target of rapamycin complex 2 (mTORC2) phosphorylates Akt at the Ser 473 residue [29]. Both of these phosphorylated residues are required for the activation of Akt.

One of Akt's most important downstream targets is Glycogen Synthase Kinase 3 (GSK-3). GSK-3 has two primary isoforms, GSK-3 α and GSK-3 β , which have a high level of structural similarity but exhibit different roles in regulating cardiac growth and the response to mechanical stress [30-32]. Both isoforms are normally constitutively active in baseline conditions, phosphorylating and deactivating pro-hypertrophic downstream targets such as the transcription factor c-jun [30]. When stimulated by growth factors or biomechanical stretch, activated Akt phosphorylates and inactivates GSK-3 β , removing GSK-3 β 's inhibition on downstream targets hence promoting hypertrophic pathways [32, 33]. Similarly, GSK-3 α negatively regulates cardiac hypertrophy, suppressing it at baseline conditions [34]. However, GSK-3 α has been demonstrated to be more important for mediating cardiomyocyte apoptosis during pressure overload than GSK-3 β [31, 32].

Figure 1.1

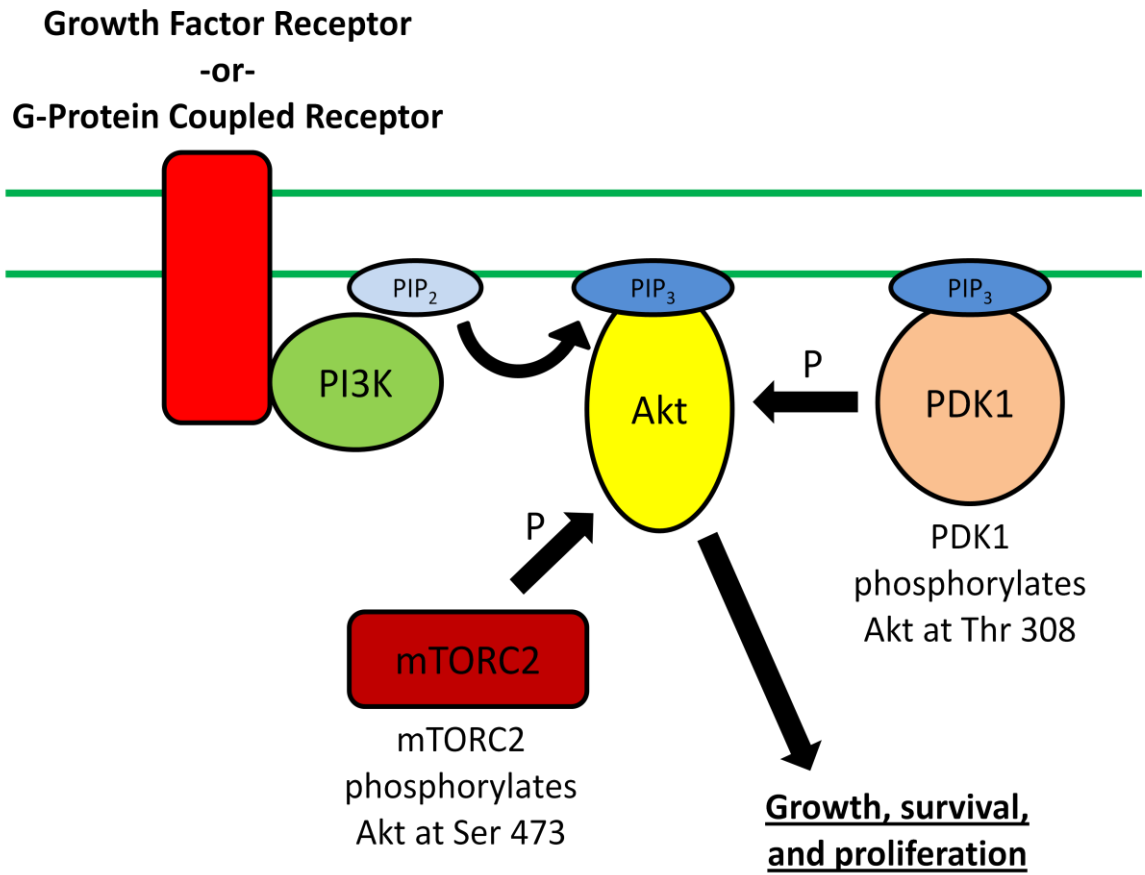


Figure 1.1 Canonical PI3K signaling cascade. RTKs or GPCRs activate PI3K, which generates PIP₃ from PIP₂. This recruits Akt to the plasma membrane, allowing it to be phosphorylated at Thr 308 by PDK1 and Ser 473 by mTORC2, resulting in Akt activation. This leads to cellular growth, survival, and proliferation.

1.5 PTEN

The tumor suppressor Phosphatase and Tensin Homolog (PTEN) is a negative regulator of PI3K kinase activity and PIP₃ concentration. PTEN is a lipid phosphatase that dephosphorylates the 3' phosphate group of PIP₃, generating PIP₂ [35, 36]. PTEN can be deactivated via phosphorylation at Ser 385, a reaction that is mediated by casein kinase 2 (CK2) [37].

At the cellular level, PTEN negatively regulates cardiac hypertrophy and survival as increased PTEN expression in neonatal rat cardiomyocytes induces apoptosis and loss of PTEN results in increased PIP₃ levels and spontaneous cardiac hypertrophy [9]. Mutants that lack PTEN activity also demonstrate an unexpected reduction in cardiomyocyte contractility, which was originally argued to be due to reduced lipid phosphatase activity [9, 23]. However, a later study demonstrated that PI3K γ KO cardiomyocytes are hyper-contractile due to kinase independent interaction with phosphodiesterase (described in more detail in chapter 3) suggesting that the altered baseline contractility of PTEN mutants likely does not originate from decreased phosphatase activity [23]. Alternatively, it is possible that PTEN mutants modulate basal contractility via increased PIP₃ concentrations as increased IGF-1 receptor expression in the heart, and hence increased PI3K α activation, leads to enhanced myocardial contractile function [38].

1.6 PI3K Mutants and Stress

1.6.1 Mutant Models

This thesis made use of three different mutant models: PI3K α DN, PI3K γ KO, and PI3K γ KD.

The PI3K α DN mutant mouse was developed by Izumo's group in an attempt to generate a PI3K α mutant mouse with suppressed PI3K α activity [3]. Previous attempts to use a PI3K α KO mutant discovered that complete ablation of p110 α results in early embryonic lethality [3]. The PI3K α DN strain expresses a non-functional p110 α that retains the ability to bind with p85, hence competing against WT p110 α . The mutated gene is attached to the alpha myosin heavy chain (α MHC) promoter region to obtain cardiomyocyte specific expression of the mutant p110 α . This mutant loses 75% of its p110 α activity, which is consistent with reduced baseline cardiomyocyte size. Interestingly, PI3K α DN mutants retain normal ventricular contractile function suggesting that PI3K α may regulate size without impeding contractility [3, 39]. This notion is supported by the PI3K α CA mutant strain, also generated by Izumo's group, which demonstrated baseline cardiac hypertrophy without a change in contractile function [3]. A limitation of the PI3K α DN mutant strain is that it requires the expression of a non-functional enzyme, which may allow for aberrant and unwanted protein interactions and signaling. This model also does not completely remove PI3K α activity.

The PI3K γ KO mutant survives through embryonic development and is phenotypically similar to WT. It was generated by Penninger's group by deleting the first 5000 base pairs from the p110 γ gene removing the first 670 amino acids containing

the PH domain and the G-protein binding domain, which completely ablates PI3K γ activity [22]. As PI3K γ normally interacts with phosphodiesterase (PDE) hence enhancing the latter's activity, PI3K γ KO mice have reduced PDE activity leading to accumulation of cAMP and enhanced cardiomyocyte contractility without hypertrophy [23]. This suggests that opposite to PI3K α , PI3K γ may regulate contractility without affect cardiomyocyte size. A weakness of the PI3K γ KO mutant strain is that PI3K γ is lost in all cells in the body. This could potentially result in systemic alterations that affect the heart.

In order to study the mechanism by which PI3K γ regulates PDE activity, Patrucco et al. generated the PI3K γ KD mutant strain, which lacks PI3K γ activity but retains PI3K γ 's protein structure. Interestingly, they observed that PI3K γ KD mice were not hyper-contractile, illustrating that PI3K γ regulates myocyte contractility via kinase independent mechanisms [23].

1.6.2 Mutant Models and Stress

The PI3K signaling cascade consists of a wide variety of downstream enzymes, many of which are activated during disease and stress. During pressure overload, WT hearts have increased phosphorylation of Akt while PI3K γ KO hearts do not, suggesting that the increase in phospho-Akt is dependent on PI3K γ [23, 40]. It has also been demonstrated that PI3K γ KO hearts have reduced ERK 1/2 activation in response to pressure overload [23]. Indeed, this reduced hypertrophic signaling partially contributes to the rapid ventricular failure and decompensation in aortic banded PI3K γ KO hearts, but it is unlikely to be the primary cause. This is because PI3K γ kinase dead (PI3K γ KD)

hearts, mutants which lack PI3K γ kinase activity, respond to pressure overload in a similar fashion as WT hearts, suggesting that a kinase independent function of PI3K γ is responsible for regulating the response to left ventricular pressure overload [23]. One possibility that was proposed by Patrucco *et al.* (2004) is that the dysregulated cAMP levels in PI3K γ KO hearts is the primary cause. PI3K γ KO hearts lack PI3K γ , which normally interacts with PDE to reduce cAMP levels and thus have elevated baseline cAMP concentration, which increases even further after pressure overload [23]. Interestingly, the use of propranolol, which reduces cAMP production, could rescue banded PI3K γ KO hearts from decompensation, providing direct evidence that elevated cAMP mediates this pathological remodeling [23, 40]. However, the exact mechanism of this remodeling was unclear and will be explored as a part of this thesis (discussed in more detail in chapter 3).

Similarly to PI3K γ KO mice, PI3K α DN hearts exposed to aortic banding also decompensate at an accelerated rate [18], though the mechanism for this is still under investigation. On the contrary, PI3K α CA hearts are protected from the deleterious effects of aortic banding, demonstrating no detectable left ventricular dilation or loss of contractile function 1 week after banding [41]. This suggests that PI3K α activity mediates protective effects against biomechanical stress.

Opposite to PI3K γ KO hearts, PI3K α DN tissue lysates demonstrate increased baseline ERK 1/2 phosphorylation. Interestingly, PI3K α CA have baseline ERK 1/2 phosphorylation similar to WT despite demonstrating baseline hypertrophy [3].

While pathological mechanical stress such as aortic banding induces hypertrophy in PI3K α DN hearts, physiological stress such as exercise does not, suggesting that PI3K α is necessary for physiological and not pathological hypertrophy [18].

1.7 PI3K and Intercellular Transmission of Mechanical Force

Intercellular transmission of mechanical signals in the heart occurs via two distinct mechanisms: by directly stretching and straining neighbouring cells and paracrine signaling. The direct transmission of force between adjacent cardiomyocytes is primarily propagated by cell-cell adhesion complexes called adherens junctions, which are composed of cadherins (with N-cadherin being the primary cardiac isoform) and catenins (α and β). Though it is often assumed that like skeletal muscles, cardiomyocytes experience mechanical stress only along its longitudinal axis via intercalated discs, cardiomyocytes actually also experience lateral strain from the surrounding ECM or from neighbouring cells, as well as exert lateral force to other cells during contraction [42]. In fact, roughly 80% of N-cadherin between adjacent cardiomyocytes is located in the peripheral membrane, away from intercalated discs [43]. Furthermore, these lateral junctions allow cardiomyocytes to adhere to other cell types, such as fibroblasts, as intercalated discs are only formed between cardiomyocytes.

Aside from propagating mechanical force, adherens junctions also interact with PI3K to mediate Akt signaling [44]. Increased and decreased adherens junctions were shown to respectively improve and weaken basal Akt phosphorylation [44]. However, it is possible that this loss of AKT stimulation is indirectly due to weakened mechanosensitivity as there is currently little evidence of direct interactions between cadherins and the PI3K pathway.

1.8 Pharmacological Inhibitors of PI3K

Development of small-molecule inhibitors for PI3K was previously focused on pan-PI3K inhibition due to the lack of understanding of isoform specific functions. The PI3K inhibitors that were widely used in research were Wortmannin and LY294002, both of which are pan-PI3K inhibitors with inhibitory effects on enzymes other than PI3K. Wortmannin is an irreversible inhibitor of PI3K that forms covalent interactions with the catalytic site of p110 [45, 46]. As all p110 catalytic sites are similar in structure, Wortmannin is able to effectively inhibit all Class I PI3K isoforms. Wortmannin also has a relatively low IC_{50} of 4 nM for PI3K α and 9 nM for PI3K γ , demonstrating its high potency as a PI3K inhibitor [46]. LY294002 is also widely used but unlike Wortmannin, it is a reversible competitive inhibitor of PI3K's ATP binding site. It has an IC_{50} of 0.55 μ M for PI3K α and 12 μ M for PI3K γ [47].

The primary concerns with these two original PI3K inhibitors were their lack of isoform specificity as well as their non-specific inhibition of non-PI3K kinases. Wortmannin has been shown to be able to inhibit mTOR, while LY294002 inhibits mTOR and Casein Kinase 2 [48-50]. In recent years, the use of Wortmannin or LY294002 has become less necessary due to the advent of ZSTK474, a pan specific PI3K inhibitor that has IC_{50} of 16 nM for PI3K α and 49 nM for PI3K γ [50]. The most beneficial aspect of this new inhibitor is that it has no known inhibitory side-effects on any other kinases.

As the understanding of isoform specific roles of PI3K emerged, demand for pharmacological inhibition of PI3K isoforms increased and a variety of specific

inhibitors were developed. This thesis will only briefly discuss a few isoform specific inhibitors of PI3K as detailed discussion of this topic can be found elsewhere [50].

PI-103 was originally developed as a PI3K α specific inhibitor as a potential therapy for cancer but was later suggested to be pan specific with an IC₅₀ of 2 nM for PI3K α and 15 nM for PI3K γ [51, 52]. However, in cardiomyocytes where PI3K β has no clear role and PI3K δ is not expressed, PI-103 can still be reasonably used as a PI3K α inhibitor, especially considering that PI3K γ does not contribute to baseline Akt activation [9]. Nevertheless, the use of PI-103 as a PI3K α inhibitor should still be confirmed via a secondary test, such as using a mutant model that lacks PI3K α activity like the PI3K α DN.

AS604850 is a PI3K γ inhibitor developed for the treatment of inflammatory diseases such as rheumatoid arthritis. It exhibits an IC₅₀ of 250 nM for PI3K γ and 4.5 μ M for PI3K α [53, 54]. Once again, its effectiveness should be confirmed with a mutant model that lacks PI3K γ activity, such as the PI3K γ KO.

1.9 Cardiac Hypertrophy

Cardiac hypertrophy is defined as the enlargement of the heart. While other cardiac cell types also alter their sizes in response to hemodynamic changes, cardiomyocyte hypertrophy is the primarily determinant of heart size as cardiomyocytes account for 70-80% of cardiac mass [55]. Cardiac hypertrophy occurs as a compensatory mechanism against biochemical and biomechanical stress. Though the augmentation of cardiac muscle generally allows for increased contractile force, cardiac hypertrophy is divided into physiological and pathological hypertrophy, with

pathological hypertrophy being further divided into eccentric and concentric hypertrophy.

Physiological hypertrophy occurs in response to exercise or growth factors. It is characterized by proportional increases in the number of sarcomeric subunits both in series and in parallel in cardiomyocytes. Ventricular weight, wall thickness, and contractile function are all enhanced during physiological hypertrophy, yielding a bigger heart in general [56]. This process is reversible and occurs in the absence of ventricular decompensation, fibrosis, or heart failure [56, 57].

Pathological hypertrophy occurs when the heart is exposed to biomechanical or biochemical stress during disease or genetic disorder, and is categorized into two types: concentric hypertrophy and eccentric hypertrophy. Concentric hypertrophy is the increase of sarcomeric subunits in parallel without proportional increase in series, leading to increased wall thickness and contractility while reducing chamber size [58]. It originally occurs as an adaptive response to pressure overload, such as in hypertension and aortic valvular stenosis, but chronic concentric hypertrophy eventually becomes maladaptive and progresses to heart failure [58]. Pressure overload can be simulated in the laboratory via aortic constriction. Concentric hypertrophy also occurs in response to neurohormonal stress, which can also be experimentally simulated using chronic chemical stimulation of the adrenergic or angiotensin pathway [24].

Eccentric hypertrophy is the increase of sarcomeric subunits in series without proportional increase in parallel, leading to elongation of ventricular walls, increased chamber size, and reduced systolic and diastolic functions [59]. This form of

hypertrophy occurs in response to volume overload primarily to accommodate the increase volumetric demand. Similarly to concentric hypertrophy, prolonged eccentric hypertrophy will also result in heart failure [59].

As pathological hypertrophy progresses into decompensation, maladaptive cellular and extracellular remodelling takes place and causes the heart to develop dilated cardiomyopathy (DCM). DCM is morphologically similar to exacerbated eccentric hypertrophy, with significant thinning of ventricular walls, severe fibrosis, and disruption of the integrity of cell-cell and cell-ECM adhesion, characteristic of end stage heart failure (reviewed in [58]). One of the cellular changes that lead to the progression of pathological hypertrophy is excessive expression and activation of matrix metalloproteinases (MMPs), which normally aid in ECM remodelling, leading to aberrant degradation of important protein complexes [40]. In some disease models, the alterations of MMPs are accompanied by changes in expression of their physiological inhibitor tissue inhibitor of metalloproteinases (TIMPs). The loss of TIMPs during stress or disease is detrimental for the heart and frequently leads to accelerated decompensation [60, 61].

1.10 Hypothesis

1.10.1 Chapter 3

Hypothesis: PI3K γ KO mice exposed to aortic banding develop rapid systolic dysfunction and left ventricular dilation due to enhanced MMP-dependent cleavage of N-cadherin adhesion complexes.

1.10.2 Chapter 4

Hypothesis: PI3K γ KO/ α DN double mutant mice will have small and hypercontractile heart compared to WT mice.

1.10.3 Chapter 5

Hypothesis: Isoproterenol and angiotensin II activation of Akt is mediated by PI3K α and not PI3K γ in a process called transactivation.

1.11 References:

1. Whitman, M., D.R. Kaplan, B. Schaffhausen, L. Cantley, and T.M. Roberts, *Association of phosphatidylinositol kinase activity with polyoma middle-T competent for transformation*. Nature, 1985. **315**(6016): p. 239-42.
2. Leever, S.J., D. Weinkove, L.K. MacDougall, E. Hafen, and M.D. Waterfield, *The Drosophila phosphoinositide 3-kinase Dp110 promotes cell growth*. EMBO J, 1996. **15**(23): p. 6584-94.
3. Shioi, T., P.M. Kang, P.S. Douglas, J. Hampe, C.M. Yballe, J. Lawitts, L.C. Cantley, and S. Izumo, *The conserved phosphoinositide 3-kinase pathway determines heart size in mice*. EMBO J, 2000. **19**(11): p. 2537-48.
4. Vanhaesebroeck, B., S.J. Leever, G. Panayotou, and M.D. Waterfield, *Phosphoinositide 3-kinases: a conserved family of signal transducers*. Trends Biochem Sci, 1997. **22**(7): p. 267-72.
5. Vanhaesebroeck, B. and M.D. Waterfield, *Signaling by distinct classes of phosphoinositide 3-kinases*. Exp Cell Res, 1999. **253**(1): p. 239-54.
6. Falasca, M. and T. Maffucci, *Role of class II phosphoinositide 3-kinase in cell signalling*. Biochem Soc Trans, 2007. **35**(Pt 2): p. 211-4.
7. Castino, R., N. Bellio, C. Follo, D. Murphy, and C. Isidoro, *Inhibition of PI3k class III-dependent autophagy prevents apoptosis and necrosis by oxidative stress in dopaminergic neuroblastoma cells*. Toxicol Sci. **117**(1): p. 152-62.
8. Oudit, G.Y., H. Sun, B.G. Kerfant, M.A. Crackower, J.M. Penninger, and P.H. Backx, *The role of phosphoinositide-3 kinase and PTEN in cardiovascular physiology and disease*. J Mol Cell Cardiol, 2004. **37**(2): p. 449-71.

9. Crackower, M.A., G.Y. Oudit, I. Kozieradzki, R. Sarao, H. Sun, T. Sasaki, E. Hirsch, A. Suzuki, T. Shioi, J. Irie-Sasaki, R. Sah, H.Y. Cheng, V.O. Rybin, G. Lembo, L. Fratta, A.J. Oliveira-dos-Santos, J.L. Benovic, C.R. Kahn, S. Izumo, S.F. Steinberg, M.P. Wymann, P.H. Backx, and J.M. Penninger, *Regulation of myocardial contractility and cell size by distinct PI3K-PTEN signaling pathways*. Cell, 2002. **110**(6): p. 737-49.
10. Guillermet-Guibert, J., K. Bjorklof, A. Salpekar, C. Gonella, F. Ramadani, A. Bilancio, S. Meek, A.J. Smith, K. Okkenhaug, and B. Vanhaesebroeck, *The p110beta isoform of phosphoinositide 3-kinase signals downstream of G protein-coupled receptors and is functionally redundant with p110gamma*. Proc Natl Acad Sci U S A, 2008. **105**(24): p. 8292-7.
11. Foster, F.M., C.J. Traer, S.M. Abraham, and M.J. Fry, *The phosphoinositide (PI) 3-kinase family*. J Cell Sci, 2003. **116**(Pt 15): p. 3037-40.
12. Pawson, T., *Specificity in signal transduction: from phosphotyrosine-SH2 domain interactions to complex cellular systems*. Cell, 2004. **116**(2): p. 191-203.
13. Stephens, L.R., T.R. Jackson, and P.T. Hawkins, *Agonist-stimulated synthesis of phosphatidylinositol(3,4,5)-trisphosphate: a new intracellular signalling system?* Biochim Biophys Acta, 1993. **1179**(1): p. 27-75.
14. Okamoto, M., T. Hayashi, S. Kono, G. Inoue, M. Kubota, H. Kuzuya, and H. Imura, *Specific activity of phosphatidylinositol 3-kinase is increased by insulin stimulation*. Biochem J, 1993. **290** (Pt 2): p. 327-33.

15. Sanchez-Margalet, V., I.D. Goldfine, C.J. Vlahos, and C.K. Sung, *Role of phosphatidylinositol-3-kinase in insulin receptor signaling: studies with inhibitor, LY294002*. *Biochem Biophys Res Commun*, 1994. **204**(2): p. 446-52.
16. Ito, H., M. Hiroe, Y. Hirata, M. Tsujino, S. Adachi, M. Shichiri, A. Koike, A. Nogami, and F. Marumo, *Insulin-like growth factor-I induces hypertrophy with enhanced expression of muscle specific genes in cultured rat cardiomyocytes*. *Circulation*, 1993. **87**(5): p. 1715-21.
17. Liang, W., G.Y. Oudit, M.M. Patel, A.M. Shah, J.R. Woodgett, R.G. Tsushima, M.E. Ward, and P.H. Backx, *Role of phosphoinositide 3-kinase {alpha}, protein kinase C, and L-type Ca²⁺ channels in mediating the complex actions of angiotensin II on mouse cardiac contractility*. *Hypertension*. **56**(3): p. 422-9.
18. McMullen, J.R., T. Shioi, L. Zhang, O. Tarnavski, M.C. Sherwood, P.M. Kang, and S. Izumo, *Phosphoinositide 3-kinase(p110alpha) plays a critical role for the induction of physiological, but not pathological, cardiac hypertrophy*. *Proc Natl Acad Sci U S A*, 2003. **100**(21): p. 12355-60.
19. Brock, C., M. Schaefer, H.P. Reusch, C. Czupalla, M. Michalke, K. Spicher, G. Schultz, and B. Nurnberg, *Roles of G beta gamma in membrane recruitment and activation of p110 gamma/p101 phosphoinositide 3-kinase gamma*. *J Cell Biol*, 2003. **160**(1): p. 89-99.
20. Naga Prasad, S.V., G. Esposito, L. Mao, W.J. Koch, and H.A. Rockman, *Gbetagamma-dependent phosphoinositide 3-kinase activation in hearts with in vivo pressure overload hypertrophy*. *J Biol Chem*, 2000. **275**(7): p. 4693-8.

21. Kubo, H., K. Hazeki, S. Takasuga, and O. Hazeki, *Specific role for p85/p110beta in GTP-binding-protein-mediated activation of Akt*. *Biochem J*, 2005. **392**(Pt 3): p. 607-14.
22. Sasaki, T., J. Irie-Sasaki, R.G. Jones, A.J. Oliveira-dos-Santos, W.L. Stanford, B. Bolon, A. Wakeham, A. Itie, D. Bouchard, I. Kozieradzki, N. Joza, T.W. Mak, P.S. Ohashi, A. Suzuki, and J.M. Penninger, *Function of PI3Kgamma in thymocyte development, T cell activation, and neutrophil migration*. *Science*, 2000. **287**(5455): p. 1040-6.
23. Patrucco, E., A. Notte, L. Barberis, G. Selvetella, A. Maffei, M. Brancaccio, S. Marengo, G. Russo, O. Azzolino, S.D. Rybalkin, L. Silengo, F. Altruda, R. Wetzker, M.P. Wymann, G. Lembo, and E. Hirsch, *PI3Kgamma modulates the cardiac response to chronic pressure overload by distinct kinase-dependent and -independent effects*. *Cell*, 2004. **118**(3): p. 375-87.
24. Oudit, G.Y., M.A. Crackower, U. Eriksson, R. Sarao, I. Kozieradzki, T. Sasaki, J. Irie-Sasaki, D. Gidrewicz, V.O. Rybin, T. Wada, S.F. Steinberg, P.H. Backx, and J.M. Penninger, *Phosphoinositide 3-kinase gamma-deficient mice are protected from isoproterenol-induced heart failure*. *Circulation*, 2003. **108**(17): p. 2147-52.
25. Shioi, T., J.R. McMullen, P.M. Kang, P.S. Douglas, T. Obata, T.F. Franke, L.C. Cantley, and S. Izumo, *Akt/protein kinase B promotes organ growth in transgenic mice*. *Mol Cell Biol*, 2002. **22**(8): p. 2799-809.
26. Bottomley, M.J., K. Salim, and G. Panayotou, *Phospholipid-binding protein domains*. *Biochim Biophys Acta*, 1998. **1436**(1-2): p. 165-83.

27. Czech, M.P., *PIP2 and PIP3: complex roles at the cell surface*. Cell, 2000. **100**(6): p. 603-6.
28. Toker, A. and A.C. Newton, *Cellular signaling: pivoting around PDK-1*. Cell, 2000. **103**(2): p. 185-8.
29. Sarbassov, D.D., D.A. Guertin, S.M. Ali, and D.M. Sabatini, *Phosphorylation and regulation of Akt/PKB by the rictor-mTOR complex*. Science, 2005. **307**(5712): p. 1098-101.
30. Delcommenne, M., C. Tan, V. Gray, L. Rue, J. Woodgett, and S. Dedhar, *Phosphoinositide-3-OH kinase-dependent regulation of glycogen synthase kinase 3 and protein kinase B/AKT by the integrin-linked kinase*. Proc Natl Acad Sci U S A, 1998. **95**(19): p. 11211-6.
31. Zhai, P., S. Gao, E. Holle, X. Yu, A. Yatani, T. Wagner, and J. Sadoshima, *Glycogen synthase kinase-3alpha reduces cardiac growth and pressure overload-induced cardiac hypertrophy by inhibition of extracellular signal-regulated kinases*. J Biol Chem, 2007. **282**(45): p. 33181-91.
32. Matsuda, T., P. Zhai, Y. Maejima, C. Hong, S. Gao, B. Tian, K. Goto, H. Takagi, M. Tamamori-Adachi, S. Kitajima, and J. Sadoshima, *Distinct roles of GSK-3alpha and GSK-3beta phosphorylation in the heart under pressure overload*. Proc Natl Acad Sci U S A, 2008. **105**(52): p. 20900-5.
33. Antos, C.L., T.A. McKinsey, N. Frey, W. Kutschke, J. McAnally, J.M. Shelton, J.A. Richardson, J.A. Hill, and E.N. Olson, *Activated glycogen synthase-3 beta suppresses cardiac hypertrophy in vivo*. Proc Natl Acad Sci U S A, 2002. **99**(2): p. 907-12.

34. Woodgett, J.R. and T. Force, *Unique and overlapping functions of GSK-3 isoforms in cellular differentiation, proliferation, and cardiovascular development*. J Biol Chem, 2008.
35. Stambolic, V., A. Suzuki, J.L. de la Pompa, G.M. Brothers, C. Mirtsos, T. Sasaki, J. Ruland, J.M. Penninger, D.P. Siderovski, and T.W. Mak, *Negative regulation of PKB/Akt-dependent cell survival by the tumor suppressor PTEN*. Cell, 1998. **95**(1): p. 29-39.
36. Sun, H., R. Lesche, D.M. Li, J. Liliental, H. Zhang, J. Gao, N. Gavrilova, B. Mueller, X. Liu, and H. Wu, *PTEN modulates cell cycle progression and cell survival by regulating phosphatidylinositol 3,4,5,-trisphosphate and Akt/protein kinase B signaling pathway*. Proc Natl Acad Sci U S A, 1999. **96**(11): p. 6199-204.
37. Zhu, D., J. Hensel, R. Hilgraf, M. Abbasian, O. Pornillos, G. Deyanat-Yazdi, X.H. Hua, and S. Cox, *Inhibition of protein kinase CK2 expression and activity blocks tumor cell growth*. Mol Cell Biochem, 2010. **333**(1-2): p. 159-67.
38. von Lewinski, D., K. Voss, S. Hulsmann, H. Kogler, and B. Pieske, *Insulin-like growth factor-1 exerts Ca²⁺-dependent positive inotropic effects in failing human myocardium*. Circ Res, 2003. **92**(2): p. 169-76.
39. O'Neill, B.T., J. Kim, A.R. Wende, H.A. Theobald, J. Tuinei, J. Buchanan, A. Guo, V.G. Zaha, D.K. Davis, J.C. Schell, S. Boudina, B. Wayment, S.E. Litwin, T. Shioi, S. Izumo, M.J. Birnbaum, and E.D. Abel, *A conserved role for phosphatidylinositol 3-kinase but not Akt signaling in mitochondrial adaptations*

- that accompany physiological cardiac hypertrophy. Cell Metab, 2007. 6(4): p. 294-306.*
40. Guo, D., Z. Kassiri, R. Basu, F.L. Chow, V. Kandalam, F. Damilano, W. Liang, S. Izumo, E. Hirsch, J.M. Penninger, P.H. Backx, and G.Y. Oudit, *Loss of PI3Kgamma enhances cAMP-dependent MMP remodeling of the myocardial N-cadherin adhesion complexes and extracellular matrix in response to early biomechanical stress. Circ Res. 107(10): p. 1275-89.*
41. McMullen, J.R., F. Amirahmadi, E.A. Woodcock, M. Schinke-Braun, R.D. Bouwman, K.A. Hewitt, J.P. Mollica, L. Zhang, Y. Zhang, T. Shioi, A. Buerger, S. Izumo, P.Y. Jay, and G.L. Jennings, *Protective effects of exercise and phosphoinositide 3-kinase(p110alpha) signaling in dilated and hypertrophic cardiomyopathy. Proc Natl Acad Sci U S A, 2007. 104(2): p. 612-7.*
42. Schoenberg, M., *Geometrical factors influencing muscle force development. II. Radial forces. Biophys J, 1980. 30(1): p. 69-77.*
43. Pedrotty, D.M., R.Y. Klinger, N. Badie, S. Hinds, A. Kardashian, and N. Bursac, *Structural coupling of cardiomyocytes and noncardiomyocytes: quantitative comparisons using a novel micropatterned cell pair assay. Am J Physiol Heart Circ Physiol, 2008. 295(1): p. H390-400.*
44. Tran, N.L., D.G. Adams, R.R. Vaillancourt, and R.L. Heimark, *Signal transduction from N-cadherin increases Bcl-2. Regulation of the phosphatidylinositol 3-kinase/Akt pathway by homophilic adhesion and actin cytoskeletal organization. J Biol Chem, 2002. 277(36): p. 32905-14.*

45. Walker, E.H., M.E. Pacold, O. Perisic, L. Stephens, P.T. Hawkins, M.P. Wymann, and R.L. Williams, *Structural determinants of phosphoinositide 3-kinase inhibition by wortmannin, LY294002, quercetin, myricetin, and staurosporine*. Mol Cell, 2000. **6**(4): p. 909-19.
46. Ui, M., T. Okada, K. Hazeki, and O. Hazeki, *Wortmannin as a unique probe for an intracellular signalling protein, phosphoinositide 3-kinase*. Trends Biochem Sci, 1995. **20**(8): p. 303-7.
47. Vlahos, C.J., W.F. Matter, K.Y. Hui, and R.F. Brown, *A specific inhibitor of phosphatidylinositol 3-kinase, 2-(4-morpholinyl)-8-phenyl-4H-1-benzopyran-4-one (LY294002)*. J Biol Chem, 1994. **269**(7): p. 5241-8.
48. Kong, D. and T. Yamori, *Phosphatidylinositol 3-kinase inhibitors: promising drug candidates for cancer therapy*. Cancer Sci, 2008. **99**(9): p. 1734-40.
49. Kong, D. and T. Yamori, *Advances in development of phosphatidylinositol 3-kinase inhibitors*. Curr Med Chem, 2009. **16**(22): p. 2839-54.
50. Marone, R., V. Cmiljanovic, B. Giese, and M.P. Wymann, *Targeting phosphoinositide 3-kinase: moving towards therapy*. Biochim Biophys Acta, 2008. **1784**(1): p. 159-85.
51. Knight, Z.A., B. Gonzalez, M.E. Feldman, E.R. Zunder, D.D. Goldenberg, O. Williams, R. Loewith, D. Stokoe, A. Balla, B. Toth, T. Balla, W.A. Weiss, R.L. Williams, and K.M. Shokat, *A pharmacological map of the PI3-K family defines a role for p110alpha in insulin signaling*. Cell, 2006. **125**(4): p. 733-47.
52. Raynaud, F.I., S. Eccles, P.A. Clarke, A. Hayes, B. Nutley, S. Alix, A. Henley, F. Di-Stefano, Z. Ahmad, S. Guillard, L.M. Bjerke, L. Kelland, M. Valenti, L.

- Patterson, S. Gowan, A. de Haven Brandon, M. Hayakawa, H. Kaizawa, T. Koizumi, T. Ohishi, S. Patel, N. Saghir, P. Parker, M. Waterfield, and P. Workman, *Pharmacologic characterization of a potent inhibitor of class I phosphatidylinositide 3-kinases*. *Cancer Res*, 2007. **67**(12): p. 5840-50.
53. Barber, D.F., A. Bartolome, C. Hernandez, J.M. Flores, C. Redondo, C. Fernandez-Arias, M. Camps, T. Ruckle, M.K. Schwarz, S. Rodriguez, A.C. Martinez, D. Balomenos, C. Rommel, and A.C. Carrera, *PI3Kgamma inhibition blocks glomerulonephritis and extends lifespan in a mouse model of systemic lupus*. *Nat Med*, 2005. **11**(9): p. 933-5.
54. Camps, M., T. Ruckle, H. Ji, V. Ardisson, F. Rintelen, J. Shaw, C. Ferrandi, C. Chabert, C. Gillieron, B. Francon, T. Martin, D. Gretener, D. Perrin, D. Leroy, P.A. Vitte, E. Hirsch, M.P. Wymann, R. Cirillo, M.K. Schwarz, and C. Rommel, *Blockade of PI3Kgamma suppresses joint inflammation and damage in mouse models of rheumatoid arthritis*. *Nat Med*, 2005. **11**(9): p. 936-43.
55. McMullen, J.R. and G.L. Jennings, *Differences between pathological and physiological cardiac hypertrophy: novel therapeutic strategies to treat heart failure*. *Clin Exp Pharmacol Physiol*, 2007. **34**(4): p. 255-62.
56. Dorn, G.W., 2nd, *The fuzzy logic of physiological cardiac hypertrophy*. *Hypertension*, 2007. **49**(5): p. 962-70.
57. Pelliccia, A., B.J. Maron, R. De Luca, F.M. Di Paolo, A. Spataro, and F. Culasso, *Remodeling of left ventricular hypertrophy in elite athletes after long-term deconditioning*. *Circulation*, 2002. **105**(8): p. 944-9.

58. Richey, P.A. and S.P. Brown, *Pathological versus physiological left ventricular hypertrophy: a review*. J Sports Sci, 1998. **16**(2): p. 129-41.
59. Eghbali, M., Y. Wang, L. Toro, and E. Stefani, *Heart hypertrophy during pregnancy: a better functioning heart?* Trends Cardiovasc Med, 2006. **16**(8): p. 285-91.
60. English, J.L., Z. Kassiri, I. Koskivirta, S.J. Atkinson, M. Di Grappa, P.D. Soloway, H. Nagase, E. Vuorio, G. Murphy, and R. Khokha, *Individual Timp deficiencies differentially impact pro-MMP-2 activation*. J Biol Chem, 2006. **281**(15): p. 10337-46.
61. Kandalam, V., R. Basu, T. Abraham, X. Wang, P.D. Soloway, D.M. Jaworski, G.Y. Oudit, and Z. Kassiri, *TIMP2 deficiency accelerates adverse post-myocardial infarction remodeling because of enhanced MT1-MMP activity despite lack of MMP2 activation*. Circ Res. **106**(4): p. 796-808.

Chapter 2

MATERIALS AND METHODS

2.1 Animal Care

All experimental animals are handled in accordance with the institutional guidelines of the Canadian Council on Animal Care. All experimental procedures have been approved by the Animal Care and Use Committee.

2.2 Heart tissue collection and gravitometry

Prior to collecting heart tissue, mice were weighed using a calibrated scale (VWR) and body mass was recorded.

Mouse hearts were excised after anesthesia via 2.25% isoflurane at 1 L/min flow rate of O₂ and sternectomy using surgical scissors. Hearts were then washed briefly in ice cold PBS to remove excess blood and weighed. The atria and right ventricle were then removed and the left ventricle (LV) was weighed and snap-frozen in liquid nitrogen.

After collecting heart tissue, the tibial length was measured using callipers to standardize LV mass. Tibial length was used instead of body weight to assess body size because body weight increases as mice age due to accumulation of body fat.

2.3 Isolation and culture of adult mouse cardiomyocytes and cardiofibroblasts

The protocol for isolation and culture of adult cardiomyocytes is derived from a previous study [1]. 9-11 week old mice were injected with 0.05 mL of 1000 units/mL heparin for 15 min and then anesthetized using 2% isoflurane (1 L/min O₂ flow rate) provided through a nose cone. After opening the chest cavity, the heart was quickly excised and perfused using a Langendorff system within 45 s. Following 3 min of

perfusion with perfusion buffer (made from stock (Table 2.1)) (Table 2.2), the heart was digested with digestion buffer (Table 2.3) for 7-8 min. After sufficient digestion, the ventricles were removed, dissociated using forceps and transfer pipettes, and resuspended in stopping buffer (Table 2.4). The isolated cardiomyocytes were then exposed to increasing calcium concentrations (100 μ M, 400 μ M, and 900 μ M) for 15 min each before being plated onto laminin coated culture dishes in plating buffer (Table 2.5) and placed at 37°C in a sterile 2% CO₂ incubator. The discarded stopping buffer was set aside for cardiofibroblasts collection. One hour after plating, the plating buffer was gently aspirated and replaced with culture buffer (Table 2.6) and then placed into the incubator for 18 h before treatment.

The discarded stopping buffer was centrifuged at 20 g for 3 min and the resulting supernatant was collected in a 15 mL conical tube. This was then centrifuged at 1500 rpm for 5 min and the pellet was collected and washed in 10 % FBS DMEM (GIBCO). The solution was once again centrifuged at 1500 rpm for 5 min and the pellet was collected and plated onto a 10 cm culture dish in fibroblast culture buffer (Table 2.7). The cardiofibroblasts were then passaged twice and placed into serum free DMEM for 24 h prior to treatment.

Table 2.1 Stock Perfusion Buffer

Reagent	Source	Concentration
NaCl	Fisher	113 mM
KCl	Fisher	4.7 mM
KH ₂ PO ₄	EMD	0.6 mM
Na ₂ HPO ₄	EMD	0.6 mM
MgSO ₄ -7(H ₂ O)	EMD	1.2 mM
NaHCO ₃	EMD	12 mM
HEPES	Fisher	10 mM
Taurine	Sigma-Aldrich	30 mM

Table 2.2 Perfusion Buffer

Reagent	Source	Quantity
Stock Perfusion Buffer	Table 2.1	490 mL
Dextrose	EMD	0.5 g
500 mM 2,3-Butanedione Monoxime Solution	BDM from Sigma-Aldrich	10 mL

Table 2.3 Digestion Buffer

Reagent	Source	Quantity
Perfusion Buffer	Table 2.2	50 mL
Collagenase Type 2	Worthington	120 mg

Table 2.4 Stopping Buffer

Reagent	Source	Quantity
Perfusion Buffer	Table 2.2	45 mL
Fetal Bovine Serum	Sigma-Aldrich	5 mL

Table 2.5 Plating Buffer

Reagent	Source	Quantity
MEM Eagle (M4780)	Sigma-Aldrich	43 mL
Fetal Bovine Serum	Sigma-Aldrich	5 mL
500 mM 2,3-Butanedione Monoxime Solution	Sigma-Aldrich	1 mL
Penicillin Streptomycin	Sigma-Aldrich	0.5 mL
Fungizone	Sigma-Aldrich	0.5 mL

Table 2.6 Culture Buffer

Reagent	Source	Quantity
MEM Eagle (M4780)	Sigma-Aldrich	47 mL
100 mg/mL Bovine Serum Albumin	Sigma-Aldrich	0.5 mL
Penicillin Streptomycin	Sigma-Aldrich	0.5 mL
Fungizone	Sigma-Aldrich	0.5 mL
500 mM 2,3-Butanedione Monoxime Solution	Sigma-Aldrich	1 mL
Insulin-Transferin-Selenium	GIBCO	0.5 mL

Table 2.7 Fibroblast Culture Buffer

Reagent	Source	Quantity
DMEM	GIBCO	44.5 mL
Penicillin Streptomycin	Sigma-Aldrich	0.5 mL
Fetal Bovine Serum	Sigma-Aldrich	5 mL

2.4 Preparation of cell lysates

Cell culture dishes were quickly aspirated to remove culture media and washed 3 times with ice cold PBS (Table 2.8). 100 μ L of cell culture RIPA buffer (Table 2.9) was then added to the plates before scraping with cell scrapers. The cell homogenates were centrifuged at 14,000 g at 4°C for 10 min and the supernatant was collected and stored at -80°C.

Table 2.8 PBS – pH 7.4

Reagent	Source	Quantity
NaCl	Fisher	8.0 g
KCl	Fisher	0.2 g
Na ₂ HPO ₄	EMD	1.44 g
KH ₂ PO ₄	EMD	0.24 g
ddH ₂ O		Add until 1 L
Total Volume		1 L

2.5 Preparation of protein extract from tissue samples

LV myocardial tissue was cut on dry ice using a surgical scalpel and suspended in RIPA protein extraction buffer (Table 2.9) with protease inhibitors (Calbiochem) and phosphatase inhibitors (Sigma-Aldrich) in a 1.5 mL eppendorf tube designed as a mini mortar. Using the appropriate pestle (VWR), the tissue was manually homogenized and then vortexed for 1 min before being incubated on ice for 30 min. The sample was then

vortexed again for 1 min and incubated on ice for 30 more min before being centrifuged at 14,000 g at 4°C for 10 min. The supernatant was collected and stored at -80°C.

Table 2.9 RIPA Buffer

Reagent	Source	Quantity
1 M Tris-HCl (pH 7.4)	Calbiochem	5 mL
1 M NaCl	Fisher	15 mL
20% Sodium dodecyl sulphate (SDS)	BioRad	0.5 mL
20% Nonidet-P40 (NP40)	Sigma-Aldrich	5 mL
10% Sodium Deoxycholate	Sigma-Aldrich	5 mL
0.5 M EDTA	Sigma-Aldrich	1 mL
ddH ₂ O		68.5 mL
Total Volume		100 mL

2.6 Membrane fractionation

Membrane fraction was extracted from LV frozen tissue in RIPA Buffer (50 mM Tris-HCl, 150 mM NaCl, and 1 mM EDTA; pH 7.4) with DTT (1 mM), PMSF (1 mM), protease inhibitor (Calbiochem) and phosphatase inhibitor cocktails (Sigma-Aldrich), and centrifuged at 29,000 g for 45 min. This high speed centrifugation separated the cytosolic protein (supernatant) from the membrane protein (pellet). The pellet was resuspended in 50 µL RIPA Buffer (containing DTT, PMSF, protease and phosphatase inhibitors, with 0.25% sodium deoxycholate and 1% NP40) and then centrifuged at 15,000 for 20 min. This supernatant was stored at -80°C as the membrane fraction.

2.7 Determination of protein concentrations

Protein concentrations were quantified using the BioRad Colorimetric Assay Kit according to the manufacturer's instructions (BioRad). Protein samples were first

diluted in 1:10 ratio using PBS and 5 μL of the diluted samples were pipetted into 96-well plates in triplicates. As well, nine protein standards (Table 2.11) dissolved in PBS were also pipetted into the same plate in triplicates. 25 μL of Reagent A' was added to each well containing samples followed by 200 μL of Reagent B (Table 2.10). The 96-well plate was then wrapped in aluminum foil and gently agitated on a rocker for 5 min at room temperature before being analyzed by a 96-well plate microplate reader. A standard absorbance-concentration curve was generated using standards and was used to determine concentrations based on absorbance at 750 nm.

Table 2.10 Protein concentration quantification solution from BioRad (per sample)

Reagent	Quantity
Reagent A	24.5 μL
Reagent B	200.0 μL
Reagent S	0.5 μL
Reagent S' (Reagent A + S)	25 μL

Table 2.11 Protein Standards

Standard	Concentration of BSA in PBS
1	2.0 mg/mL
2	1.5 mg/mL
3	1.0 mg/mL
4	0.8 mg/mL
5	0.6 mg/mL
6	0.4 mg/mL
7	0.2 mg/mL
8	0.1 mg/mL
9 (Blank)	0.0 mg/mL

2.8 Western blot analysis

After protein quantification (Chapter 2.7), protein samples were mixed with loading buffer (Table 2.18) before being loaded into a 5% acrylamide loading gel (Table 2.12), separated by 8-12% SDS-PAGE gel electrophoresis (Table 2.13 and 2.15) and transferred to nitrocellulose membrane (Millipore) (Table 2.17). The membrane was blocked with 5% milk in Tris-Buffered Saline Tween-20 (TBST) for 2 h and then incubated overnight at 4°C with a primary antibody. After the primary antibody was removed, the membrane was washed 3 times with TBST for 15 min each. The membrane was then incubated with an appropriate horseradish peroxidase coupled secondary antibody at 1:5000 dilution in TBST for 2 h at room temperature, then washed 3 times with TBST for 15 min each. Proteins were detected by enhanced chemiluminescence (GE) using X-ray film (Fuji) and analyzed by the ImageJ software (U.S. National Institutes of Health, Bethesda, MD).

Coomassie Blue staining was used as a protein loading control for several western blots. Coomassie Blue was added to acrylamide gels after transferring and incubated at room temperature for 30 min. The Coomassie Blue was then removed and replaced with water and incubated overnight before being scanned.

Table 2.12 Loading Gel (5%)

Reagent	Source	Quantity
ddH ₂ O		2.70 mL
1.0 M Tris-HCl (pH 6.8)	Calbiochem	0.50 mL
10% SDS	BioRad	0.04 mL
30% acrylamide	BioRad	0.67 mL
10% ammonium persulfate	BioRad	0.04 mL
TEMED	J.T. Baker	0.004 mL
Total Volume		4 mL

Table 2.13 Separating Gel

Reagent	Source	Quantity		
		8%	10%	12%
ddH ₂ O		4.62 mL	4.96 mL	3.29 mL
1.5 M Tris-HCl (pH 8.8)	Calbiochem	2.50 mL	2.50 mL	2.50 mL
10% SDS	BioRad	0.10 mL	0.10 mL	0.10 mL
30% acrylamide	BioRad	2.67 mL	3.33 mL	4.00 mL
10% ammonium persulfate	BioRad	0.10 mL	0.10 mL	0.10 mL
TEMED	J.T. Baker	0.01 mL	0.01 mL	0.01 mL
Total Volume		10.00 mL	10.00 mL	10.00 mL

Table 2.14 Running Buffer (10x) pH 8.3

Reagent	Source	Quantity
Tris Base	Calbiochem	30.3 g
Glycine	EMD	144 g
SDS	BioRad	10 g
ddH ₂ O		Add until 1 L
Total Volume		1 L

Table 2.15 Running Buffer (1x)

Reagent	Source	Quantity
10x Running Buffer	Table 2.15	100 mL
ddH ₂ O		900 mL
Total Volume		1 L

Table 2.16 Transfer Buffer (10x) pH 8.3

Reagent	Source	Quantity
Tris Base	Calbiochem	30.3 g
Glycine	EMD	144 g
ddH ₂ O		Add until 1 L
Total Volume		1 L

Table 2.17 Transfer Buffer (1x)

Reagent	Source	Quantity
10x Transfer Buffer	Table 2.18	100 mL
Methanol	Fisher	200 mL
ddH ₂ O		700 mL
Total Volume		1 L

Table 2.18 Loading Buffer (5x)

Reagent	Source	Quantity
Glycerol	Sigma-Aldrich	3.0 mL
SDS	BioRad	0.8 g
0.5 M Tris-HCl (pH 6.8)	Calbiochem	5.0 mL
0.1% bromophenol blue	EMD	1.9 mL
100 μ M DTT	Thermo Scientific	0.1 mL

2.9 Stripping western blot membranes

Nitrocellulose membranes were briefly rinsed in room temperature TBST before being incubated in stripping buffer (Table 2.19) at 60°C for 30 min. The membranes were then washed three times with TBST for 15 min each.

Table 2.19 Stripping Buffer

Reagent	Source	Quantity
ddH ₂ O		16.6 mL
20% SDS	BioRad	2.0 mL
1M Tris-HCl (pH 6.8)	Calbiochem	1.26 mL
Beta-mercaptoethanol	Sigma Aldrich	140 μ L
Total Volume		20 mL

2.10 Measurement of cAMP levels

The cAMP assay was performed following the protocol provided with the GE Healthcare Amersham cAMP Biotrak Enzyme Immunoassay System. Isolated

ventricular cells and LV myocardial tissue were homogenized with the provided lysis reagent and centrifuged to remove debris. The homogenate was placed into the appropriate wells in the provided 96-well plate and incubated with antiserum for 2 h at 4°C. After the incubation, cAMP peroxidase conjugate was pipetted into all the wells except blanks and the plate was then incubated at 4°C for 1 h before the wells were aspirated, washed, and dried. Enzyme substrate was then added to each well for 30 min at room temperature before collecting the OD values at 630 nm. The OD values were converted to concentrations using a standard curve prepared with provided standards. The effects of beta adrenergic blockade using propranolol (25 µM) (Sigma) and specific adenylate cyclase inhibition using 2',5'-dideoxyadenosine (DIDA; 30 µM) (Sigma) on isoproterenol-induced elevation of cAMP were also examined using this assay.

2.11 RNA Extraction and cDNA Preparation

Total RNA was extracted from flash-frozen tissue or cardiofibroblasts using TRIzol extraction protocol, and cDNA was synthesized from 1 µg RNA by using cDNA PCR Solution (Table 2.20).

Table 2.20 cDNA PCR Solution (per sample)

Reagent	Source	Quantity
5X Buffer	Invitrogen	4 µL
0.1 M Dithiothreitol	Invitrogen	2 µL
25 mM dNTP	Invitrogen	1 µL
Superscript II	Invitrogen	1 µL
RNase inhibitor	Invitrogen	1 µL
Total Volume		9 µL

2.12 TaqMan Real-time PCR

For each gene, a standard curve was generated using known concentrations of cDNA (Table 2.21) as a function of the cycle threshold (CT). Expression analysis of the reported genes was performed by TaqMan Real-Time PCR using ABI 7900 Sequence Detection System (Table 2.22). The SDS2.2 software (integral to ABI 7900 real-time machine) fits the CT values for the experimental samples and generates values for cDNA levels. All samples were run in triplicates in 384 well plates. 18S rRNA was used as an endogenous control.

Table 2.21 TaqMan cDNA Standards

Standard	Concentration (cDNA in PCR H₂O)
1	2.00 ng/nL
2	1.00 ng/nL
3	0.50 ng/nL
4	0.25 ng/nL
5	0.125 ng/nL
6	0.0625 ng/nL

Table 2.22 TaqMan reaction mix (per sample)

Reagent	Source	Quantity
Mastermix	Applied Biosystems	8.33 μ L
Forward Primer		0.50 μ L
Reverse Primer		0.50 μ L
Probe		0.50 μ L
PCR H ₂ O		5.17 μ L
Total Volume		15.00 μ L

2.13 Echocardiography

Transthoracic M-mode and Doppler echocardiographic examination at 1 wk and 3 wk post-AB were performed using an Acuson (R) Sequoia C256 system equipped

with a 15-MHz linear transducer (15L8) (Version 4.0, Acuson Corporation, Mountain View, California) as previously described. Mice were placed on a heating pad and a nose cone with 0.75-1% isoflurane in 100% oxygen was applied at 1 L/min. The temperature was maintained at 36.5 to 37.5°C. Hair was removed using a surgical shaver. Ultrasound gel was placed on the bare chest of the anesthetized mouse and the ultrasound probe was placed in contact with the gel and scanning was performed over 30 min. Body temperature, heart rate, and blood pressures were constantly monitored throughout the procedure. M-mode images were obtained for measurements of LV wall thickness, LV end-diastolic diameter, and LV end-systolic diameter. M-mode images were used to measure LV chamber sizes and wall thicknesses. Fractional shortening and velocity of circumferential fractional shortening were calculated.

For the propranolol experiments, the echocardiographic measurements were made using the Vevo 770 high-resolution imaging system equipped with a 30 MHz transducer (RMV-707B; VisualSonics, Toronto, Canada).

2.14 Hemodynamic Measurements

The protocol for Hemodynamic Measurements is derived from a previous study [2]. Mice were anesthetized via I.P. injection of ketamine and xylazine and laid in a supine position; a small incision was made above the rib cage. The right carotid artery was identified and subsequently cannulated with a 1.4 French Millar catheter, which was inserted through the aorta into the left ventricle. Left ventricular pressures were then recorded and assessed for left ventricular end diastolic pressure (LVEDP),

maximum rate of pressure generation ($+dP/dt_{\max}$) and maximum rate of pressure loss ($-dP/dt_{\min}$).

2.15 Statistical analysis

All data were plotted using the mean value \pm standard error mean with n representing the sample size. One-way ANOVA was used to test for overall significance, followed by the Student-Newman-Keuls test for multiple-comparison testing between the various groups. All statistical analyses were performed with the SPSS software (version 10.1).

2.16 References:

1. O'Connell, T.D., M.C. Rodrigo, and P.C. Simpson, *Isolation and culture of adult mouse cardiac myocytes*. *Methods Mol Biol*, 2007. **357**: p. 271-96.
2. Zvaritch, E., P.H. Backx, F. Jirik, Y. Kimura, S. de Leon, A.G. Schmidt, B.D. Hoit, J.W. Lester, E.G. Kranias, and D.H. MacLennan, *The transgenic expression of highly inhibitory monomeric forms of phospholamban in mouse heart impairs cardiac contractility*. *J Biol Chem*, 2000. **275**(20): p. 14985-91.

Chapter 3

PI3K γ KO AND PRESSURE OVERLOAD

A version of this chapter has been published in *Circulation Research*. Guo D, Kassiri Z, Basu R, Chow FL, Kandalam V, Damilano F, Liang W, Izumo S, Hirsch E, Penninger JM, Backx PH, Oudit GY. *Circ Res*. 2010 Nov 12;107(10):1275-89.

PSR, TUNEL assay, echocardiography, cardiomyocyte contractility assay, immunofluorescence staining, zymography, and collagenase activity assay were conducted by Dr. Gavin Oudit. Taqman RT-PCR was performed by Dr. Xiuhua Wang. Hydroxyproline assay was conducted by Vijay Kandalam. Invasive hemodynamic analysis and aortic banding were conducted by Fung Lan Chow.

3.1 Introduction:

Mechanotransduction plays a fundamental role in cardiac function and involves interactions between the extracellular matrix (ECM) and intracellular cytoskeletal proteins via cell adhesion complexes which are modulated by Class I PI3Ks [1]. Although PI3Ks and lipid phosphatases can modulate cytoskeletal interactions, stretch can in turn activate Akt and GSK-3 β activity in cardiomyocytes [2]. In the myocardium, cell adhesion and cardiomyocyte stretch sensor machinery play key roles in the complex mechanism leading to human DCM and associated heart failures, which are associated with marked remodeling of ECM and cell adhesion complexes [3].

Loss of p110 γ , the catalytic subunit of the PI3K γ complex, leads to enhanced cAMP generation due to the loss of phosphodiesterase activity, resulting in enhanced Ca²⁺ cycling attributable primarily to increased phosphorylation and inhibition of phospholamban (PLN) and increased SERCA2a activity [4-6]. As this is a key regulator of myocardial contractility, baseline enhancements in Ca²⁺ cycling, such as observed in PI3K γ KO hearts, can protect the heart from systolic dysfunction and DCM.

Aortic banding (AB) is the chronic constriction of the aorta leading to a constant increase in left ventricular pressure and mechanical workload. WT hearts exposed to AB demonstrate progressive pathological and concentric hypertrophy, fibrosis, and loss of left ventricular contractile function as early as 4 weeks post AB [7, 8]. The conditions of these hearts continue to deteriorate until they begin to decompensate and develop DCM [9, 10]. Interestingly, PI3K γ KO hearts develop rapid left ventricular dysfunction

and DCM one wk post AB despite its enhanced Ca^{2+} cycling, though the exact mechanism leading to this paradoxical failure has not been described [5].

This chapter will explore the role of mechanotransduction and intercellular adhesion complexes in the observed systolic dysfunction and DCM in PI3K γ KO hearts post AB.

3.2 Methods:

3.2.1 Experimental animals

PI3K γ KO, PI3K α DN, and PI3K γ KD mice in C57Bl/6 background have been described [5, 11]. All experiments were performed in accordance with institutional guidelines and Canadian Council on Animal Care. Only male mice of 8 to 9 weeks of age and littermate WT controls were used. For the propranolol experiments, mice were treated with propranolol in their drinking water (0.2 g/L) to deliver 15 mg/kg per day; propranolol was withdrawn 1 day before the echocardiographic and hemodynamic measurements. The broad-spectrum MMP inhibitor PD166793 (Pfizer Inc) was administered orally by daily gavage. Because the rapid onset of ventricular dilation in PI3K γ KO mice, PD166793 treatment (30 mg/kg/day) began 3 days before AB and continued until mice were euthanized.

3.2.2 Aortic Banding

8-9 wk old male mice weighing 20-25 g were anesthetized with ketamine (100 mg/kg) and xylazine (10 mg/kg). A topical depilatory agent was applied to the neck and chest area to remove fur at and around the area of incision. The skin was cleaned with Germex and Betadine. One dose of penicillin (10 mg/kg, 0.1 mL I.P.) was administered prior to start of surgery. Mice were placed supine and body temperature was maintained at 37°C with a heating pad. Once the mouse reached surgical plane of anaesthesia as confirmed by toe-pinching on both hind feet, a horizontal skin incision of 1 cm in length was made at the level of second intercostal space. A 6-0 silk suture was passed under the aortic arch. A bent 26-gauge needle was then placed next to the aortic arch and the

suture was snugly tied around the needle and aorta between the left carotid artery and the brachiocephalic trunk. The needle was quickly removed allowing the suture to constrict the aorta. The incision was closed in layers and the mice were allowed to recover on a warming pad until they were fully awake. Immediately after the surgery, mice received one dose of buprenorphine and for the first 24 hours. The sham animals underwent the same procedure without the aortic banding.

3.2.3 Hydroxyproline Assay

20 mg pieces of frozen LV tissue were sliced and placed into Eppendorf tubes for lyophilisation at -110°C and 96 mTorr overnight. After lyophilisation, the frozen tissue was crushed, weighed, transfer into glass test tubes, and suspended in 2 mL of 6 N HCl. The samples were then incubated at 120°C for 3-5 hours until the acid fully evaporated and then resuspended with 100 μL of ddH₂O.

Samples were loaded onto a 96-well microplate and incubated with Chloramine T (Table 3.1) at room temperature for 20 min to oxidize hydroxyproline, then Ehrlich's reagent (Sigma) was added, and plates were wrapped in aluminum foil and incubated at 60°C for 20 min. The concentration of hydroxyproline was determined using standards (Table 3.3).

Table 3.1 Chloramine T (per sample)

Reagent	Source	Quantity
n-propanol	Sigma-Aldrich	3.75 μL
Acetate-citrate buffer	Table 3.2	30 μL
ddH ₂ O		3.75 μL
Total Volume		37.5 μL

Table 3.2 Acetate-citrate Buffer

Reagent	Source	Quantity
Sodium acetate trihydrate	Sigma-Aldrich	120 g
Citric acid	Sigma-Aldrich	46 g
Acetic acid (100%)	Sigma-Aldrich	12 mL
Sodium hydroxide	Sigma-Aldrich	34 g
ddH ₂ O		To 1 L
Total Volume		1 L

Table 3.3 Hydroxyproline Standards

Standard	Concentration of L-4-Hydroxyproline methyl ester hydrochloride (Sigma)
1	1.000 mg/mL
2	0.500 mg/mL
3	0.250 mg/mL
4	0.100 mg/mL
5	0.075 mg/mL
6	0.050 mg/mL
7	0.025 mg/mL
8	0.010 mg/mL
Blank	0.000 mg/mL

3.2.4 Tissue fixation, histology, and TUNEL assay

For formalin fixation, hearts were excised as described in Chapter 2.2, arrested with 1 M KCl, and fixed in 10% phosphate buffered formalin (VWR). After 36 hr of fixation, the hearts were embedded in paraffin for sectioning at 10 μ m thickness per section. Collagen volume fraction was measured using picosirius red staining of the section hearts and confocal microscopy. TUNEL assays were performed using ApopTag Plus kit (Oncor, Gaithersburg, MD) to determine apoptosis via DNA fragmentation.

3.2.5 Isolated cardiomyocyte contractility

Ventricular cardiomyocytes were placed in a Plexiglass chamber and continuously perfused with oxygenated Tyrodes buffer (137 mM NaCl, 5.4 mM KCl, 10 mM glucose, 10 mM HEPES, 0.5 mM NaH₂PO₄, 1 mM MgCl₂, 1.2 mM CaCl₂, and pH 7.4) at 2.5 mL/min at 36°C. Cardiomyocytes were stimulated at 1 Hz with a Grass S44 stimulator (pulse duration 3 ms; 15-20 V) and a video edge detector (Crescent Electronics) was used to track myocyte contractions. Steady state contractions were recorded at 1 kHz following a 4 min equilibrium period using a Phillips 800 camera system (240 Hz) and Felix acquisition software (Photon Technologies Inc.). Cardiomyocyte length, percent fractional shortening, shortening rate (+dL/dt) and relaxation rate (-dL/dt) were determined at baseline.

3.2.6 Cell Adhesion Assay

The cell adhesion assay was performed in accordance with the protocol provided by CELL BIOLABS, INC. CytoSelect 48-Well Cell Adhesion Assay (ECM Array, Colorimetric Format) as previously described. Adult murine cardiomyocytes from sham and 1 wk post AB hearts were freshly isolated and a hemocytometer was used to determine cell concentration per mL. The concentration was adjusted to 100,000 cells/mL and the cells were plated into each well at 20,000 cells/well. The cells were then placed into a 2% CO₂ sterile 37°C incubator for 60 min for cells to adhere. The adherent cells were washed with PBS before 200 µL of the Cell Stain solution was added for 10 min. The cells were then washed five times with PBS to remove excess staining solution and left to air dry for 10 min. 200 µL of extraction solution was then

added to each well and the plate was incubated for 10 min on a rocker. Once the color of the solution stabilized, the 48-well plate was placed in a plate reader and absorbance (A) was recorded at 560 nm. The reported A values are the raw A values of samples minus the A value of a blank.

3.2.7 Gelatin Zymography

LV myocardial tissue was extracted as described in Chapter 2 using RIPA buffer without EDTA (Table 3.8). After preparing samples and mixing with loading buffer, the samples were loaded into the gel containing gelatin (Table 3.4). The gel was run at 30 mA per gel (set to constant Amps) for 1 hour, followed by 3 successive 20 min incubations with 2.5% Triton X-100 solution at room temperature. The Triton X-100 solution was then replaced with incubation buffer (Table 3.5) and placed in a 37°C non-sterile incubator for 48 hr. Gels were then stained with staining buffer (Table 3.6) in room temperature overnight. Destaining buffer (Table 3.7) is then added to visualize MMP2 and MMP9 bands. These zymograms were scanned using a GS 800 (BioRad) calibrated densitometer.

Table 3.4 Separating Gel for Zymography (8% with gelatine type-A)

Reagent	Source	Quantity
Gelatin type-A	Sigma-Aldrich	36 mg
ddH ₂ O		6.90 mL
1.5 M Tris-HCl (pH 8.8)	Calbiochem	3.80 mL
10% SDS	BioRad	0.15 mL
30% acrylamide	BioRad	6.90 mL
10% ammonium persulfate	BioRad	0.15 mL
TEMED	J.T. Baker	0.06 mL
Total Volume		18 mL

Table 3.5 Incubation Buffer

Reagent	Source	Quantity
2 M Tris-HCl	Calbiochem	15 mL
2 M CaCl ₂	Fisher	1.5 mL
NaCl	Fisher	5.25 g
5% NaN ₃	EMD	6.0 mL
ddH ₂ O		Add until 600 mL
Total Volume		600 mL

Table 3.6 Staining Solution

Reagent	Source	Quantity
Coomassie blue	EMD	4 mL
Methanol	Fisher	50 mL
Acetic acid	VWR	20 mL
ddH ₂ O		126 mL
Total Volume		200 mL

Table 3.7 Destaining Solution

Reagent	Source	Quantity
Methanol	Fisher	10 mL
Acetic acid	VWR	20 mL
ddH ₂ O		470 mL
Total Volume		500 mL

Table 3.8 RIPA Buffer without EDTA

Reagent	Source	Quantity
1 M Tris-HCl (pH 7.4)	Calbiochem	5 mL
1 M NaCl	Fisher	15 mL
20% Sodium dodecyl sulphate (SDS)	BioRad	0.5 mL
20% Nonidet-P40 (NP40)	Sigma-Aldrich	5 mL
10% Sodium Deoxycholate	Sigma-Aldrich	5 mL
ddH ₂ O		69.5 mL
Total Volume		100 mL

3.2.8 Collagenase Activity Assay

The collagenase activity assay was conducted as described in the provided protocol for EnzChek Gelatinase/Collagenase Assay Kit (Molecular Probes Inc). Cytobuster extraction buffer (Table 3.9) was used to extract protein instead of RIPA.

Table 3.9 Cytobuster extraction buffer

Reagent	Source	Quantity
Cytobuster buffer	Novagen	980.0 μ L
Phosphatase inhibitor cocktail	Calbiochem	10 μ L
Protease inhibitor cocktail	Calbiochem	10 μ L

3.2.9 Confocal Fluorescence Microscopy

Formalin-fixed sections were permeabilized with ice-cold methanol for 10 min, blocked with goat serum and incubated with primary antibodies overnight at 4°C in a humidified chamber. After several washes, the appropriate secondary antibodies were added and the sections were incubated for 30 min at room temperature. The sections were evaluated with a confocal microscope and associated software.

3.2.10 MMP/N-cadherin cleavage assay

N-cadherin Fc Chimera, which is a chimeric protein containing only the extracellular domain of N-cadherin, was incubated with 1 nM, 10 nM, and 100 nM of MMP2 and MT1-MMP for 15 min at 37°C. The 100 nM group was also incubated with the MMP inhibitor, PD166793. Western blot analysis was used to test for cleavage of N-cadherin.

3.3 Results:

3.3.1 Accelerated Development of Ventricular Dilation and Pathological Hypertrophy in PI3K γ KO Mice in Response to Biomechanical Stress

In response to pressure overload, WT mice developed concentric hypertrophy with increased wall thickness and reduction in chamber size at 1 and 3 weeks following AB (Figure 3.1 A). In contrast, LV size dilated rapidly in PI3K γ KO mice, characteristic of eccentric remodeling at 1 and 3 week following AB as shown by trichrome-stained four-chamber views (Figure 3.1 B). The early development of dilated cardiomyopathy in the banded PI3K γ KO mice was associated with increased interstitial myocardial fibrosis at 3 weeks after AB as illustrated by picrosirius red staining (Figure 3.1 C) and quantified as collagen volume fraction (Figure 3.1 D). Increased myocardial fibrosis in banded PI3K γ KO mice was confirmed by the biochemical assessment of hydroxyproline content (Figure 3.1 D) and occurred without a significant increase in apoptosis (Figure 3.1 E-F). In banded PI3K γ KO mice, mRNA expression profile showed greater myocardial expression of the disease markers, atrial natriuretic factor (ANF) (Figure 3.1 G), b-type natriuretic peptide (BNP) (Figure 3.1 H), and beta myosin heavy chain (β MHC) (Figure 3.1 I) with morphometric features of hypertrophy (Table 3.10). Activation of several signaling pathways is a key mediator of the response to biomechanical stress [12, 13]. Unlike in WT, phosphorylation of extracellular signal-regulated kinase (ERK) 1/2 (Figure 3.2 A) and Akt (Figure 3.2 B) were not increased in banded PI3K γ KO mice after one week of pressure overload. However, following three weeks of pressure overload, phosphorylation of ERK 1/2 was significantly increased in PI3K γ KO mice (Figure 3.2 A). The GSK-3 system is an important downstream

mediator of PI3K/Akt signaling [8] and consistent with a loss of Akt signaling, phosphorylated (phospho)-GSK-3 α (Figure 3.2 C) and phospho-GSK-3 β (Figure 3.2 D) were not affected initially at one week and then showed a drastic reduction at three weeks after AB in PI3K γ KO mice. Interestingly, baseline level of phospho-GSK-3 β was significantly greater in PI3K γ KO compared with WT mice (Figure 3.2 D). The phosphorylation of focal adhesion kinase (FAK) is a fundamental response in myocardial mechanical stretch and hypertrophy [14]. In the banded PI3K γ KO mice, increased phospho-FAK occurred earlier than in WT mice, consistent with an aberrant response to biomechanical stress (Figure 3.2 E). These results show that PI3K γ KO mice developed rapid onset of adverse myocardial remodeling and pathological hypertrophy in response to biomechanical stress with resultant alteration in the activation of mechano-sensitive and Akt-dependent signaling cascades.

3.3.2 Uncoupling Between In Vivo Myocardial Contractility and Single-Cardiomyocyte Contractility in Pressure Overloaded PI3K γ KO Mice

To examine whether these differences in myocardial remodeling in WT and PI3K γ KO mice result in functional alteration, we used transthoracic echocardiography to assess heart function. The LV chamber rapidly dilated with progressive decrements in systolic function at 1 and 3 weeks in PI3K γ KO mice (Figure 3.3 A-E; Table 3.11). In contrast, banded WT mice developed increased wall thickness with reduced ventricular size and preserved systolic function (Figure 3.3 A-D; Table 3.11). We further characterized these functional alterations using invasive hemodynamic measurements, which showed greater elevation in LV end diastolic pressure (Table 3.11) and reduced myocardial contractility as assessed by $+dP/dt_{max}$ (Figure 3.3 D; Table 3.11) and -

dP/dt_{\min} (Figure 3.3 E; Table 3.11) in banded PI3K γ KO mice. The early decompensation of banded PI3K γ KO hearts despite enhanced Ca^{2+} cycling and increased basal myocardial contractility (Figure 3.3; Table 3.11) [4-6] illustrate that the cause of the systolic dysfunction may be extracellular, suggesting that myocardial cell adhesion is compromised. Therefore, we hypothesized that isolated cardiomyocyte contractility would remain elevated in banded PI3K γ KO mice. Increased phosphorylation of PLN is a critical target of the elevated cAMP levels in PI3K γ KO mice [4, 6]. Western blot analyses confirmed increased Ser 16 phospho-PLN in PI3K γ KO compared with WT mice, which was preserved in response to pressure overload (Figure 3.3 F).

Analysis of cAMP levels in the LV from PI3K γ KO mice confirmed an elevated basal level of cAMP, which was maintained 1 wk after AB (Figure 3.3 G). Indeed, ventricular cardiomyocytes isolated from banded PI3K γ KO hearts showed increased cell shortening (Figure 3.3 H) and rate of contractility (Figure 3.3 I) compared to WT cardiomyocytes. Whereas ECM-based cell adhesion was intact in the PI3K γ KO cardiomyocytes under baseline conditions (sham), there was a reduction of cardiomyocyte adhesion to collagen IV and laminin in response to pressure overload (Figure 3.3 J). In contrast, cardiomyocyte adhesion from WT mice remained intact following pressure overload (Figure 3.3 J). These results show that isolated cardiomyocytes maintain increased contractility despite the early deterioration in whole heart systolic function providing evidence that a primary defect in banded PI3K γ KO mice is disorganization of ECM and cell adhesion. Furthermore, this was evident without significant increases in apoptosis (Figure 3.1E).

3.3.3 Selective Upregulation of MMP2 and MT1-MMP and MMP Inhibition Mediated Rescue of Pressure Overloaded PI3K γ KO Mice

Adverse remodeling of the ECM by MMPs is a key determinant of the response to biomechanical stress. MMP2 (gelatinase A) and MMP13 (collagenase-3) genes contain promoter regions encoding cAMP-response elements (CRE), which binds CRE binding protein (CREB) [15] and mediates cAMP-dependent increase in the synthesis of MMP2 [16] and MMP13 [17] whereas MT1-MMP expression is also positively regulated by cAMP [18]. We hypothesize that elevated cAMP levels and increased biomechanical stress synergistically increase MMP expression and/or activity in banded PI3K γ KO mice. In accordance, both MMP2 (Figure 3.4 A) and MT1-MMP (Figure 3.4 B) myocardial mRNA expression increased within 1 week of AB and persisted at 3 weeks in PI3K γ KO but not WT mice, whereas MMP13 expression was drastically increased in PI3K γ KO mice at 3 weeks after AB (Figure 3.4 C). In contrast, the non-cAMP-responsive MMP, MMP9 (gelatinase B) (Figure 3.4 D), showed no change in expression in response to AB. To provide a more definitive connection between cAMP and MMP expression/activity, we also examined the mRNA expression of these MMPs in banded PI3K α DN mice, which also develop an early dilated cardiomyopathy [19] and in banded PI3K γ KD mice, which lack PI3K γ kinase activity and signaling without elevation of cAMP levels [5]. Consistent with our hypothesis, myocardial expression levels of MMP2 (Figure 3.4 A), MT1-MMP (Figure 3.4 B), and MMP13 (Figure 3.4 C) were not increased in PI3K α DN and PI3K γ KD mice at 1 or 3 weeks post AB. Next, we examined the changes in MMP expression in cultured adult ventricular cardiomyocyte and cardiofibroblast fractions in response to the activation of cAMP signaling using the

β -adrenergic agonist, isoproterenol. The levels of cAMP in cardiomyocytes increase significantly in response to isoproterenol stimulation preventable by β -adrenergic blockade using propranolol (25 μ M) and adenylate cyclase inhibition using 2,5-dideoxyadenosine (DIDA) (30 μ M; Figure 3.4 E). Western blot analysis showed an early increase in Ser 133 CREB phosphorylation in cultured cardiomyocytes and cardiofibroblasts (Figure 3.4 F) and shown quantitatively (Figure 3.4 G) in response to β -adrenergic receptor stimulation. Consistent with activation of CREB, adult cardiomyocytes stimulated with 100 nM isoproterenol for 24 hours showed increased mRNA expression of cAMP-responsive MMPs, MMP2 (Figure 3.4 H), MT1-MMP (Figure 3.4 I), and MMP13 (Figure 3.4 J). Importantly, the corresponding increases in mRNA expression of MMP2, MT1-MMP, and MMP13 in both cardiomyocytes and cardiofibroblasts were suppressible by both propranolol and DIDA (Figure 3.4 H-J).

We next assessed for biochemical evidence of increased MMP activity in the PI3K γ KO mice in response to pressure overload. Myocardial collagenase activity significantly increased at 1 and 3 weeks after AB in PI3K γ KO mice compared to WT mice, which was suppressible by the MMP inhibitor PD166793 (Figure 3.5 A), whereas gelatin zymography showed activation of MMP2 in banded PI3K γ KO compared with WT mice (Figure 3.5 B). MMP9 protein levels did not change in banded WT hearts, whereas at 3 weeks post AB PI3K γ KO hearts showed an increase (Figure 3.11), despite minimal, in mRNA levels (Figure 3.4 D), suggesting a post-transcriptional mechanism for the increased MMP9 activity. Given the absence of increased MMP expression in banded PI3K γ KD mice, their myocardial collagenase activity was not elevated (Figure 3.5 A). Consistent with gelatin zymography analysis, Western blot analysis (Figure 5B)

revealed increased myocardial levels of active MMP2 (64 kDa) and pro-MMP2 (72 kDa) in banded PI3K γ KO mice at 1 and 3 weeks after AB. Similarly, membrane fractionation and analysis of MT1-MMP levels showed an earlier and greater increase in MT1-MMP levels in banded PI3K γ KO mice compared to WT mice (Figure 3.5 C).

The activity of MMPs is physiologically inhibited by tissue inhibitor of matrix metalloproteinases (TIMPs), TIMP1, TIMP2, TIMP3, and TIMP4 with TIMP3 playing a key role in the myocardial response to biomechanical stress [20, 21]. Interestingly, TIMP1 expression levels increased similarly, whereas the expression of TIMP2 did not change in banded WT and PI3K γ KO mice (Figure 3.5 D). In contrast, expressions of TIMP3 and TIMP4 increased at 3 weeks post AB in PI3K γ KO mice possibly attributable to a negative-feedback response to increased MMP expression and activity (Figure 3.5 D). Our data provide a link between the adverse myocardial remodeling in banded PI3K γ KO mice and the increase in expression and activity of MMPs.

Human recombinant MMP2 rather than MT1-MMP cleaved human recombinant N-cadherin Fc chimera *in vitro* and was inhibited by the MMP inhibitor, PD166793 (Figure 3.10). We hypothesized that MMP inhibition would lead to a marked protection in banded PI3K γ KO mice. Daily treatment of banded PI3K γ KO mice with the broad-spectrum MMP inhibitor, PD166793 (30 mg/kg/day) [20], prevented the dilated cardiomyopathy and fibrosis (Figure 3.5 E). This also reversed the upregulation of disease markers, ANF and BNP, and ventricular dilation at end-diastole and end-systole, resulting in improved systolic performance in banded PI3K γ KO mice (Figure 3.5 F). These results illustrate a key role of cAMP-mediated upregulation of MMP2 and MT1-

MMP expressions in mediating the adverse myocardial remodeling in pressure overloaded PI3K γ KO mice.

3.3.4 Specific Loss of N-Cadherin from Adhesion Complexes While β -Adrenergic Blocker Prevents Upregulation of MMP and Loss of N-Cadherin in Banded PI3K γ KO Mice

In addition to the degradation of the ECM, N-cadherin/ β -catenin cell adhesion complexes are also important cellular targets of activated MMPs [22, 23]. Western blot analysis of the myocardial membrane fraction in banded WT and PI3K α DN mice showed a modest increase in N-cadherin levels (Figure 3.6 A-B), whereas in banded PI3K γ KO mice, there was a 75% loss of N-cadherin levels (Figure 3.6 A-B). In contrast, in the banded PI3K γ KO (and PI3K α DN) mice, levels of β -catenin in the heart were significantly increased compared to banded WT mice (Figure 3.6 C). The relative preservation of N-cadherin levels in the PI3K γ KD hearts is consistent with the critical role of cAMP in mediating the loss of N-cadherin from cell adhesion complexes independent of the PI3K γ lipid kinase activity. The quality of Western blot analysis was confirmed by absence of the membrane specific protein (toll-like receptor 4) in the cytosolic fraction and absence of the cytosol-specific protein (caspase-3) in the membrane fraction (Figure 3.9). Immunofluorescence microscopy confirmed co-localization of N-cadherin and β -catenin in the end-to-end and side-to-side connections between cardiomyocytes in banded WT hearts (Figure 3.6 D). Consistent with our Western blot analysis, there was an almost complete loss of N-cadherin from end-to-end and side-to-side connections in the pressure overloaded PI3K γ KO myocardium (Figure 3.6 E). Consistent with the ability of PD166793 to prevent MMP2-mediated cleavage of

N-cadherin (Figure 3.10) and rescue the DCM in banded PI3K γ KO mice (Figure 3.5), Western blot analysis confirmed that PD166793 prevents the loss of membrane-associated N-cadherin (Figure 3.6 F-G), resulting in more pronounced staining of N-cadherin in myocardial cell adhesion junctions (Figure 3.6 H) in banded PI3K γ KO mice treated with PD166793.

Given the key role of integrin complexes in mediating cell adhesion in the heart [24], we also examined changes in integrin levels in response to pressure overload. Western blot analysis of membrane fractions showed increased protein levels of integrins in WT hearts at 1 and 3 weeks after AB and a delayed increase in the PI3K γ KO hearts, which significantly increased only at 3 weeks after AB (Figure 3.12).

We then tested the hypothesis that elevated cAMP plays a key *in vivo* role in the adverse remodeling in banded PI3K γ KO mice by using the nonspecific β -adrenergic blocker propranolol at a dose that has been previously shown to normalize elevated cAMP levels [5]. Propranolol treatment normalized the mRNA expression of MMP2, MT1-MMP, and MMP13 (Figure 3.7 A-C) with similar changes seen in the expression of disease markers, ANF, β MHC, and BNP (Figure 3.7 D-F). Consistent with a reduction in MMP expression, elevated collagenase activity in the banded PI3K γ KO mice was normalized in response to propranolol (Figure 3.7 C) with relative preservation of N-cadherin levels in the myocardial membrane fraction (Figure 3.7 D). These biochemical and cellular changes imply that cardiac function was rescued in banded PI3K γ KO mice treated with propranolol. Echocardiographic assessment showed a near normalization of the increased LV dilation and improved fractional shortening with invasive hemodynamic parameters showing marked increase in $+dP/dt_{\max}$ and -

dP/dt_{\min} in the banded PI3K γ KO mice treated with propranolol (Figure 3.7 L-M). These results highlight a key reversible defect in the N-cadherin system in the PI3K γ KO mice in response to biomechanical stress caused by cAMP-dependent upregulation of MMP activity.

3.3.5 Beta-Blocker Therapy Prevents the Adverse Remodeling in Response to Chronic Pressure Overload

The beneficial effects of β -blocker therapy in the banded PI3K γ KO mice suggest that β -blockade may have a similar protective role in a long-term (9 weeks) WT AB model as the PI3K γ KO AB model. Aortic banding for nine weeks resulted in marked increase in expression of hypertrophy markers, α -skeletal actin, β MHC and BNP (Figure 3.8 A) in association with LV dilation and reduced systolic function (Figure 3.8 B). Propranolol treatment prevented the adverse remodeling and systolic dysfunction in response to chronic biomechanical stress (Figure 3.8 A-B). Quantitative assessment of cardiac systolic function using echocardiography showed significant improvement in fractional shortening and reduction in LV end-diastolic dimension (Figure 3.8 B). Similarly, invasive hemodynamic measurements revealed a restoration of an elevated LV end-diastolic pressure and normalization of $+dP/dt_{\max}$ and $-dP/dt_{\min}$ in response to chronic β -blocker therapy (Figure 3.8 C). These functional changes correlated with a reduction of MMP2 and MT1-MMP expression without a differential effect on MMP13 expression (Figure 3.8 D), suggesting that propranolol exerts cardioprotection by reducing MMP expression in fibroblasts. Western blot analysis showed a higher level of membrane-associated N-cadherin with an equivalent increase in β -catenin levels resulting in preservation of the myocardial N-cadherin/ β -catenin ratio (Figure 3.8 E) in

response to chronic β -blocker therapy. Our results highlight a novel mechanism of chronic β -blocker therapy in preventing the adverse myocardial remodeling in pressure overload–induced heart failure.

3.4 Discussion:

The response to biomechanical stress is a fundamental response in heart disease and plays a key adaptive role in response to a pressure overloaded state characteristic of hypertension and aortic valvular stenosis. Mechanotransduction plays a fundamental role in cardiac structure and function and involves a concerted interaction between ECM, intracellular cytoskeletal proteins, and cell adhesion complexes [1, 25]. Advanced heart failure in response to myocardial injury including biomechanical stress leads to impaired Ca^{2+} cycling and strategies aimed at enhancing Ca^{2+} cycling are currently being developed as therapies for heart failure [26, 27]. Loss of PI3K γ increases basal cAMP levels, enhances SERCA2 function and Ca^{2+} cycling, and increases basal myocardial contractility [4-6]. In the heart, loss of PI3K γ prevents phosphorylation of Akt in response to GPCR agonists [5, 28, 29], and PI3K γ KO mice are resistant to the pathological effects of β -adrenergic stimulation [28]. Despite these biochemical changes, PI3K γ KO mice show enhanced susceptibility to biomechanical stress [5], and we provide direct evidence that the primary defect is compromised cell-adhesion/ECM linked to elevated cAMP levels. In contrast, in PI3K γ KD mice, which have normal myocardial cAMP levels [5], there is no upregulation of MMPs with preservation of N-cadherin levels, consistent with the ability of these mice to maintain normal systolic function in response to early biomechanical stress [5].

The PI3K/PTEN system may also have a more direct role in the cardiac response to biomechanical stress [1, 2]. Whereas PI3K and lipid phosphatases can modulate cytoskeletal interactions, stretch can in turn activate Akt and GSK-3 β activity [2]. Indeed, loss of PTEN prevents pressure overload-induced heart failure [9], whereas loss

of Akt1/PKB α leads to a rapid onset of ventricular dilation and systolic dysfunction in response to pressure overload [30]. Consistent with a critical role of PI3K γ in pathological GPCR signaling [5, 28, 29], phosphorylation of ERK 1/2 is impaired in response to early biomechanical stress in the PI3K γ KO mice [5]. However, this differential response is lost at three weeks post AB, which is likely driven by severe disruption of the ECM and/or cell adhesion leading to GPCR-independent activation of ERK 1/2 in the PI3K γ KO mice. Despite equivalent basal phospho-Akt levels in WT and PI3K γ KO hearts, basal phospho-GSK-3 β was increased in the PI3K γ KO mice, likely mediated by PKA [31] given the chronic elevation of myocardial cAMP levels in these mice. The diverse downstream effects of elevated basal phospho-GSK-3 β [32] may have contributed to the adverse remodeling in the PI3K γ KO mice. Elevated cAMP levels in response to increased biomechanical stress leads to increased MMP expression, active (cleaved) MMP2 and collagenase activity, resulting in adverse myocardial remodeling. As MMP2 and MT1-MMP expressions are increased at 1 week post AB and they are primarily expressed by fibroblasts, the early decompensation and heart failure is likely due to fibroblast mediated degradation of intercalated discs. In addition to degrading various components of the ECM, increased MMP activity can also adversely modify cell-cell adhesion complexes. Cardiomyocyte cell adhesion complexes provide an important mechanism by which cardiomyocytes (and cardiofibroblasts) are anchored to the ECM while allowing force transmission to the intracellular cytoskeletal network [25, 26]. In particular, we have shown that increased MMP expression and activity can regulate N-cadherin function through proteolytic degradation [22, 23, 33]. Cardiac-specific loss of N-cadherin in the heart leads to DCM

attributable to loss of the integrity of cell adhesion junctions [34]. Because of their homophilic binding and adhesive specificities, N-cadherin/ β -catenin complex is required for cadherin-mediated cell adhesion and linkage to the actin cytoskeleton. The delayed increase in membrane β 1D and α 7B integrins in the banded PI3K γ KO hearts may have also contributed to the early onset of DCM [24]. In addition, MT1-MMP is a potent collagenase that also targets other ECM components, such as fibronectin [35], laminin [35], and integrin [36] while activating MMP13 (collagenase-3), thereby amplifying the collagen-degradation process [37, 38].

Our results are consistent with the conclusion that elevated cAMP (and its downstream effects) is the primary driver of the adverse remodeling in banded PI3K γ KO mice rather than loss of PI3K γ kinase activity and signaling. Our findings may help to explain the cardiomyopathy in experimental models with enhanced β -adrenergic signaling (and cAMP levels) [39, 40] and lack of a protection against pressure overload and tumor necrosis factor–induced heart failure despite enhanced Ca²⁺ cycling in the PLN knockout mice [41, 42]; specifically, we demonstrated that PI3K γ KO mice, which also have enhanced Ca²⁺ cycling like the PLN knockout, rapidly develop heart failure in response to stress. Although Ca²⁺ transients in cardiomyocytes were normalized in tumor necrosis factor–induced cardiomyopathy in a PLN-null background, global systolic function remained depressed and unchanged [42]. We propose that enhancing cell–cell adhesion and cell–ECM interaction promotes the salutary effects of enhanced intracellular Ca²⁺ cycling on whole heart function and booster the therapeutic potential of normalizing intracellular Ca²⁺ cycling in patients with heart failure. Increased sympathetic nervous system activity and β -adrenergic

receptor signaling are key aspects of the pathophysiology of heart failure [43] and in catecholamine-mediated cardiomyopathies [44, 45]. β -adrenergic receptor blockers improve clinical outcomes in patients with chronic heart failure [43]. In contrast, agents that increase myocardial cAMP such as PDE3 inhibitors are associated with adverse outcomes and increased mortality in patients with heart failure [46]. Our data support a novel role of β -adrenergic blocker in reducing MMP expression and/or activity and preservation of cell adhesion, thereby curtailing adverse myocardial remodeling.

Figure 3.1

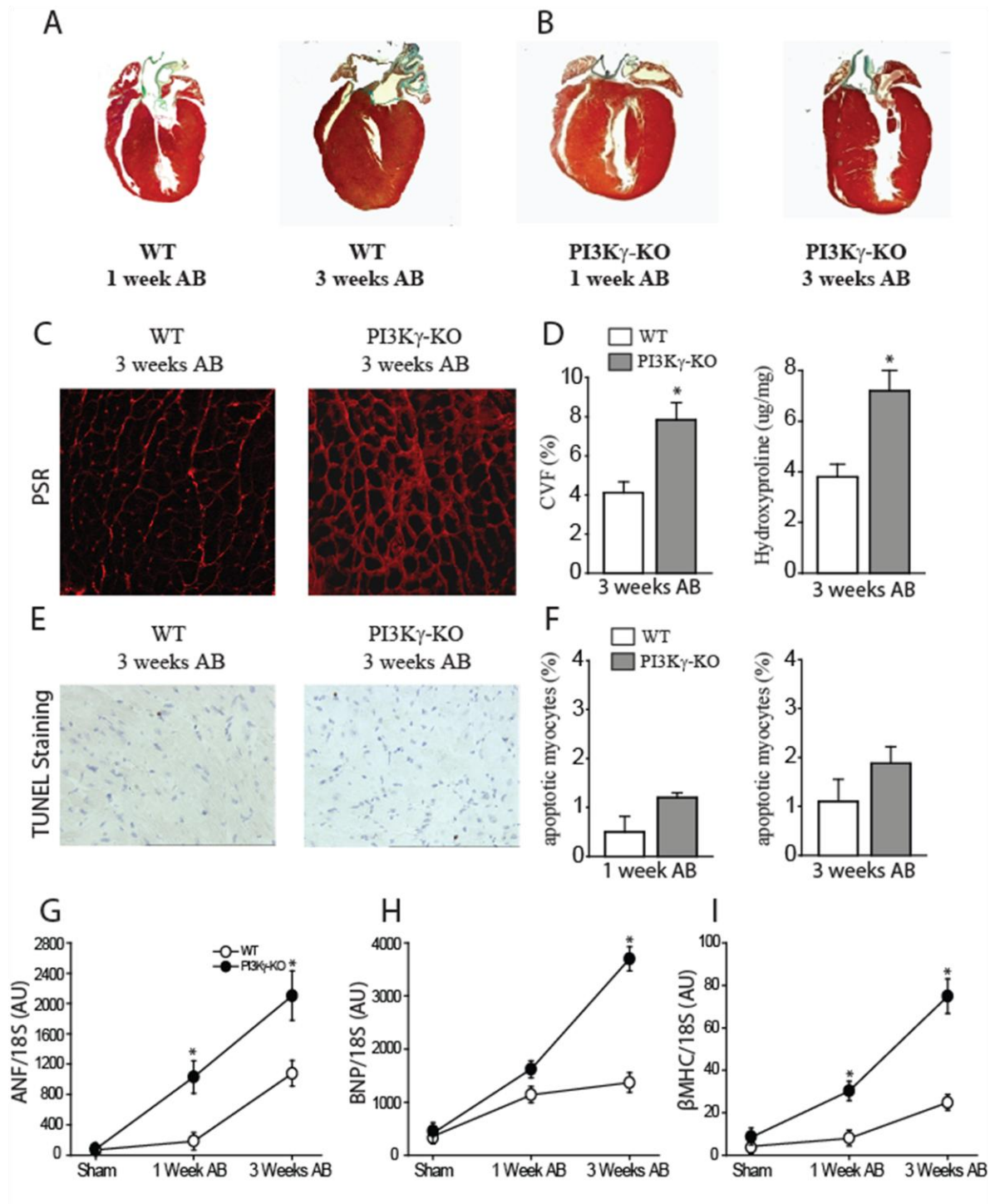


Figure 3.1 Development of early-onset dilated cardiomyopathy in response to biomechanical stress in PI3K γ KO mice. Four-chamber trichrome stained heart sections showed concentric hypertrophy in WT mice (A) with ventricular dilation and eccentric remodeling in PI3K γ KO mice (B) in response to aortic banding. Increased interstitial fibrosis shown using PSR staining (left panel) (C) and quantification of the collagen volume fraction (CVF) (D) without differences in apoptosis between WT and PI3K γ KO was shown using TUNEL staining (left panel) (E) and quantified as percent of apoptotic nuclei (right panel) (F). (n = 5 per group). RT-PCR demonstrated that expression of hypertrophy disease markers showed early and markedly increased expression of ANF (G), BNP (H) and β MHC (I) in banded PI3K γ KO mice compared to WT mice. (n = 5 for sham groups and n = 7 for AB groups; *p < 0.05 compared with the WT group; graphs are plotted as mean \pm SEM)

Figure 3.2

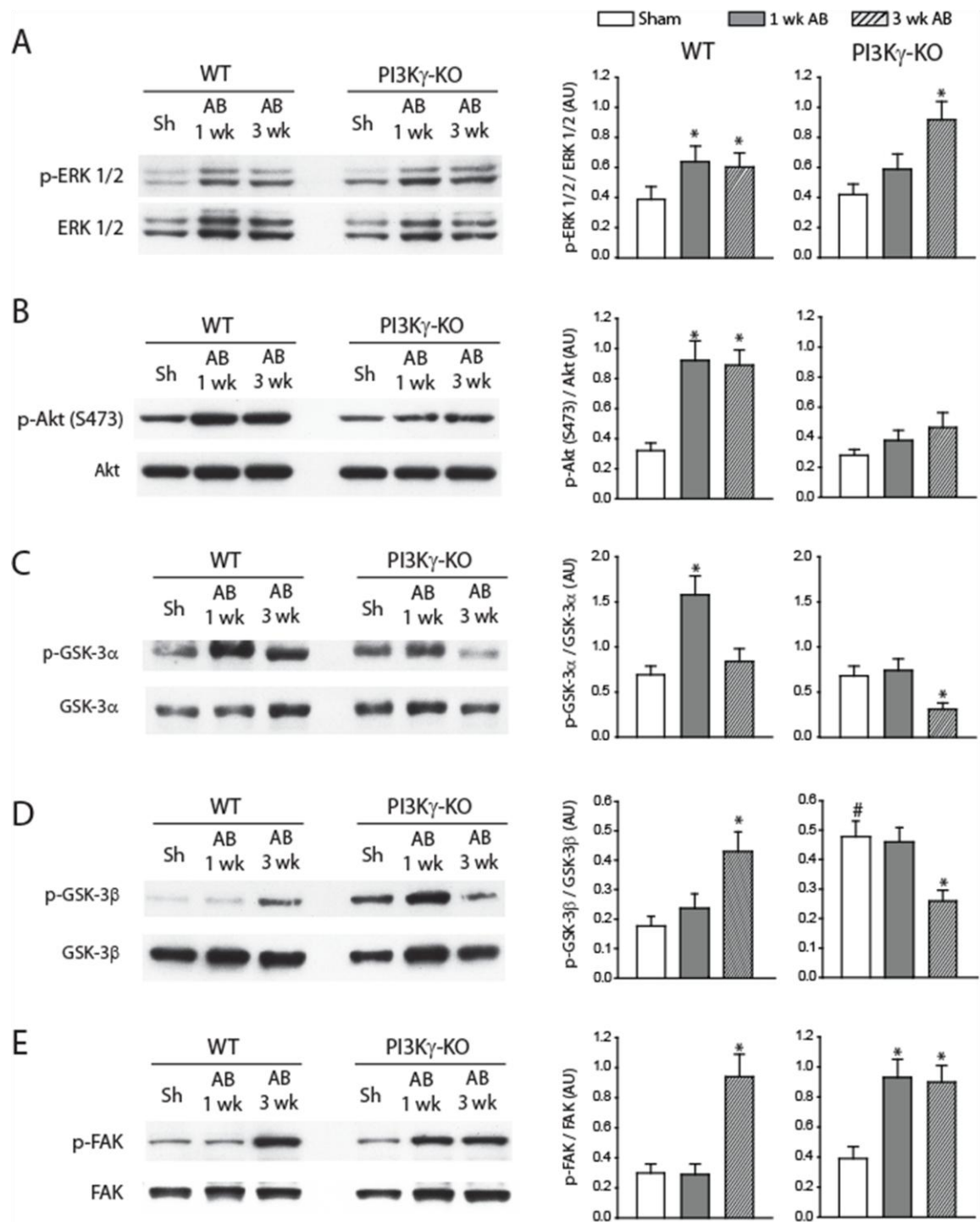


Figure 3.2 Alterations in signaling are observed in response to biomechanical stress in PI3K γ KO mice. Western blot analysis (left panel) and quantification (right panel) showing increased phosphorylation of the MAPK, extracellular regulated kinase 1/2 (ERK 1/2) (A) with loss of Ser 473 Akt phosphorylation (B) in the banded PI3K γ KO mice. Western blot analysis (left panel) and quantification (right panel) showing preservation of glycogen synthase kinase 3 α (GSK-3 α) (C) and GSK-3 β (D) phosphorylation in banded WT mice but with a loss of phosphorylation in the banded PI3K γ KO mice while earlier phosphorylation of focal adhesion kinase (FAK) occurs in the banded PI3K γ KO mice (E). Open column = sham; full column = 1 wk post aortic-banding; hatched column = 3 wks post aortic-banding. (n = 5 per group; *p < 0.05 compared with the corresponding sham group; #p < 0.05 compared with WT sham; graphs are plotted as mean \pm SEM)

Figure 3.3

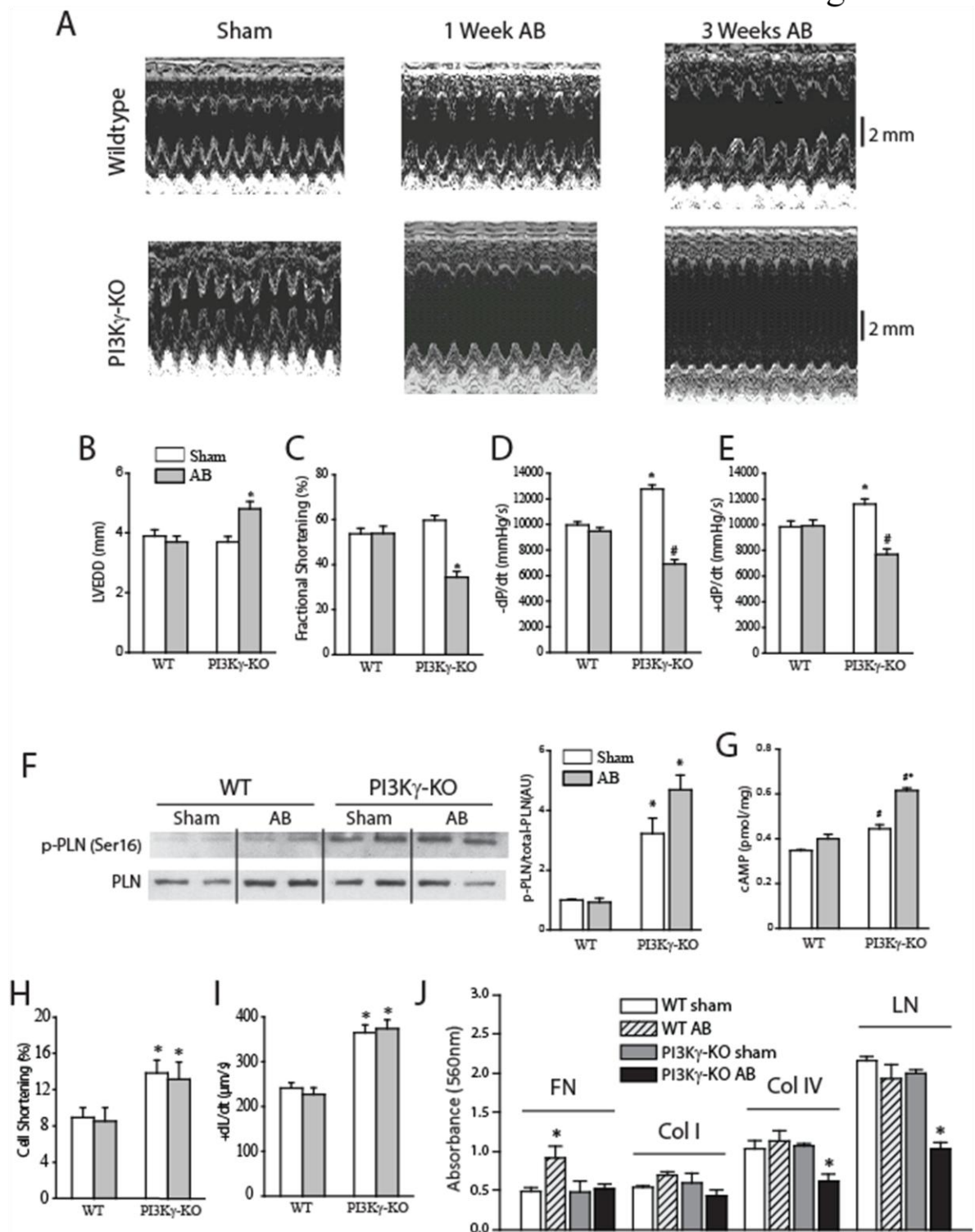


Figure 3.3 Uncoupling between *in vivo* myocardial contractility and isolated single cardiomyocyte contractility in PI3K γ KO mice in response to early biomechanical stress. M-mode echocardiograms (A) and *in vivo* quantitative assessment of heart function showing baseline hyper-contraction followed by rapid and marked ventricular dilation (B) and reduction in systolic function based on fractional shortening (C) and invasive hemodynamic measurement of $-dP/dt_{min}$ (D) and $+dP/dt_{max}$ (E) at 1 week post aortic banding. LVEDD = LV End-Diastolic Dimension. (n = 8 for sham groups; n = 12 for AB groups.) Western blot analysis (left) and quantification (right) using myocardial membrane fractions showing increased phosphorylated PLN (F) at baseline and in banded PI3K γ KO mice with myocardial cAMP levels (G) showing elevated levels in PI3K γ KO at baseline and at 1 week post AB (H). (n = 5 for all groups.) Single cardiomyocyte contractility measurements showing basal hyper-contraction based on percent (H) and rate of change ($+dL/dt$) (I) of cell shortening in PI3K γ KO mice, which persists in response to 1 week of pressure overload. (n = 8 for sham groups; n = 12 for AB groups.) (J) ECM-based cell adhesion of isolated adult LV cardiomyocytes following 1 week of aortic banding showing an increase in fibronectin adhesion in WT cardiomyocytes and a marked decrease in adhesion to collagen IV and laminin in PI3K γ KO cardiomyocytes. FN = fibronectin; Col I = collagen I; Col IV = collagen IV and LN = laminin; (n = 4 for WT and PI3K γ KO; *p < 0.05 compared with corresponding WT group; graphs are plotted as mean \pm SEM)

Figure 3.4

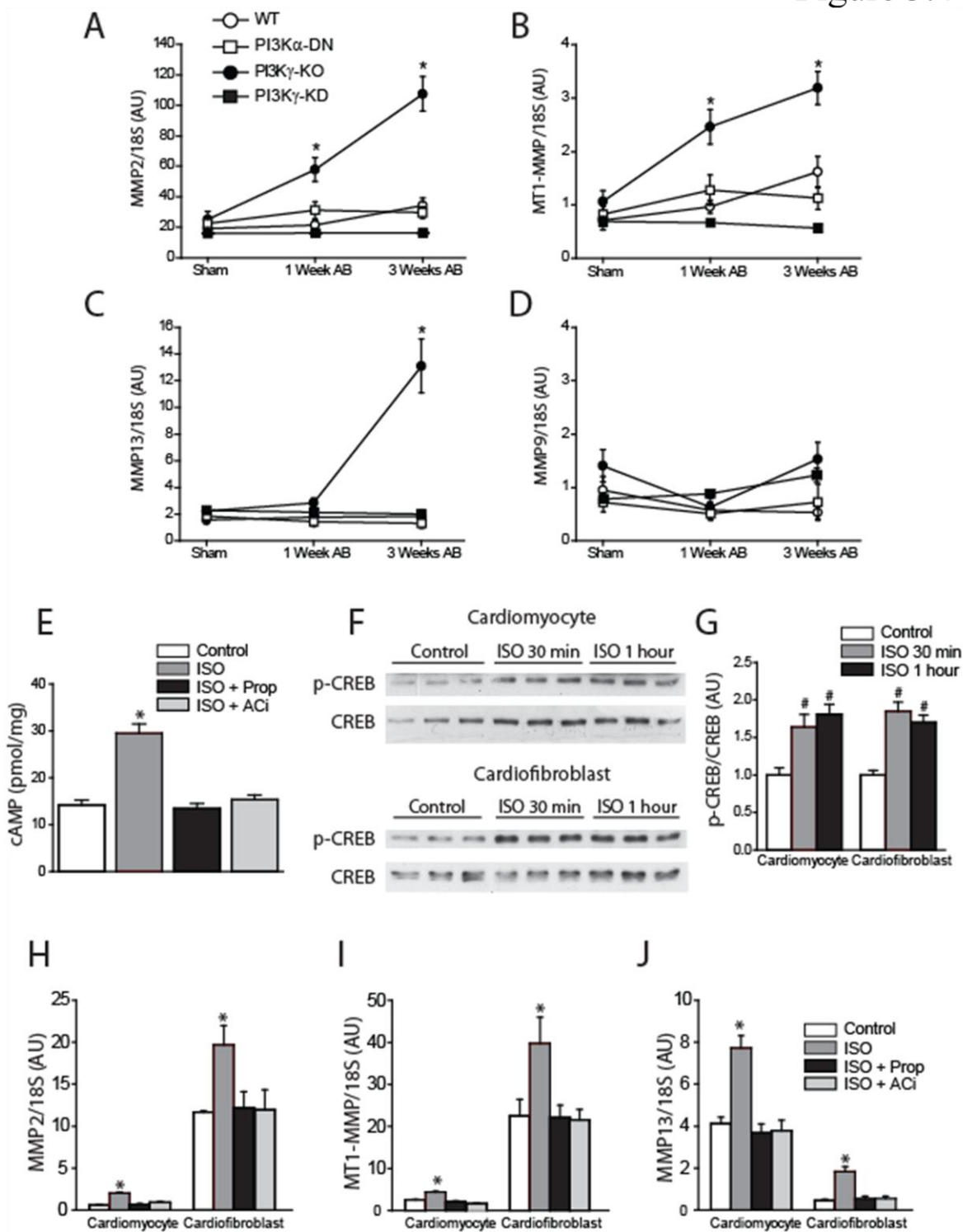


Figure 3.4 Upregulation of myocardial matrix metalloproteinase expression in banded PI3K γ KO mice with beta-adrenergic receptor stimulation of MMPs expression in isolated adult cardiomyocytes and cardiofibroblasts. Expression profiling of MMPs revealed upregulation of myocardial MMP2 (A), MT1-MMP (B) and MMP13 (C) expression without a change in MMP9 (D) expression in the banded PI3K γ KO mice compared to banded WT, PI3K α DN and PI3K γ -KD mice. (*p < 0.05 compared with all other groups) (E) Normalization of elevated cAMP levels in cultured adult cardiomyocytes in response to beta adrenergic receptor stimulation using isoproterenol (100 nM) by beta adrenergic receptor blockade using propranolol (25 μ M) and adenylate cyclase inhibition using 2',5'-dideoxyadenosine (DIDA; 30 μ M); (n = 5 for each group.) Western blot analyses showed early phosphorylation of cAMP-response element (CRE) binding protein (CREB) in response to beta adrenergic receptor stimulation using isoproterenol (100 nM) in cultured adult cardiomyocytes and cardiofibroblasts (F) and shown quantitatively (G). (n = 5 for each group. #p < 0.05 compared with the control group. Analysis of mRNA expression showed that long-term beta adrenergic receptor stimulation using isoproterenol (100 nM) leads to an upregulation of mRNA expression of MMP2 (H), MT1-MMP (I) and MMP13 (J) in cultured adult cardiomyocytes and cardiofibroblasts which was prevented by the beta adrenergic receptor blocker, propranolol (25 μ M) and adenylate cyclase inhibition using 2',5'-dideoxyadenosine (DIDA; 30 μ M). (n = 5 for each group; *p < 0.05 compared with all other groups; graphs are plotted as mean \pm SEM)

Figure 3.5

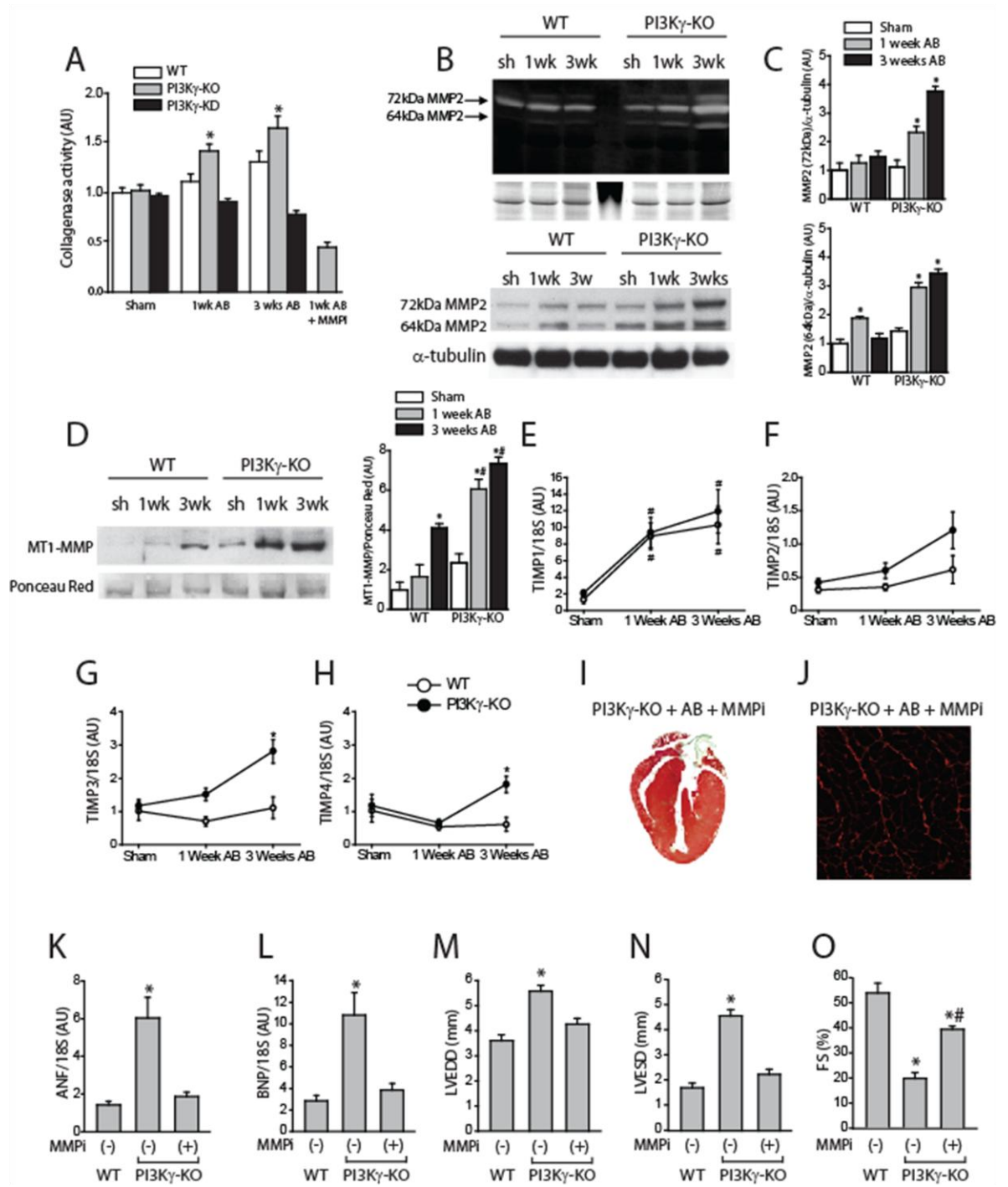


Figure 3.5 Increased collagenase activity and MMP2 activation with prevention of the dilated cardiomyopathy by broad spectrum MMP inhibition was observed in banded PI3K γ KO mice. Increased myocardial collagenase activity in banded PI3K γ KO mice (A) was suppressed by the MMP inhibitor, PD166793 (30 mg/kg/day), while gelatin zymography showed increased pro-MMP2 and active MMP2 levels in the banded PI3K γ KO mice (B). Western blot analysis and quantification showed increased expression of active MMP2 (64 kDa) and pro-MMP2 (72 kDa) (C) and membrane-fractionated MT1-MMP (D) in banded PI3K γ KO tissue lysate at 1 week and 3 weeks post AB. (n = 4 for sham group and AB groups; *p < 0.05 compared with the sham group.) Expression profile of tissue inhibitors of matrix metalloproteinases (TIMPs) showed equivalent upregulation in TIMP1 (E) without alteration in TIMP2 (F), while TIMP3 (G) and TIMP4 (H) levels increased in banded PI3K γ KO mice. (n = 6 for sham group and n = 8 for AB groups; #p < 0.05 compared with the sham group; *p < 0.05 compared with the WT group.) Treatment with the broad spectrum MMP inhibitor, PD166793 (30 mg/kg/day), prevented the dilated cardiomyopathy (I) and disruption of the extracellular collagen network shown as picrosirius red staining (J) while reversing the upregulation of disease markers, ANF (K) and BNP (L), ventricular dilation at end-diastole (M) and end-systole (N), and reduction in systolic performance (O) in banded PI3K γ KO mice. (n = 8 for each group; *p < 0.05 compared with all other groups; graphs are plotted as mean \pm SEM)

Figure 3.6

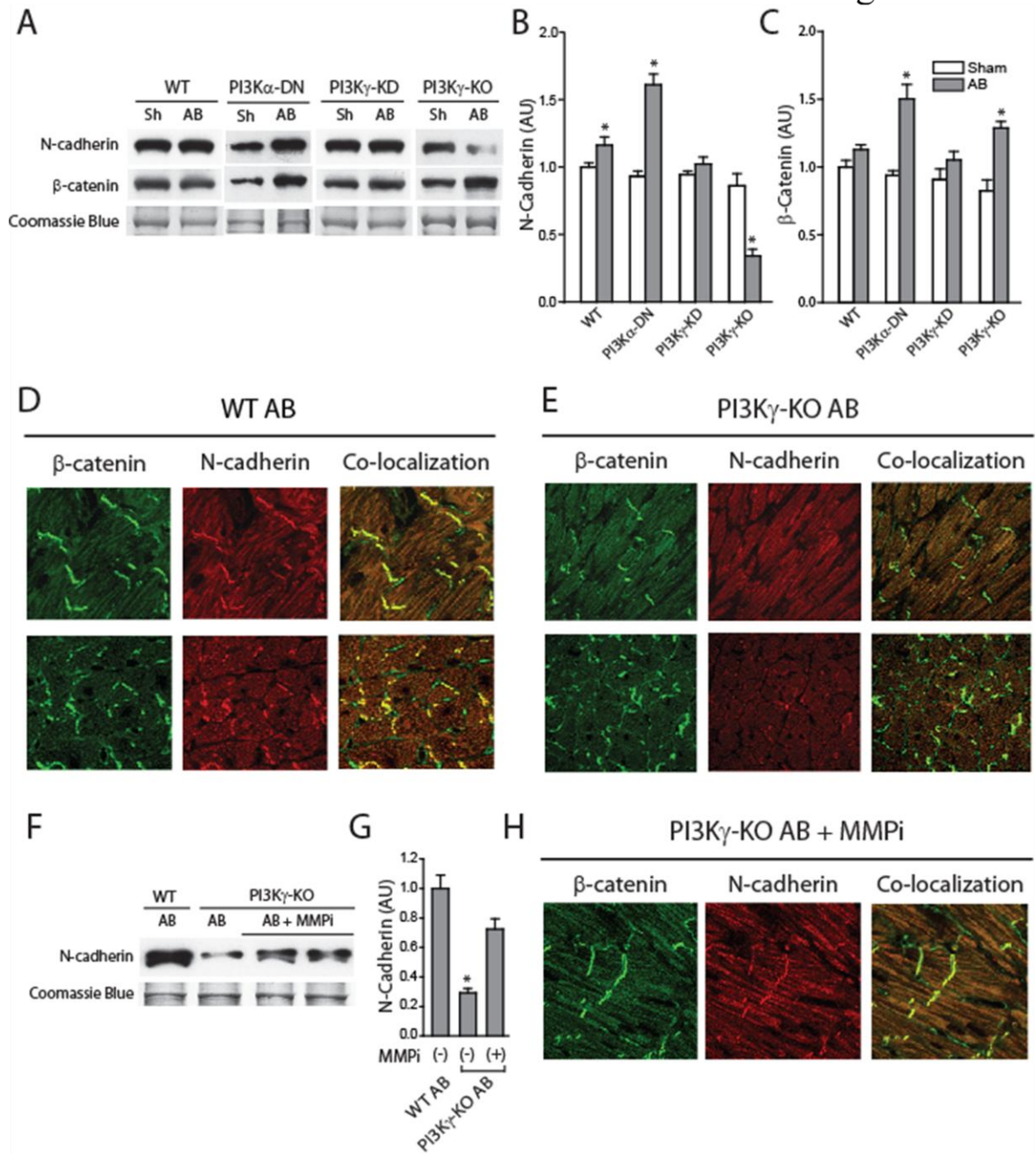


Figure 3.6 Selective loss of N-cadherin from myocardial membrane fraction and the cell-adhesion complexes in the myocardium from banded PI3K γ KO mice.

Western blot analysis of the myocardial membrane fraction (A) and quantification (B) showing a selective loss of N-cadherin levels without alterations in β -catenin levels (C) in banded PI3K γ KO mice while the level of N-cadherin increases in banded WT and PI3K α DN mice (*p < 0.05 compared with the corresponding sham group). Immunofluorescence microscopy of the myocardial β -catenin and N-cadherin proteins showing end-to-end connections (top panel) and side-to-side connections (bottom panel) in banded WT (D) and PI3K γ KO (E) mice with a distinct loss of N-cadherin in the banded PI3K γ KO mice. Western blot analysis of the myocardial membrane fraction (F) and quantification (G), and immunofluorescence microscopy of myocardial β -catenin and N-cadherin proteins (H) showing that MMP inhibitor preserved N-cadherin in banded PI3K γ KO mice (n = 5 for all groups; *p < 0.05 compared with all other groups; graphs are plotted as mean \pm SEM).

Figure 3.7

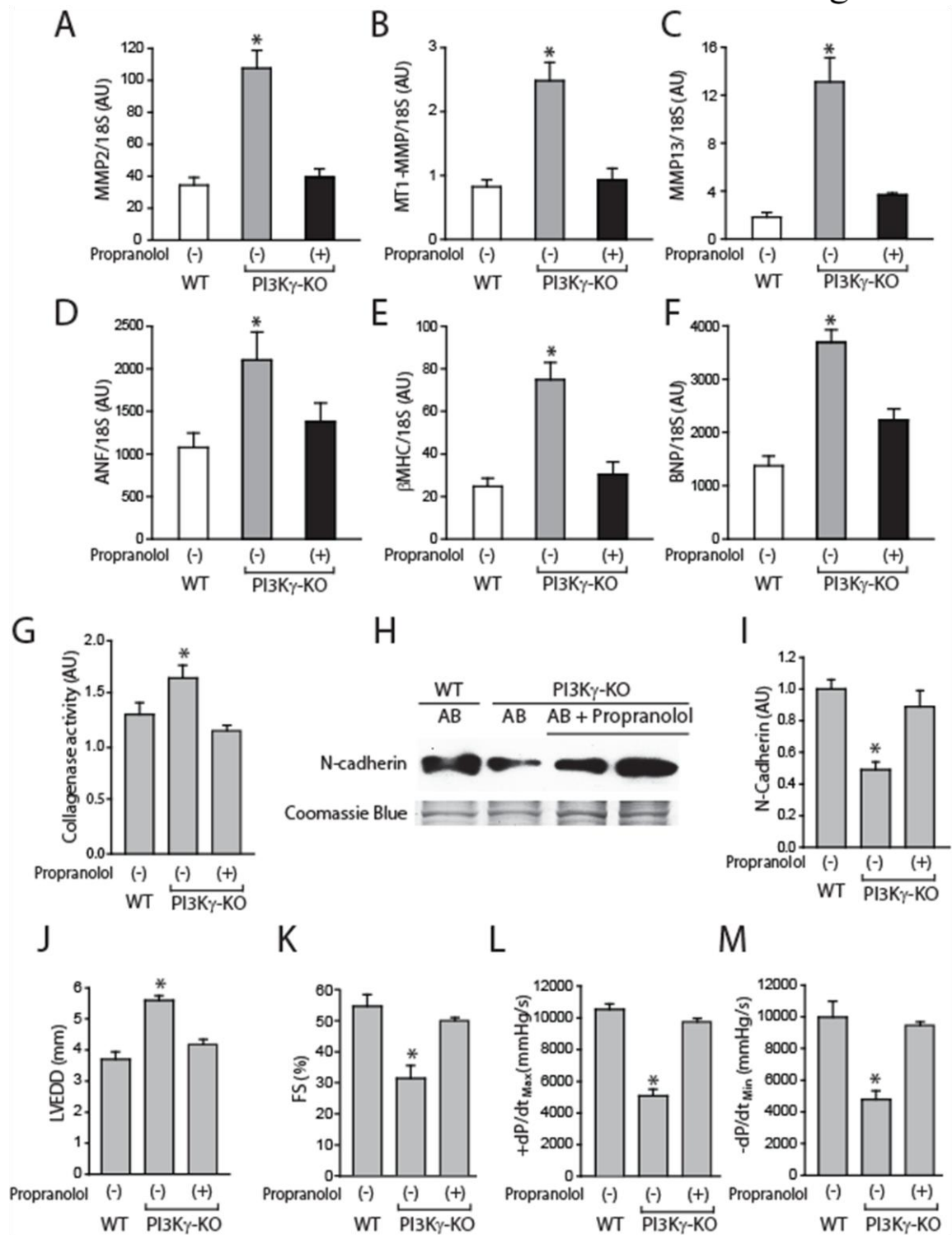


Figure 3.7 The non-specific beta receptor blocker, propranolol (15 mg/kg/day), prevents the molecular, biochemical and functional deterioration in response to biomechanical stress in PI3K γ KO mice. Treatment with propranolol prevents the increased expression of MMPs including MMP2 (A), MT1-MMP (B) and MMP13 (C) and disease markers such as ANF (D), β MHC (E) and BNP (F) in banded PI3K γ KO mice (*p < 0.05 compared with all other groups). Propranolol suppressed of the increased myocardial collagenase activity (G). Western blot analysis (H) and quantitative analysis (I) showed restoration of the membrane N-cadherin levels in banded PI3K γ KO mice (*p < 0.05 compared with all other groups). Reduction in LV dilation and preservation of systolic function in banded PI3K γ KO mice based on echocardiographic parameters, LV end diastolic dimension (J) and fractional shortening (K), and hemodynamic assessment, +dP/dt_{max} (L) and -dP/dt_{min} (M) in response to treatment with propranolol. (n=8 for all groups; *p < 0.05 compared with all other groups; graphs are plotted as mean \pm SEM).

Figure 3.8

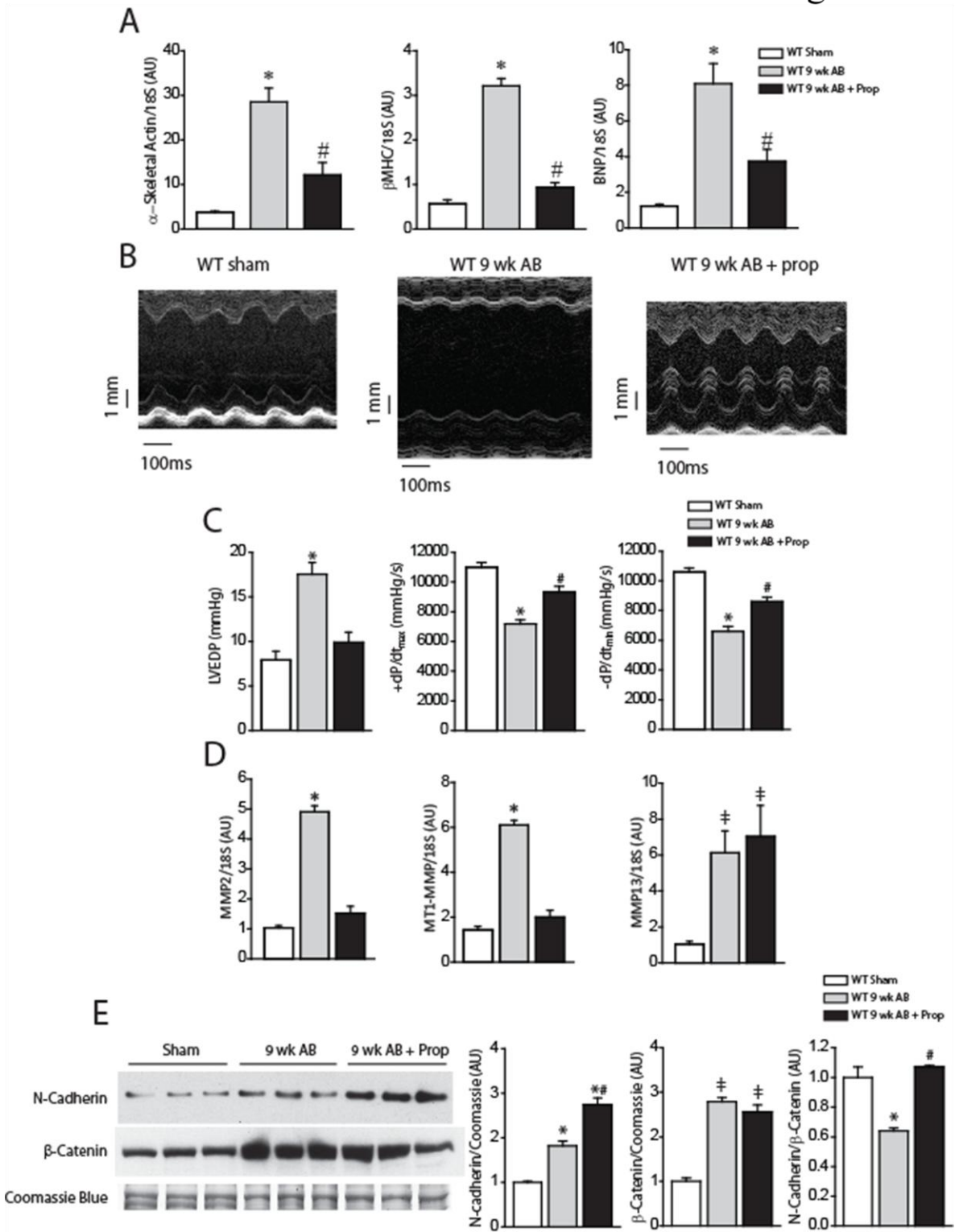


Figure 3.8 Chronic beta-blocker prevents pressure-overload induced adverse remodeling and preserves systolic function in WT mice. Expression profile of hypertrophy disease markers show increased expression of α -skeletal actin, β MHC and BNP in banded WT mice at 9 week, which was not observed with propranolol treatment (A) (n = 5 per group). Echocardiographic assessment of systolic function with M-mode echocardiograms, fractional shortening and LV end-diastolic dimension showing a marked reduction in LV dilation and increase in fractional shortening in response to propranolol (B). FS = fractional shortening; LVEDD = LV end-diastolic dimension. Invasive hemodynamic assessment show marked reduction in LVEDP and prevention of the deterioration in myocardial contractility based on $+dP/dt_{max}$ and $-dP/dt_{min}$ in response to chronic beta blocker therapy (C) (n = 6 for WT sham and n = 8 for WT AB groups). Expression of MMPs show a marked increase in MMP2, MT1-MMP and MMP-13 levels and a normalization of MMP and MT1-MMP in response to chronic beta blocker therapy (D) (n = 5 per group). Western blot analysis revealed a greater increase in myocardial N-cadherin levels with equivalent increase in β -catenin levels leading to a relative preservation of the N-cadherin/ β -catenin ratio in response to chronic beta blocker therapy (E). (n = 5 per group; *p < 0.05 compared with all other groups; #p < 0.05 compared with WT + AB 9 wk; †p < 0.05 compared with WT sham group; graphs are plotted as mean \pm SEM).

Figure 3.9

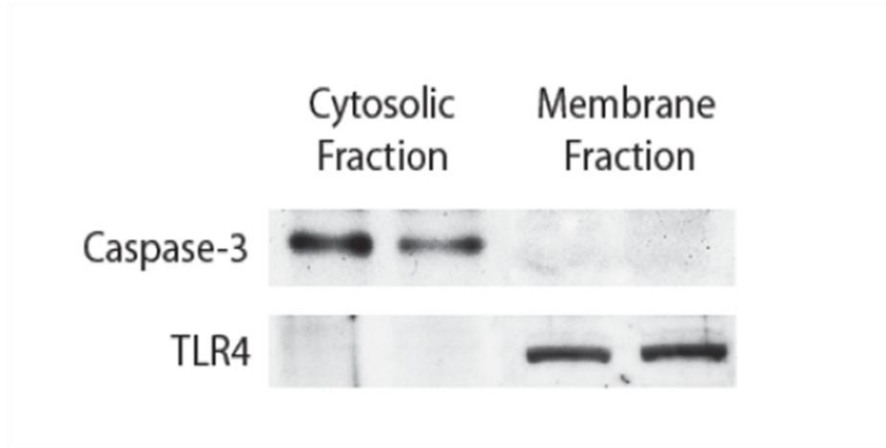


Figure 3.9 Purity of membrane fractionation. The purity of protein fractionation was confirmed using western blot for caspase-3 (a cytosolic protein) and toll-like receptor 4 (a membrane bound protein). Caspase-3 protein was only found in the cytosolic fraction and not the membrane fraction whereas toll-like receptor 4 protein was present in the membrane fraction but not in the cytosolic fraction.

Figure 3.10

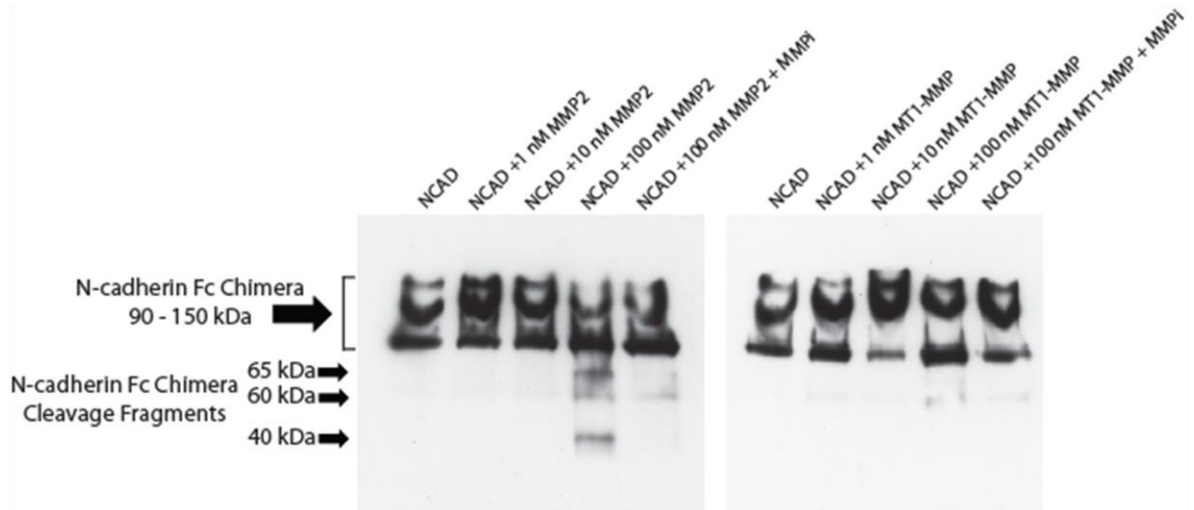


Figure 3.10 MMP2, but not MT1-MMP, cleaves human recombinant N-cadherin Fc Chimera. N-cadherin Fc Chimera (NCAD, 100 ng) was incubated with 3 different concentrations of human recombinant MMP2 or MT1-MMP and the MMP inhibitor (MMPi, PD166793 (10 μ M)) for 4 hours at 37°C. Western blot detected bands at 65, 60, and 40 kDa representing fragments of the N-cadherin Fc Chimera.

Figure 3.11

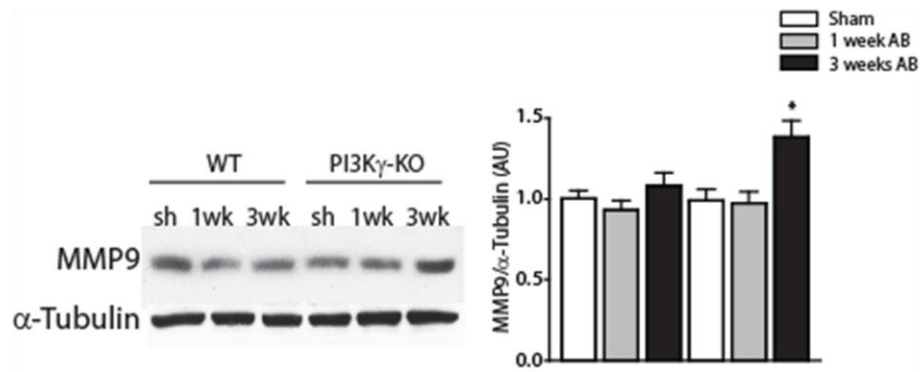


Figure 3.11 MMP9 protein levels in WT and PI3K γ KO hearts. MMP9 protein levels increase in the PI3K γ KO hearts 3 weeks after AB but not at 1 week after AB whereas WT hearts showed no changes in MMP9 protein levels. (n = 4 for each group; *p < 0.05 compared with WT sham; graphs are plotted as mean \pm SEM)

Figure 3.12

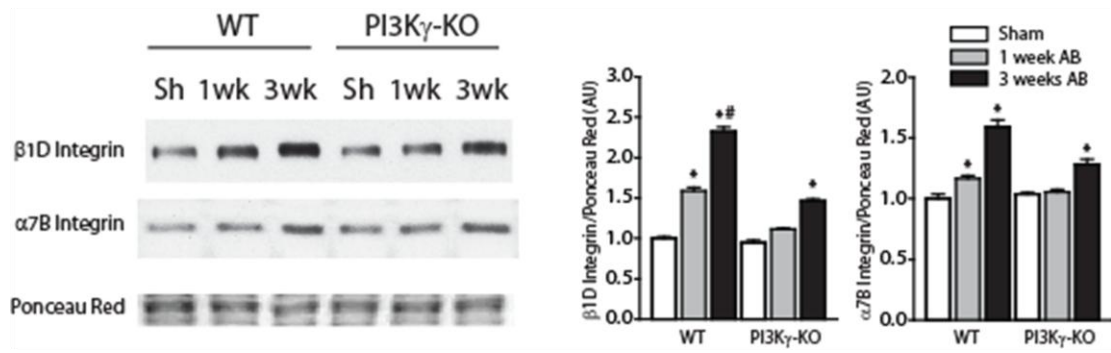


Figure 3.12 β 1D and α 7B integrin protein levels in WT and PI3K γ KO hearts. β 1D and α 7B integrin protein levels increased in WT hearts 1 and 3 weeks after AB. Both integrins increased in the PI3K γ KO at 3 weeks after AB. (n = 4 for each group; *p < 0.05 compared with sham. #p < 0.05 compared with 1 week AB; graphs are plotted as mean \pm SEM)

Table 3.10

<i>TIMP 1</i>	Forward Primer: Reverse Primer: Probe:	5'-CATGGAAAGCCTCTGTGGATATG-3' 5'-AAGCTGCAGGCACTGATGTG-3' 5'-FAM-CTCATCACGGGCCGCCTAAGGAAC-TAMRA-3'
<i>TIMP 2</i>	Forward Primer: Reverse Primer: Probe:	5'-CCAGAAGAAGAGCCTGAACCA-3' 5'-GTCCATCCAGAGGCACTCATC-3' 5'-FAM-ACTCGCTGTCCCATGATCCCTTGC-TAMRA-3'
<i>TIMP3</i>	Forward Primer (294): Reverse Primer (427): Probe (376): Reverse primer2 (423):	5'- CCG CAG CGG ACC ACA AC-3' 5'- CCG GAT CAC GAT GTC GGA G-3' 5'- FAM-CTA CCA TGA CTC CCT GGC TT-TAMRA-3' 5'- GGA TCA CGA TGT CGG AGT TGC-3'
<i>TIMP 4</i>	Forward Primer: Reverse Primer: Probe:	5'-TGCAGAGGGAGAGCCTGAA-3' 5'-GGTACATGGCACTGCATAGCA-3' 5'-FAM-CCACCAGAAGTGTGGCTGCCAAATC-TAMRA-3'
<i>MMP-9</i>	Forward Primer: Reverse Primer: Probe:	5'-CGAACTTCGACACTGACAAGAAGT -3' 5'- GCACGCTGGAATGATCTAAGC-3' 5'-TCTGTCCAGACCAAGGGTACAGCCTGTTC -3'
<i>MMP-2</i>	Forward Primer: Reverse Primer:	5'-AACTACGATGATGACCGGAAGTG -3' 5'-TGGCATGGCCGAAGTCA -3'
<i>MMP-13</i>	Forward Primer: Reverse Primer: Probe:	5'-GGGCTCTGAATGGTTATGACATTC -3' 5'-AGCGCTCAGTCTCTTCACCTCTT -3' 5'-AAGGTTATCCCAGAAAAATATCTGACCTGGGATTC -3'
<i>MMP-14</i> <i>MT1-MMP</i>	Forward Primer: Reverse Primer: Probe:	5'- AGGAGACAGAGGTGATCATCATTG -3' 5'- GTCCCATGGCGTCTGAAGA -3' 5'-FAM- CCTGCCGGTACTACTGCTGCTCCTG-TAMRA -3'
<i>ANF</i>	Forward Primer: Reverse Primer: Probe:	5'-GGA GGA GAA GAT GCC GGT AGA-3' 5'-GCT TCC TCA GTC TGC TCA CTC A-3' 5'-TGA GGT CAT GCC CCC GCA GG-3'
<i>BNP</i>	Forward Primer: Reverse Primer: Probe:	5'-CTG CTG GAG CTG ATA AGA GA-3' 5'-TGC CCA AAG CAG CTT GAG AT-3' 5'-FAM-CTC AAG GCA GCA CCC TCC GGG-TAMRA-3'
<i>β-MHC</i>	Forward Primer: Reverse Primer: Probe:	5'-GTGCCAAGGGCCTGAATGAG-3' 5'-GCAAAGGCTCCAGGTCTGA-3' 5'-ATCTTGTGCTACCCAGCTCTAA-3'

Table 3.10 RT-PCR primers and probes. The sequence to all RT-PCR primers and probes used in TaqMan analysis.

Table 3.11

	WT+ SHAM	PI3K γ KO+ SHAM	WT+AB 1wk post-AB	PI3K γ KO+AB 1 wk post-AB	WT+AB 3 wks post-AB	PI3K γ KO+AB 3 wks post-AB
N	8	8	10	10	10	10
HR (bpm)	554±14	549±12	561±14	548±15	539±16	568±17
PWT (mm)	0.68±0.06	0.67±0.05	0.74±0.09	0.73±0.11	0.86±0.12 [#]	0.84±0.14 [#]
LVEDD (mm)	3.81±0.11	3.79±0.12	3.78±0.14	4.41±0.2*	3.65±0.17	5.53±0.23*
LVESD (mm)	1.71±0.09	1.52±0.1*	1.69±0.16	2.63±0.18*	1.69±0.21	4.58±0.19*
FS (%)	55.1±1.8	59.9±1.9*	55.3±2.5	40.3±2.8*	53.8±3.1	17.2±4.2*
VCFc (circ/s)	10.8±0.32	12.94±0.4*	10.9±0.38	7.48±0.31*	10.9±0.45	4.52±0.361*
+dP/dt _{max} (mmHg/s)	10131±301	12893±276*	9935±378	7138±330*	9984±423	5012±359*
-dP/dt _{min} (mmHg/s)	9945±252	12671±311	9471±283	6902±363*	6145±369	4875±408*
LVEDP (mmHg)	5.23±1.96	6.56±2.7	7.71±2.8	12.8±2.2*	9.23±4.1	19.3±3.9*
LVW/BW (mg/g)	3.75±0.13	3.71±0.17	4.17±0.21	4.22±0.24	5.63±0.22 [#]	5.69±0.29 [#]
HW/BW (mg/g)	4.9±0.15	4.88±0.15	5.21±0.23	5.28±0.27	6.27±0.41 [#]	6.31±0.38 [#]

AB, aortic banded; SHAM, sham-operated; HR, heart rate; PWT, posterior left ventricular wall thickness; LVEDD, left ventricular end diastolic diameter; LVESD, left ventricular end systolic diameter; FS, fractional shortening; VCFc, velocity of circumferential shortening corrected for heart rate; +dP/dt_{max}, maximum first derivative of the change in left ventricular pressure; and -dP/dt_{min}, minimum first derivative of the change in left ventricular pressure; LVEDP, left ventricular end-diastolic pressure. *p<0.05 compared with the corresponding WT+AB group; [#]p<0.05 compared with corresponding SHAM group.

3.5 References:

1. Sugden, P.H., *Ras, Akt, and mechanotransduction in the cardiac myocyte*. *Circ Res*, 2003. **93**(12): p. 1179-92.
2. Baba, H.A., J. Stypmann, F. Grabellus, P. Kirchhof, A. Sokoll, M. Schafers, A. Takeda, M.J. Wilhelm, H.H. Scheld, N. Takeda, G. Breithardt, and B. Levkau, *Dynamic regulation of MEK/Erks and Akt/GSK-3beta in human end-stage heart failure after left ventricular mechanical support: myocardial mechanotransduction-sensitivity as a possible molecular mechanism*. *Cardiovasc Res*, 2003. **59**(2): p. 390-9.
3. Knoll, R., M. Hoshijima, H.M. Hoffman, V. Person, I. Lorenzen-Schmidt, M.L. Bang, T. Hayashi, N. Shiga, H. Yasukawa, W. Schaper, W. McKenna, M. Yokoyama, N.J. Schork, J.H. Omens, A.D. McCulloch, A. Kimura, C.C. Gregorio, W. Poller, J. Schaper, H.P. Schultheiss, and K.R. Chien, *The cardiac mechanical stretch sensor machinery involves a Z disc complex that is defective in a subset of human dilated cardiomyopathy*. *Cell*, 2002. **111**(7): p. 943-55.
4. Crackower, M.A., G.Y. Oudit, I. Kozieradzki, R. Sarao, H. Sun, T. Sasaki, E. Hirsch, A. Suzuki, T. Shioi, J. Irie-Sasaki, R. Sah, H.Y. Cheng, V.O. Rybin, G. Lembo, L. Fratta, A.J. Oliveira-dos-Santos, J.L. Benovic, C.R. Kahn, S. Izumo, S.F. Steinberg, M.P. Wymann, P.H. Backx, and J.M. Penninger, *Regulation of myocardial contractility and cell size by distinct PI3K-PTEN signaling pathways*. *Cell*, 2002. **110**(6): p. 737-49.
5. Patrucco, E., A. Notte, L. Barberis, G. Selvetella, A. Maffei, M. Brancaccio, S. Marengo, G. Russo, O. Azzolino, S.D. Rybalkin, L. Silengo, F. Altruda, R.

- Wetzker, M.P. Wymann, G. Lembo, and E. Hirsch, *PI3Kgamma modulates the cardiac response to chronic pressure overload by distinct kinase-dependent and -independent effects*. Cell, 2004. **118**(3): p. 375-87.
6. Kerfant, B.G., D. Gidrewicz, H. Sun, G.Y. Oudit, J.M. Penninger, and P.H. Backx, *Cardiac sarcoplasmic reticulum calcium release and load are enhanced by subcellular cAMP elevations in PI3Kgamma-deficient mice*. Circ Res, 2005. **96**(10): p. 1079-86.
 7. Zhai, P., S. Gao, E. Holle, X. Yu, A. Yatani, T. Wagner, and J. Sadoshima, *Glycogen synthase kinase-3alpha reduces cardiac growth and pressure overload-induced cardiac hypertrophy by inhibition of extracellular signal-regulated kinases*. J Biol Chem, 2007. **282**(45): p. 33181-91.
 8. Matsuda, T., P. Zhai, Y. Maejima, C. Hong, S. Gao, B. Tian, K. Goto, H. Takagi, M. Tamamori-Adachi, S. Kitajima, and J. Sadoshima, *Distinct roles of GSK-3alpha and GSK-3beta phosphorylation in the heart under pressure overload*. Proc Natl Acad Sci U S A, 2008. **105**(52): p. 20900-5.
 9. Oudit, G.Y., Z. Kassiri, J. Zhou, Q.C. Liu, P.P. Liu, P.H. Backx, F. Dawood, M.A. Crackower, J.W. Scholey, and J.M. Penninger, *Loss of PTEN attenuates the development of pathological hypertrophy and heart failure in response to biomechanical stress*. Cardiovasc Res, 2008. **78**(3): p. 505-14.
 10. Guo, D., Z. Kassiri, R. Basu, F.L. Chow, V. Kandalam, F. Damilano, W. Liang, S. Izumo, E. Hirsch, J.M. Penninger, P.H. Backx, and G.Y. Oudit, *Loss of PI3Kgamma enhances cAMP-dependent MMP remodeling of the myocardial N-*

- cadherin adhesion complexes and extracellular matrix in response to early biomechanical stress.* Circ Res. **107**(10): p. 1275-89.
11. Shioi, T., P.M. Kang, P.S. Douglas, J. Hampe, C.M. Yballe, J. Lawitts, L.C. Cantley, and S. Izumo, *The conserved phosphoinositide 3-kinase pathway determines heart size in mice.* EMBO J, 2000. **19**(11): p. 2537-48.
 12. Sussman, M.A., A. McCulloch, and T.K. Borg, *Dance band on the Titanic: biomechanical signaling in cardiac hypertrophy.* Circ Res, 2002. **91**(10): p. 888-98.
 13. Heineke, J. and J.D. Molkentin, *Regulation of cardiac hypertrophy by intracellular signalling pathways.* Nat Rev Mol Cell Biol, 2006. **7**(8): p. 589-600.
 14. Romer, L.H., K.G. Birukov, and J.G. Garcia, *Focal adhesions: paradigm for a signaling nexus.* Circ Res, 2006. **98**(5): p. 606-16.
 15. Sands, W.A. and T.M. Palmer, *Regulating gene transcription in response to cyclic AMP elevation.* Cell Signal, 2008. **20**(3): p. 460-6.
 16. Melnikova, V.O., A.A. Mourad-Zeidan, D.C. Lev, and M. Bar-Eli, *Platelet-activating factor mediates MMP-2 expression and activation via phosphorylation of cAMP-response element-binding protein and contributes to melanoma metastasis.* J Biol Chem, 2006. **281**(5): p. 2911-22.
 17. Quinn, C.O., R.A. Rajakumar, and O.A. Agapova, *Parathyroid hormone induces rat interstitial collagenase mRNA through Ets-1 facilitated by cyclic AMP response element-binding protein and Ca(2+)/calmodulin-dependent protein kinase II in osteoblastic cells.* J Mol Endocrinol, 2000. **25**(1): p. 73-84.

18. Shankavaram, U.T., W.C. Lai, S. Netzel-Arnett, P.R. Mangan, J.A. Ardans, N. Caterina, W.G. Stetler-Stevenson, H. Birkedal-Hansen, and L.M. Wahl, *Monocyte membrane type 1-matrix metalloproteinase. Prostaglandin-dependent regulation and role in metalloproteinase-2 activation.* J Biol Chem, 2001. **276**(22): p. 19027-32.
19. McMullen, J.R., T. Shioi, L. Zhang, O. Tarnavski, M.C. Sherwood, P.M. Kang, and S. Izumo, *Phosphoinositide 3-kinase(p110alpha) plays a critical role for the induction of physiological, but not pathological, cardiac hypertrophy.* Proc Natl Acad Sci U S A, 2003. **100**(21): p. 12355-60.
20. Kassiri, Z., G.Y. Oudit, O. Sanchez, F. Dawood, F.F. Mohammed, R.K. Nuttall, D.R. Edwards, P.P. Liu, P.H. Backx, and R. Khokha, *Combination of tumor necrosis factor-alpha ablation and matrix metalloproteinase inhibition prevents heart failure after pressure overload in tissue inhibitor of metalloproteinase-3 knock-out mice.* Circ Res, 2005. **97**(4): p. 380-90.
21. Kassiri, Z. and R. Khokha, *Myocardial extra-cellular matrix and its regulation by metalloproteinases and their inhibitors.* Thromb Haemost, 2005. **93**(2): p. 212-9.
22. Ho, A.T., E.B. Voura, P.D. Soloway, K.L. Watson, and R. Khokha, *MMP inhibitors augment fibroblast adhesion through stabilization of focal adhesion contacts and up-regulation of cadherin function.* J Biol Chem, 2001. **276**(43): p. 40215-24.

23. Covington, M.D., R.C. Burghardt, and A.R. Parrish, *Ischemia-induced cleavage of cadherins in NRK cells requires MT1-MMP (MMP-14)*. Am J Physiol Renal Physiol, 2006. **290**(1): p. F43-51.
24. Babbitt, C.J., S.Y. Shai, A.E. Harpf, C.G. Pham, and R.S. Ross, *Modulation of integrins and integrin signaling molecules in the pressure-loaded murine ventricle*. Histochem Cell Biol, 2002. **118**(6): p. 431-9.
25. Jamora, C. and E. Fuchs, *Intercellular adhesion, signalling and the cytoskeleton*. Nat Cell Biol, 2002. **4**(4): p. E101-8.
26. Chien, K.R., J. Ross, Jr., and M. Hoshijima, *Calcium and heart failure: the cycle game*. Nat Med, 2003. **9**(5): p. 508-9.
27. Jaski, B.E., M.L. Jessup, D.M. Mancini, T.P. Cappola, D.F. Pauly, B. Greenberg, K. Borow, H. Dittrich, K.M. Zsebo, and R.J. Hajjar, *Calcium upregulation by percutaneous administration of gene therapy in cardiac disease (CUPID Trial), a first-in-human phase 1/2 clinical trial*. J Card Fail, 2009. **15**(3): p. 171-81.
28. Oudit, G.Y., M.A. Crackower, U. Eriksson, R. Sarao, I. Kozieradzki, T. Sasaki, J. Irie-Sasaki, D. Gidrewicz, V.O. Rybin, T. Wada, S.F. Steinberg, P.H. Backx, and J.M. Penninger, *Phosphoinositide 3-kinase gamma-deficient mice are protected from isoproterenol-induced heart failure*. Circulation, 2003. **108**(17): p. 2147-52.
29. Naga Prasad, S.V., G. Esposito, L. Mao, W.J. Koch, and H.A. Rockman, *Gbetagamma-dependent phosphoinositide 3-kinase activation in hearts with in vivo pressure overload hypertrophy*. J Biol Chem, 2000. **275**(7): p. 4693-8.

30. DeBosch, B., I. Treskov, T.S. Lupu, C. Weinheimer, A. Kovacs, M. Courtois, and A.J. Muslin, *Akt1 is required for physiological cardiac growth*. *Circulation*, 2006. **113**(17): p. 2097-104.
31. Tanji, C., H. Yamamoto, N. Yorioka, N. Kohno, K. Kikuchi, and A. Kikuchi, *A-kinase anchoring protein AKAP220 binds to glycogen synthase kinase-3beta (GSK-3beta) and mediates protein kinase A-dependent inhibition of GSK-3beta*. *J Biol Chem*, 2002. **277**(40): p. 36955-61.
32. Hardt, S.E. and J. Sadoshima, *Glycogen synthase kinase-3beta: a novel regulator of cardiac hypertrophy and development*. *Circ Res*, 2002. **90**(10): p. 1055-63.
33. Pon, Y.L., N. Auersperg, and A.S. Wong, *Gonadotropins regulate N-cadherin-mediated human ovarian surface epithelial cell survival at both post-translational and transcriptional levels through a cyclic AMP/protein kinase A pathway*. *J Biol Chem*, 2005. **280**(15): p. 15438-48.
34. Kostetskii, I., J. Li, Y. Xiong, R. Zhou, V.A. Ferrari, V.V. Patel, J.D. Molkentin, and G.L. Radice, *Induced deletion of the N-cadherin gene in the heart leads to dissolution of the intercalated disc structure*. *Circ Res*, 2005. **96**(3): p. 346-54.
35. Ohtake, Y., H. Tojo, and M. Seiki, *Multifunctional roles of MT1-MMP in myofiber formation and morphostatic maintenance of skeletal muscle*. *J Cell Sci*, 2006. **119**(Pt 18): p. 3822-32.
36. Deryugina, E.I., B.I. Ratnikov, T.I. Postnova, D.V. Rozanov, and A.Y. Strongin, *Processing of integrin alpha(v) subunit by membrane type 1 matrix metalloproteinase stimulates migration of breast carcinoma cells on vitronectin*

- and enhances tyrosine phosphorylation of focal adhesion kinase. J Biol Chem, 2002. 277(12): p. 9749-56.*
37. Kandalam, V., R. Basu, T. Abraham, X. Wang, P.D. Soloway, D.M. Jaworski, G.Y. Oudit, and Z. Kassiri, *TIMP2 deficiency accelerates adverse post-myocardial infarction remodeling because of enhanced MT1-MMP activity despite lack of MMP2 activation. Circ Res. 106(4): p. 796-808.*
38. Itoh, Y. and M. Seiki, *MT1-MMP: a potent modifier of pericellular microenvironment. J Cell Physiol, 2006. 206(1): p. 1-8.*
39. Engelhardt, S., L. Hein, F. Wiesmann, and M.J. Lohse, *Progressive hypertrophy and heart failure in beta1-adrenergic receptor transgenic mice. Proc Natl Acad Sci U S A, 1999. 96(12): p. 7059-64.*
40. Liggett, S.B., N.M. Tepe, J.N. Lorenz, A.M. Canning, T.D. Jantz, S. Mitarai, A. Yatani, and G.W. Dorn, 2nd, *Early and delayed consequences of beta(2)-adrenergic receptor overexpression in mouse hearts: critical role for expression level. Circulation, 2000. 101(14): p. 1707-14.*
41. Kiriazis, H., Y. Sato, V.J. Kadambi, A.G. Schmidt, M.J. Gerst, B.D. Hoit, and E.G. Kranias, *Hypertrophy and functional alterations in hyperdynamic phospholamban-knockout mouse hearts under chronic aortic stenosis. Cardiovasc Res, 2002. 53(2): p. 372-81.*
42. Janczewski, A.M., M. Zahid, B.H. Lemster, C.S. Frye, G. Gibson, Y. Higuchi, E.G. Kranias, A.M. Feldman, and C.F. McTiernan, *Phospholamban gene ablation improves calcium transients but not cardiac function in a heart failure model. Cardiovasc Res, 2004. 62(3): p. 468-80.*

43. Triposkiadis, F., G. Karayannis, G. Giamouzis, J. Skoularigis, G. Louridas, and J. Butler, *The sympathetic nervous system in heart failure physiology, pathophysiology, and clinical implications*. J Am Coll Cardiol, 2009. **54**(19): p. 1747-62.
44. Kloner, R.A., S. Hale, K. Alker, and S. Rezkalla, *The effects of acute and chronic cocaine use on the heart*. Circulation, 1992. **85**(2): p. 407-19.
45. Gianni, M., F. Dentali, A.M. Grandi, G. Sumner, R. Hiralal, and E. Lonn, *Apical ballooning syndrome or takotsubo cardiomyopathy: a systematic review*. Eur Heart J, 2006. **27**(13): p. 1523-9.
46. Nony, P., J.P. Boissel, M. Lievre, A. Leizorovicz, M.C. Haugh, S. Fareh, and B. de Breyne, *Evaluation of the effect of phosphodiesterase inhibitors on mortality in chronic heart failure patients. A meta-analysis*. Eur J Clin Pharmacol, 1994. **46**(3): p. 191-6.

Chapter 4

PI3K γ KO/ α DN DOUBLE MUTANT HEARTS

Taqman RT-PCR was performed by Dr. Xiuhua Wang. Invasive hemodynamic analysis was conducted by Fung Lan Chow. Echocardiography was performed by CVRC core and analyzed by Ratnadeep Basu.

4.1 Introduction:

In the heart, the two primary PI3K isoforms are PI3K α and PI3K γ . Although PI3K β is also expressed, its role in the myocardium remains unknown. Previous studies showed that PI3K α and PI3K γ have unique roles in the heart and they are activated by RTKs and GPCRs, respectively [1]. Each also regulates a different aspect of cardiac physiology. Specifically, PI3K α has been linked to the regulation of cardiomyocyte size and PI3K γ to the regulation of cardiomyocyte contractility via interacting with PDE and regulating intracellular cAMP levels [2, 3].

As mentioned in chapter 1, PTEN dephosphorylates PIP₃ into PIP₂ as the primary indirect negative regulator of PI3K activity. PTEN loss of function mutant mice were used to demonstrate the isoform specific functions of PI3K α and PI3K γ as the PTEN mutant mouse has a hypertrophic heart that reduced ventricular contractility, the exact opposite of PI3K α DN and PI3K γ KO mutant strains combined [3, 4].

Though the isoform specific roles of PI3K α and PI3K γ in the heart have each been independently described, no study has investigated whether their roles overlap or whether they compensate for each other in the absence of each other. Crackower and Oudit et al. (2002) suggested that PI3K α and PI3K γ 's respective regulation of morphology and function may be independent of each other [3]. This study will generate a PI3K γ / α loss of function double mutant (PI3K γ KO/ α DN) to investigate the redundant and non-redundant regulatory roles of PI3K α and PI3K γ on cardiomyocyte size and contractility.

4.2 Methods:

4.2.1 Heart tissue collection

Left ventricles from WT, PI3K α DN, PI3K γ KO, and PI3K γ KO/ α DN were collected at 3 and 6 months of age and snap frozen in liquid nitrogen.

4.2.2 Western blot analysis

Protein extracts were analyzed via western blot using the following antibodies: Akt (phospho-(Ser 473) Akt, phospho-(Thr 308) Akt, and total-Akt), GSK-3 β (phospho-(Ser 9) GSK-3 β and total-GSK-3 β), GSK-3 α (phospho-(Ser 21) GSK-3 α and total-GSK-3 α), ERK 1/2 (phospho-(Thr 202/Tyr 204) ERK 1/2 and total ERK 1/2), p110 β (total p110 β and total α -tubulin), and CK2 (CK2 α and CK2 α').

4.2.3 Immunoprecipitation assay

LV myocardial tissue were homogenized with RIPA buffer (Table 2.9) and centrifuged to remove debris. 1:1000 of PTEN antibody (Cell Signaling) was added and the samples were incubated for 1 hour at 4°C under gentle agitation. 20 mg of Protein A Sepharose (Sigma Aldrich) was then added and the samples were incubated at 4°C overnight under rotary agitation. After the incubation period, samples were centrifuged and the supernatant was removed. Pellets were washed with ice-cold PBS five times and then resuspended in RIPA buffer. SDS loading buffer (Table 2.18) was then added and the samples were incubated in 95°C for 5 min prior to freezing and storing in a -80°C freezer.

4.2.4 Phosphatase Activity Assay

Phosphatase Activity Assay was conducted using the Echelon Malachite Green Phosphatase Activity Assay. Phosphate standards are first prepared using the provided 0.1 mM phosphate standard solution and 25 μL of each standard is pipetted into each well in a 96-well plate pre-coated with PIP_3 . 25 μL of enzyme reactions and blanks were then pipetted into the appropriate wells. This is followed by adding 100 μL of Malachite Green Solution and incubation for 15 min at room temperature. Absorbance was recorded at 660 nm and converted into free phosphate concentration using standards (Table 4.1).

Table 4.1 Phosphate standard for phosphatase activity assay

Standard	Phosphate concentration (pmol/25 μL)
1	2,000
2	1,800
3	1,600
4	1,400
5	1,200
6	1,000
7	800
8	600
9	400
10	200
11 (Blank)	0

4.3 Results:

4.3.1 Left Ventricular mass in WT, PI3K γ KO, PI3K α DN, and PI3K γ KO/PI3K α DN (DM) mice at 3 and 6 months.

Baseline LV mass was measured at 3 and 6 months of age and standardized to tibial length (Figure 4.1). Similar to previous studies, there is no difference in LV mass between WT and PI3K γ KO, while PI3K α DN LV mass is significantly lower than the WT at both time points [2, 3]. At 3 months, DM LV mass was significantly lower than WT and PI3K γ KO and is comparable to PI3K α DN. However, the LV mass of DM mice at 6 months is significantly higher than PI3K α DN mice and comparable to both WT and PI3K γ KO.

mRNA expression profiling of LV extracts demonstrated that DM hearts have significantly higher baseline levels of atrial natriuretic factor (ANF) (Figure 4.2 A), b-type natriuretic peptide (BNP) (Figure 4.2 B), and beta myosin heavy chain (β MHC) (Figure 4.2 C), all indicators of hypertrophy and stress [5, 6], as compared to WT, PI3K γ KO, and PI3K α DN.

4.3.2 Augmented activation of Akt and MAPK signaling cascades and expression of hypertrophy markers in DM LV as compared to WT, PI3K γ KO, and PI3K α DN.

Despite DM hearts having a smaller LV size at 3 months compared to WT, Akt and MAPK signaling cascades are hyper-activated compared to of WT, PI3K γ KO, and PI3K α DN (Figure 4.3). Specifically, westerns blot analysis of DM LV protein extract demonstrated markedly increased phosphorylation of Akt at both Ser 473 and Thr 308 residues (Figure 4.3 A). In accordance, both GSK-3 β and GSK-3 α , which are well-

known downstream substrates of the PI3K/Akt signaling cascade [7, 8], are both hyper-phosphorylated in the DM hearts as compared to the other three genotypes (Figure 4.3 B), which stimulates downstream pro-hypertrophic and pro-survival pathways. When comparing to WT and PI3K γ KO, PI3K α DN exhibited lower baseline phosphorylation of both Akt and GSK-3 β (Figure 4.3 C). This is expected as PI3K α regulates Akt activity under unstressed conditions [2, 5, 9]. Interestingly, baseline phospho-GSK-3 α was not decreased in PI3K α DN hearts, suggesting that basal GSK-3 α activity may be regulated by another enzyme (Figure 4.3 D).

ERK is a well investigated MAPK that closely participates in both physiological and pathological growth of the heart. As previously reported, basal phosphorylation of ERK 1/2 is similar among WT, PI3K γ KO, and PI3K α DN hearts [2, 10]. On the other hand, DM hearts exhibited hyper-phosphorylation of ERK 1/2 (Figure 4.3 B). Whether this is a PI3K dependent process is unknown as ERK can be phosphorylated independently of PI3K [11, 12]. Furthermore, protein levels of PI3K β were not different between the four genotypes, as measured by western blot analysis of p110 β , the catalytic unit of PI3K β (Figure 4.4 A).

4.3.3 Increased phosphorylation and deactivation of PTEN in DM mice as compared to WT, PI3K γ KO, and PI3K α DN.

Consistent with the hyper-activation of PI3K/Akt and MAPK signaling cascades, phosphorylation of PTEN at the Ser 385 residue, and hence deactivation, is augmented in DM LV as compared to WT, PI3K γ KO, and PI3K α DN (Figure 4.4 B). Similarly,

purified PTEN from the LV protein extracts from the four genotypes indicate that DM hearts have reduced PIP₃ phosphatase activity (Figure 4.4 C).

To test the hypothesis that PTEN activity is reduced due to deactivation of PTEN instead of due to reduced expression of PTEN, immunoblot analysis of total PTEN levels from LV extracts were standardized to α -tubulin levels. This confirmed that the observed difference in PTEN activity is primarily due to increased phosphorylation of PTEN in DM as compared to WT, PI3K γ KO, and PI3K α DN (Figure 4.4 A).

4.3.4 Increased CK2 α ' protein level in DM mice as compared to WT, PI3K γ KO, and PI3K α DN.

Western blot analysis of DM LV protein extracts were used to measure Casein Kinase 2 α ' (CK2 α ') and CK2 α protein levels. CK2 α ' and CK2 α are the catalytic subunits of CK2, an endogenous PTEN kinase [13]. Baseline level of the CK2 α ' catalytic subunit in DM was higher compared to WT, PI3K γ KO, and PI3K α DN (Figure 4.5). On the other hand, this increase is not observed in the CK2 α catalytic subunit, suggesting partial alteration in CK2 activity in DM hearts (Figure 4.5).

4.3.5 Partial enhancement of systolic function in DM hearts as compared to WT and PI3K α DN hearts.

B-mode and M-mode echocardiography demonstrated significant increases in the contractile function of DM hearts compared to WT and PI3K α DN as measured by enhanced velocity of circumferential fractional shortening (VcFc) (Figure 4.6 C). Not surprisingly, VcFc values were similar between DM hearts and PI3K γ KO hearts as

previous studies have indicated that lack of the physical presence of p110 γ increases basal contractility via enhancing calcium cycling (Figure 4.6 C).

Invasive hemodynamic measurements were used to assess systolic and diastolic function via determining the maximum rate of pressure generation (+dP/dt_{max}) and pressure loss (-dP/dt_{min}) in the LV (Figure 4.6 A-B). The +dP/dt_{max} value of the DM LV is significantly higher than WT and PI3K α DN and closely resemble PI3K γ KO, suggesting a hyper-contractile phenotype (Figure 4.6 A). Interestingly, the -dP/dt_{min} value of DM hearts is not enhanced and resembles WT and PI3K α DN instead of PI3K γ KO suggesting that the mechanism of contractility regulation may differ between DM and PI3K γ KO (Figure 4.6 B). Overall, the functional phenotype of DM hearts demonstrates enhanced systolic function and preserved diastolic function.

4.3.6 Increased baseline cAMP levels and phosphorylation of PLN in PI3K γ KO and DM mice compared to WT and PI3K α DN.

cAMP levels were measured from LV extracts from WT, PI3K γ KO, PI3K α DN, and DM hearts using the GE Amersham cAMP Enzyme Immunoassay Kit. DM hearts have significantly higher baseline cAMP levels as compared to WT and PI3K α DN hearts, but have similar cAMP levels as PI3K γ KO hearts (Figure 4.6 D). This result is consistent with previous studies investigating the basal contractility of the PI3K γ KO mutant [3, 10]. A similar pattern is observed in PLN phosphorylation, where DM and PI3K γ KO have similar phospho-PLN levels and both are higher than that of WT and PI3K α DN (Figure 4.6 E).

4.4 Discussion:

The complex regulation and structure of the PI3K signaling pathway is an active area in cardiac research and the use of PI3K isoform specific inhibitors proves to be a potential treatment in the future. However, more research is currently necessary for the identification of redundant and non-redundant roles of PI3K α and PI3K γ before the pursuit of drug development. While the traditional model views PI3K α and PI3K γ as having distinct up-stream activation but similar down-stream signaling cascades, the current study suggests that this simple concept does not fully represent the actuality of PI3K α and PI3K γ signaling in the heart.

The suppression of PI3K α activity in PI3K α DN hearts leads to reduction of baseline cardiomyocyte and ventricular size [3, 14]. Similarly Akt, GSK-3 β , and GSK-3 α activation is also reduced accordingly while no changes are observed in ERK 1/2 activation. Furthermore, as previously described, no changes in contractile function are observed in PI3K α DN hearts [3]. These findings suggest that PI3K α regulates heart size independently of contractile function.

On the other hand, the loss of PI3K γ in PI3K γ KO hearts does not result in alterations in the Akt signaling cascade or changes in cardiomyocyte or ventricular size, but instead enhances baseline contractility, demonstrating that contrary to PI3K α , PI3K γ regulates contractile function independently of heart size.

These observations indicate that the PI3K α and PI3K γ pathways may be dissimilar despite having almost identical kinase activities. Interestingly, the current study shows that the dual loss of PI3K α and PI3K γ results in an early paradoxical

increase in Akt, GSK-3 β , GSK-3 α , and ERK phosphorylation, which are accompanied by a delayed hypertrophic response observable by 6 months of age. This radical change in signaling is likely due to a compensatory pro-survival response by cardiomyocytes in the absence of the two primary PI3K isoforms in the heart. We investigated two potential causes for this paradoxical signaling, which are an increase in PI3K β activity or a decrease in PTEN activity.

We found no significant differences in p110 β protein levels suggesting that alteration of PI3K β activity may not be the cause of the augmented Akt signaling pathways. On the other hand, it remains a possibility that over-expression of the p110 α DN protein outcompetes p110 β interaction with p85 thus limiting the latter's signaling capacity in PI3K α DN and DM hearts.

Although there are also no significant differences in PTEN protein levels between the four genotypes, PTEN phosphorylation/deactivation is significantly increased in DM hearts, which is accompanied by a similar reduction of PTEN phosphatase activity. It is possible that the loss of PTEN activity over-compensates the loss of PI3K activity leading to the hyper-activation of downstream pathways.

Studies in tumour cells have suggested that PTEN activity is directly regulated via phosphorylation by Casein Kinase 2 (CK2) at the Ser 385 residue [13, 15] (Figure 4.7). Our results illustrate that CK2 α' , one of the catalytic subunits of CK2, but not CK2 α , is upregulated in DM hearts compared to the other three genotypes. One potential explanation for the increased CK2 mediated inhibition of PTEN is that in the absence of PI3K, p53 activity increases, leading to increased expression of CK2 α' [16].

Our findings suggest that in the absence of both PI3K α and PI3K γ , there is a paradoxical activation of the PI3K signaling cascade due to upregulation of CK2 mediated deactivation of PTEN activity.

Figure 4.1

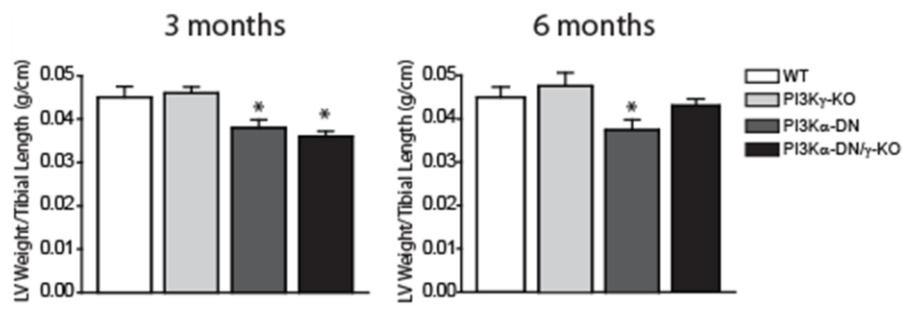


Figure 4.1 DM hearts have reduced LV weight at 3 months but not at 6 months of age. Baseline left ventricular weights were standardized to tibial length at 3 and 6 months of age and plotted as bar graphs (n = 8; *p < 0.05 compared with WT group; graphs are plotted as mean \pm SEM).

Figure 4.2

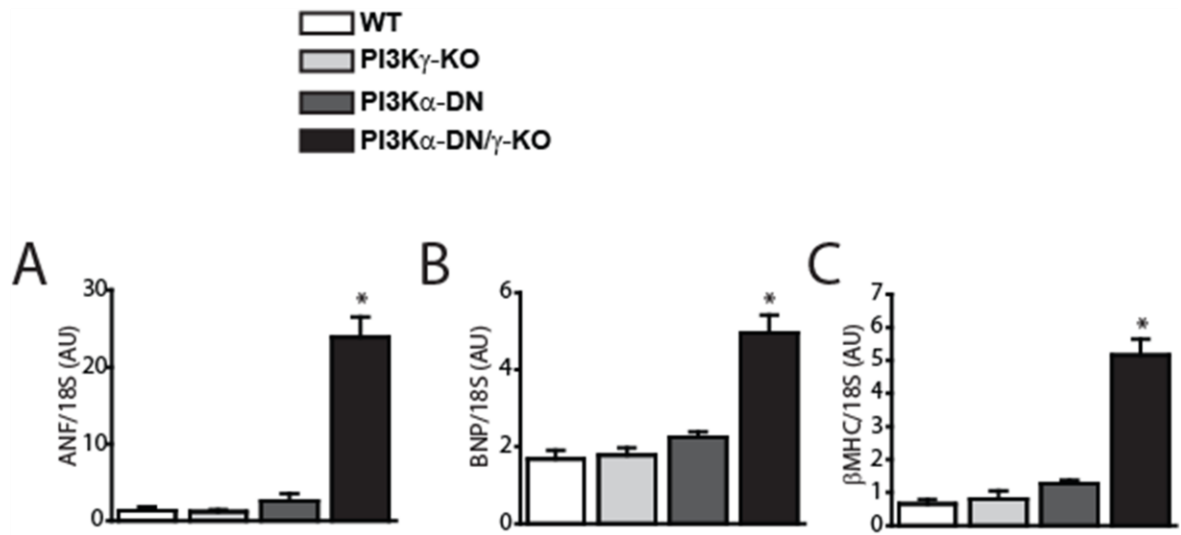


Figure 4.2 DM hearts demonstrated enhanced baseline expression of ANF, BNP, and β MHC. mRNA expression levels of the hypertrophy markers ANF (A), BNP (B), β MHC (C) are standardized against mRNA expression of 18S. The quantified values of gene expression are displayed in bar graphs (n = 6; *p < 0.05 compared with WT group; graphs are plotted as mean \pm SEM).

Figure 4.3

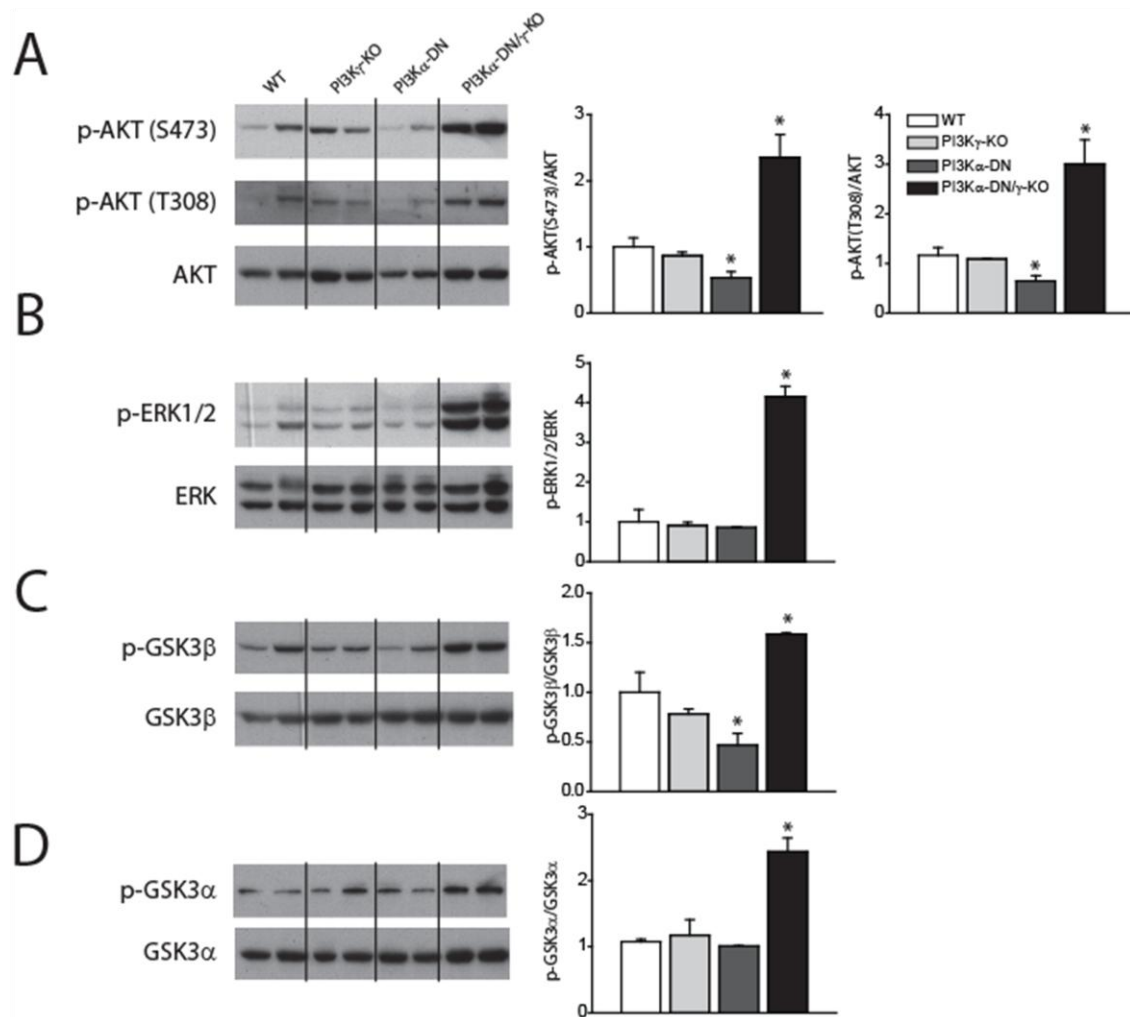


Figure 4.3 Western blot analysis shows that DM hearts have enhanced baseline phosphorylation of PI3K signaling cascade. Left ventricular protein extracts from the respective genotypes were subjected to western blot analysis. The western blots shown are representative of Akt (phospho-(Ser 473) Akt, phospho-(Thr 308) Akt, and total Akt) (A), GSK-3 β (phospho-(Ser 9) GSK-3 β and total GSK-3 β) (B), GSK-3 α (phospho-(Ser 21) GSK-3 α and total GSK-3 α) (C), and ERK 1/2 (phospho-(Thr 202/Tyr 204) ERK 1/2 and total ERK 1/2) (D) (n = 8; *p < 0.05 compared with WT group; graphs are plotted as mean \pm SEM).

Figure 4.4

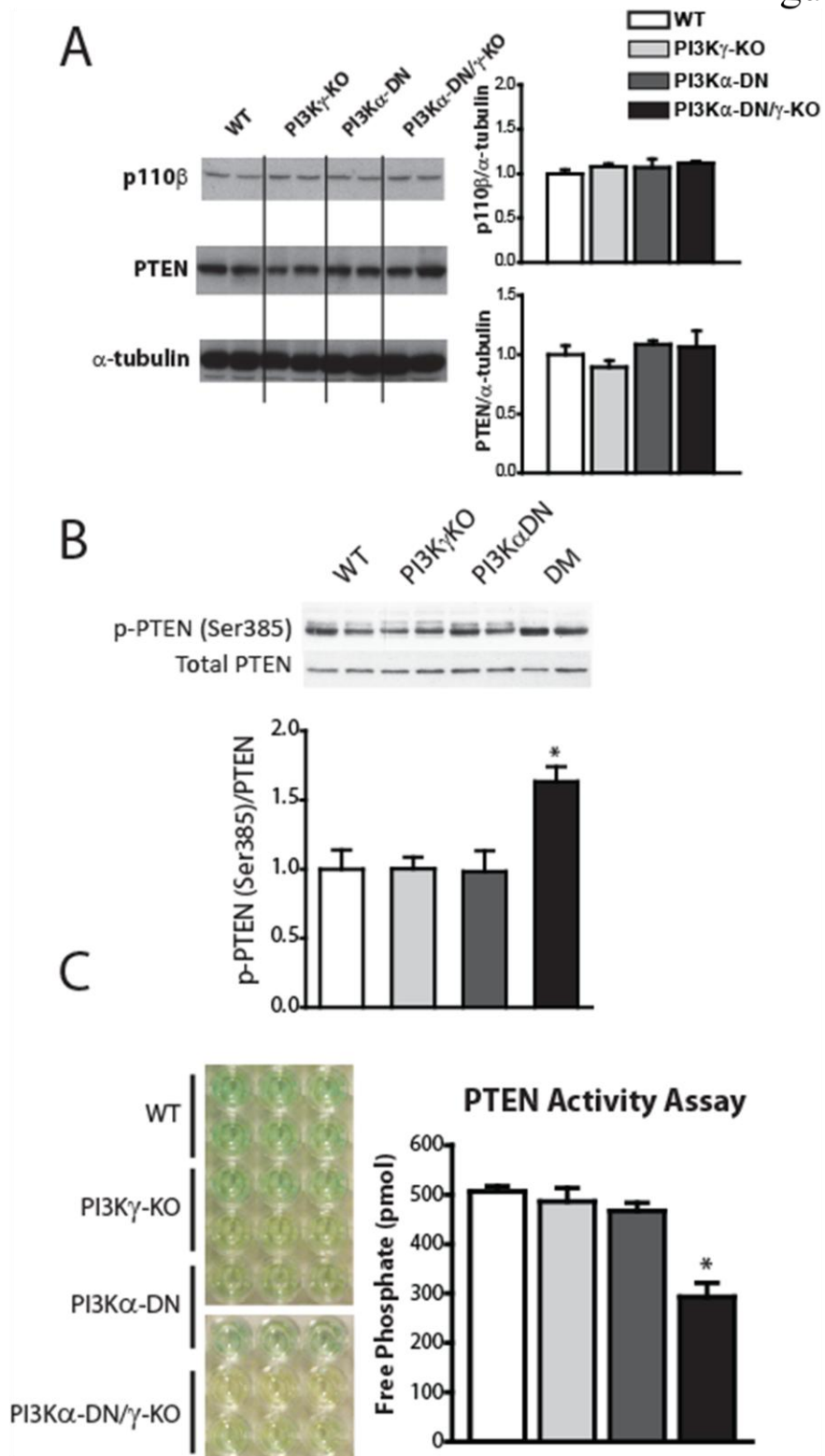


Figure 4.4 DM hearts have reduced baseline PTEN phosphatase activity without changes in PTEN protein levels due to enhanced phosphorylation of PTEN. Left ventricular protein extracts from the respective genotypes were subjected to western blot analysis (A-B) and immunoprecipitation for PTEN followed by PIP₃ phosphatase activity assay (C). The western blot shown is representative of baseline PTEN (phospho-(Ser 385) PTEN and total PTEN) signaling (A-B) and p110 β (A). The quantified values of the western blot and the PIP₃ phosphatase activity assay are displayed in bar graphs (n = 8; *p < 0.05 compared with WT group; graphs are plotted as mean \pm SEM).

Figure 4.5

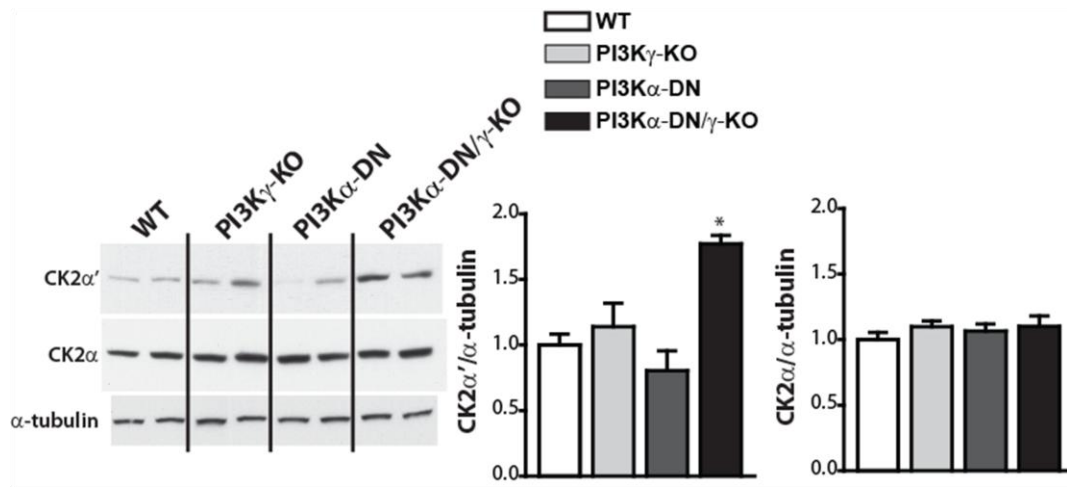


Figure 4.5 DM hearts have increased protein levels of CK2 α' but not CK2 α than WT, PI3K γ KO, and PI3K α DN. Left ventricular protein extracts from the respective genotypes were subjected to western blot analysis. The western blots shown are representative for CK2 α' and CK2 α as standardized to α -tubulin. The quantified values of the western blots are displayed in the bar graphs (n = 8; *p < 0.05 compared with WT group; graphs are plotted as mean \pm SEM).

Figure 4.6

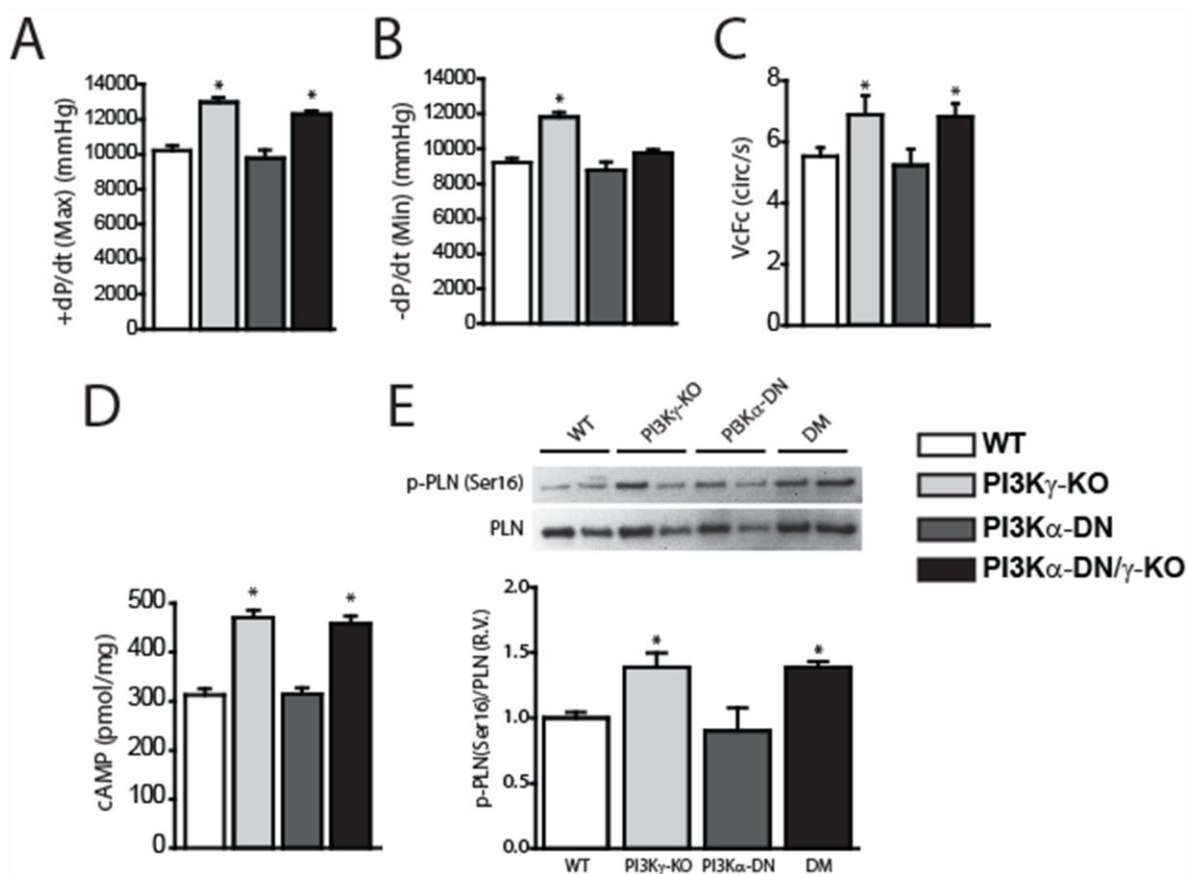


Figure 4.6 Echocardiographic and hemodynamic measurements of LV function demonstrated that DM and PI3K γ KO hearts have enhanced contractile function than WT or PI3K α DN. Echocardiography was used to measure the velocity of circumferential fractional shortening (VcFc) (C) while invasive hemodynamics were used to measure the maximum rate of contraction (+dP/dt_{max}) (A) and the maximum rate of relaxation (-dP/dt_{min}) (B). cAMP levels were measured using LV myocardial tissue extracted from the respective genotype (D). LV protein extracts from the respective genotypes were subjected western blot analysis. The western blot shown is representative of baseline PLN (phospho-(Ser 16) PLN and total PLN) (E). The quantified values of each experiment are displayed in the bar graphs (n = 9; *p < 0.05 compared with WT group; graphs are plotted as mean \pm SEM).

Figure 4.7

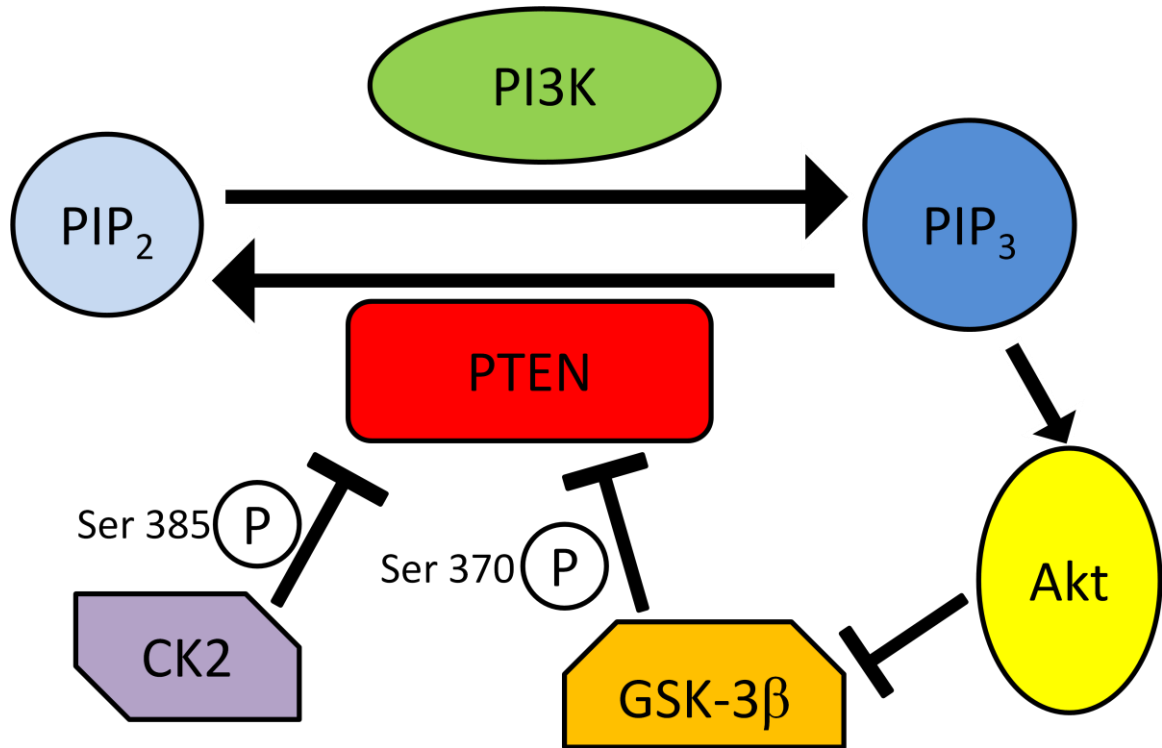


Figure 4.7 A schematic of PTEN phosphorylation and deactivation. PTEN is phosphorylated and inactivated by GSK-3 β and CK2. GSK-3 β phosphorylates PTEN at Ser 370 and CK2 phosphorylate PTEN at Ser 385.

Table 4.2

<i>ANF</i>	Forward Primer: Reverse Primer: Probe:	5'-GGA GGA GAA GAT GCC GGT AGA-3' 5'-GCT TCC TCA GTC TGC TCA CTC A-3' 5'-TGA GGT CAT GCC CCC GCA GG-3'
<i>BNP</i>	Forward Primer: Reverse Primer: Probe:	5'-CTG CTG GAG CTG ATA AGA GA-3' 5'-TGC CCA AAG CAG CTT GAG AT-3' 5'-FAM-CTC AAG GCA GCA CCC TCC GGG-TAMRA-3'
<i>β-MHC</i>	Forward Primer: Reverse Primer: Probe:	5'-GTGCCAAGGGCCTGAATGAG-3' 5'-GCAAAGGCTCCAGGTCTGA-3' 5'-ATCTTGTGCTACCCAGCTCTAA-3'

Table 4.2 RT-PCR primers and probes. The sequence to all RT-PCR primers and probes used in TaqMan analysis.

4.5 References:

1. Vanhaesebroeck, B. and M.D. Waterfield, *Signaling by distinct classes of phosphoinositide 3-kinases*. Exp Cell Res, 1999. **253**(1): p. 239-54.
2. Shioi, T., P.M. Kang, P.S. Douglas, J. Hampe, C.M. Yballe, J. Lawitts, L.C. Cantley, and S. Izumo, *The conserved phosphoinositide 3-kinase pathway determines heart size in mice*. EMBO J, 2000. **19**(11): p. 2537-48.
3. Crackower, M.A., G.Y. Oudit, I. Kozieradzki, R. Sarao, H. Sun, T. Sasaki, E. Hirsch, A. Suzuki, T. Shioi, J. Irie-Sasaki, R. Sah, H.Y. Cheng, V.O. Rybin, G. Lembo, L. Fratta, A.J. Oliveira-dos-Santos, J.L. Benovic, C.R. Kahn, S. Izumo, S.F. Steinberg, M.P. Wymann, P.H. Backx, and J.M. Penninger, *Regulation of myocardial contractility and cell size by distinct PI3K-PTEN signaling pathways*. Cell, 2002. **110**(6): p. 737-49.
4. Oudit, G.Y., Z. Kassiri, J. Zhou, Q.C. Liu, P.P. Liu, P.H. Backx, F. Dawood, M.A. Crackower, J.W. Scholey, and J.M. Penninger, *Loss of PTEN attenuates the development of pathological hypertrophy and heart failure in response to biomechanical stress*. Cardiovasc Res, 2008. **78**(3): p. 505-14.
5. McMullen, J.R., T. Shioi, L. Zhang, O. Tarnavski, M.C. Sherwood, P.M. Kang, and S. Izumo, *Phosphoinositide 3-kinase(p110alpha) plays a critical role for the induction of physiological, but not pathological, cardiac hypertrophy*. Proc Natl Acad Sci U S A, 2003. **100**(21): p. 12355-60.
6. Oudit, G.Y., M.A. Crackower, U. Eriksson, R. Sarao, I. Kozieradzki, T. Sasaki, J. Irie-Sasaki, D. Gidrewicz, V.O. Rybin, T. Wada, S.F. Steinberg, P.H. Backx, and J.M. Penninger, *Phosphoinositide 3-kinase gamma-deficient mice are*

- protected from isoproterenol-induced heart failure. Circulation, 2003. 108(17): p. 2147-52.*
7. Sugden, P.H., S.J. Fuller, S.C. Weiss, and A. Clerk, *Glycogen synthase kinase 3 (GSK3) in the heart: a point of integration in hypertrophic signalling and a therapeutic target? A critical analysis. Br J Pharmacol, 2008. 153 Suppl 1: p. S137-53.*
 8. Matsuda, T., P. Zhai, Y. Maejima, C. Hong, S. Gao, B. Tian, K. Goto, H. Takagi, M. Tamamori-Adachi, S. Kitajima, and J. Sadoshima, *Distinct roles of GSK-3alpha and GSK-3beta phosphorylation in the heart under pressure overload. Proc Natl Acad Sci U S A, 2008. 105(52): p. 20900-5.*
 9. Shioi, T., J.R. McMullen, P.M. Kang, P.S. Douglas, T. Obata, T.F. Franke, L.C. Cantley, and S. Izumo, *Akt/protein kinase B promotes organ growth in transgenic mice. Mol Cell Biol, 2002. 22(8): p. 2799-809.*
 10. Patrucco, E., A. Notte, L. Barberis, G. Selvetella, A. Maffei, M. Brancaccio, S. Marengo, G. Russo, O. Azzolino, S.D. Rybalkin, L. Silengo, F. Altruda, R. Wetzker, M.P. Wymann, G. Lembo, and E. Hirsch, *PI3Kgamma modulates the cardiac response to chronic pressure overload by distinct kinase-dependent and -independent effects. Cell, 2004. 118(3): p. 375-87.*
 11. Lorenz, K., J.P. Schmitt, E.M. Schmitteckert, and M.J. Lohse, *A new type of ERK1/2 autophosphorylation causes cardiac hypertrophy. Nat Med, 2009. 15(1): p. 75-83.*
 12. Seko, Y., N. Takahashi, K. Tobe, T. Kadowaki, and Y. Yazaki, *Pulsatile stretch activates mitogen-activated protein kinase (MAPK) family members and focal*

- adhesion kinase (p125(FAK)) in cultured rat cardiac myocytes. Biochem Biophys Res Commun, 1999. 259(1): p. 8-14.*
13. Zhu, D., J. Hensel, R. Hilgraf, M. Abbasian, O. Pornillos, G. Deyanat-Yazdi, X.H. Hua, and S. Cox, *Inhibition of protein kinase CK2 expression and activity blocks tumor cell growth. Mol Cell Biochem, 2010. 333(1-2): p. 159-67.*
 14. O'Neill, B.T., J. Kim, A.R. Wende, H.A. Theobald, J. Tuinei, J. Buchanan, A. Guo, V.G. Zaha, D.K. Davis, J.C. Schell, S. Boudina, B. Wayment, S.E. Litwin, T. Shioi, S. Izumo, M.J. Birnbaum, and E.D. Abel, *A conserved role for phosphatidylinositol 3-kinase but not Akt signaling in mitochondrial adaptations that accompany physiological cardiac hypertrophy. Cell Metab, 2007. 6(4): p. 294-306.*
 15. Maccario, H., N.M. Perera, L. Davidson, C.P. Downes, and N.R. Leslie, *PTEN is destabilized by phosphorylation on Thr366. Biochem J, 2007. 405(3): p. 439-44.*
 16. Zhou, Y., H. Zhen, Y. Mei, Y. Wang, J. Feng, S. Xu, and X. Fu, *PI3K/AKT mediated p53 down-regulation participates in CpG DNA inhibition of spontaneous B cell apoptosis. Cell Mol Immunol, 2009. 6(3): p. 175-80.*

Chapter 5

TRANSACTIVATION OF PI3K α

5.1 Introduction:

PI3K is a family of conserved lipid kinases that are responsible for activation of growth and survival pathways in response to extracellular agonist mediated signals [1]. The two types of receptors that activate PI3K signaling are RTKs and GPCRs. In cardiomyocytes, RTKs and GPCRs have traditionally been known to activate PI3K α and PI3K γ respectively, each leading to a similar downstream modulation of Akt and MAPK activity [1, 2]. However, recent studies suggested that growth factor receptors may also be necessary for mediating MAPK activation by GPCR agonists and this novel signaling pathway has been termed transactivation [3-5]. For example, angiotensin II mediated activation of the MAPK pathway in cancer cell lines requires the activation of EGFR [6, 7].

In cardiomyocytes, transactivation is initiated by GPCR stimulation and followed the activation of extracellular proteases and sheddases. These proteolytic enzymes exert autocrine and paracrine cleavage of membrane bound growth factors, which subsequently activate their respective receptors, leading to transactivation of PI3K α [3, 4]. Indeed, Noma et al (2007) demonstrated in cancer cell lines and neonatal cardiomyocytes that isoproterenol stimulation of ERK 1/2 can be blocked via the pharmacological inhibition of either growth factor receptors or MMPs [3]. Similarly, Chen et al (2006) found that angiotensin II treatment of porcine kidney cells increased the phosphorylation of EGFR and that angiotensin II mediated hypertrophy was blocked with treatment of an EGFR inhibitor [8]. Several studies have also demonstrated similar EGFR dependent transactivation pathways in other cell types [9-11]. Gefitinib is a potent EGFR inhibitor that selectively binds to EGFR with higher potency than other

ErbB receptors [12]. As EGFR inhibitors are clinically used for certain types of cancer treatment, the use of Gefitinib in mitigating agonist mediated heart disease may prove effective.

Given PI3K α 's role in regulating cardiac hypertrophy in adult cardiomyocytes, it is possible that transactivation of EGFR by GPCR agonists activates hypertrophic signaling cascades via PI3K α . This chapter will focus on identifying the transactivation pathway in adult cardiomyocytes using PI3K isoform specific inhibitors and PI3K mutant strains.

5.2 Methods:

5.2.1 Cell culture

Adult cardiomyocytes were pre-treated with either 10 μ M gefitinib, 10 nM of PI-103, or 1 μ M of AS604850 for 15 min then treated with either 100 nM isoproterenol or 100 nM angiotensin II for 15 min. After, the cells were washed with ice cold PBS and cell lysate was collected according to Chapter 2.4.

5.3 Results:

5.3.1 Isoproterenol mediated activation of Akt signaling requires PI3K α but not PI3K γ .

WT, PI3K α DN, and PI3K γ KO adult cardiomyocytes were pre-treated with PI-103 or AS604850 (Figure 5.1) before being treated with 100 nM of isoproterenol. WT cardiomyocytes showed a significant increase in Akt phosphorylation in response to isoproterenol (Figure 5.1 A) and this response was blocked by PI-103 but not by AS604850 demonstrating that PI3K α but not PI3K γ is needed for this response. Indeed, while PI3K α DN cardiomyocytes did not have increased Akt phosphorylation when treated with isoproterenol, PI3K γ KO cardiomyocytes showed normal Akt phosphorylation similar to WT (Figure 5.1 B-C).

Consistent with the fact that PI3K α DN mutants retain 25% of PI3K α activity, application of PI-103 in PI3K α DN further suppressed baseline Akt phosphorylation (Figure 5.1 C). While it is true that PI-103 reduces baseline Akt phosphorylation, the fact that PI3K α DN cardiomyocytes lacked a response to isoproterenol demonstrated that PI3K α activity is necessary for isoproterenol induced Akt phosphorylation (Figure 5.2).

5.3.2 Gefitinib blocks angiotensin II but not isoproterenol mediated activation of Akt.

Pre-treatment of adult cardiomyocytes with EGFR inhibitor gefitinib inhibited angiotensin II mediated phosphorylation of Akt at both the Ser 473 and Thr 308 residues (Figure 5.3 A) demonstrating the linkage between angiotensin receptor and

EGFR. However, gefitinib only inhibits isoproterenol mediated phosphorylation of Akt at the Thr 308 and not Ser 473 residue (Figure 5.2 B).

5.4 Discussion:

The traditional PI3K signaling cascade consists of exclusive activation of PI3K α and PI3K γ by RTKs and GPCRs, respectively. Our results showed that this canonical perspective does not fully represent the complexity of the PI3K signaling cascade *in vivo*, particularly in adult cardiomyocytes. Interestingly, our results have demonstrated that isoproterenol induced transactivation of Akt in cardiomyocytes via stimulation of EGFR and subsequent transactivation of PI3K α . The use of the EGFR inhibitor, gefitinib, only partially blocked isoproterenol mediated Akt phosphorylation, preventing phosphorylation of Thr 308 but not Ser 473 residue, suggesting that β adrenergic receptor induced transactivation is not limited to the EGFR pathway. It is possible, however, that the unknown pathway make still involve activation of proteases leading to shedding of other membrane bound growth factors; hence, future analysis of the potential of protease inhibitors in blocking transactivation will be required. It is also possible that the initial activation of the β adrenergic receptor leads to activation of kinases that activates PI3K α intracellularly, such as the Src kinase [3].

On the other hand, angiotensin II mediated activation of Akt was completely ablated by pre-treatment with gefitinib, likely due to intrinsic differences in downstream activation of signaling cascades between adrenergic receptors and angiotensin receptors. Indeed, it has been suggested that angiotensin receptors rely entirely on EGFR for transactivation [6].

We also showed that the transactivation of EGFR by isoproterenol requires PI3K α , as the loss of PI3K α activity in PI3K α DN cardiomyocytes and in WT cardiomyocytes

treated with the PI3K α inhibitor prevented Akt phosphorylation. Though it is arguable that the reduction in Akt phosphorylation upon treatment of the PI3K α inhibitor is due to the inhibitor's effects on baseline Akt activation, the use of PI3K α DN mutants further validated that PI3K α is indeed necessary for isoproterenol mediated transactivation of Akt. We also demonstrated that the transactivation of Akt via isoproterenol treatment is mediated solely by PI3K α as PI3K γ inhibitors and PI3K γ KO mutant cardiomyocytes exhibited similar Akt phosphorylation in response to isoproterenol as WT.

Figure 5.1

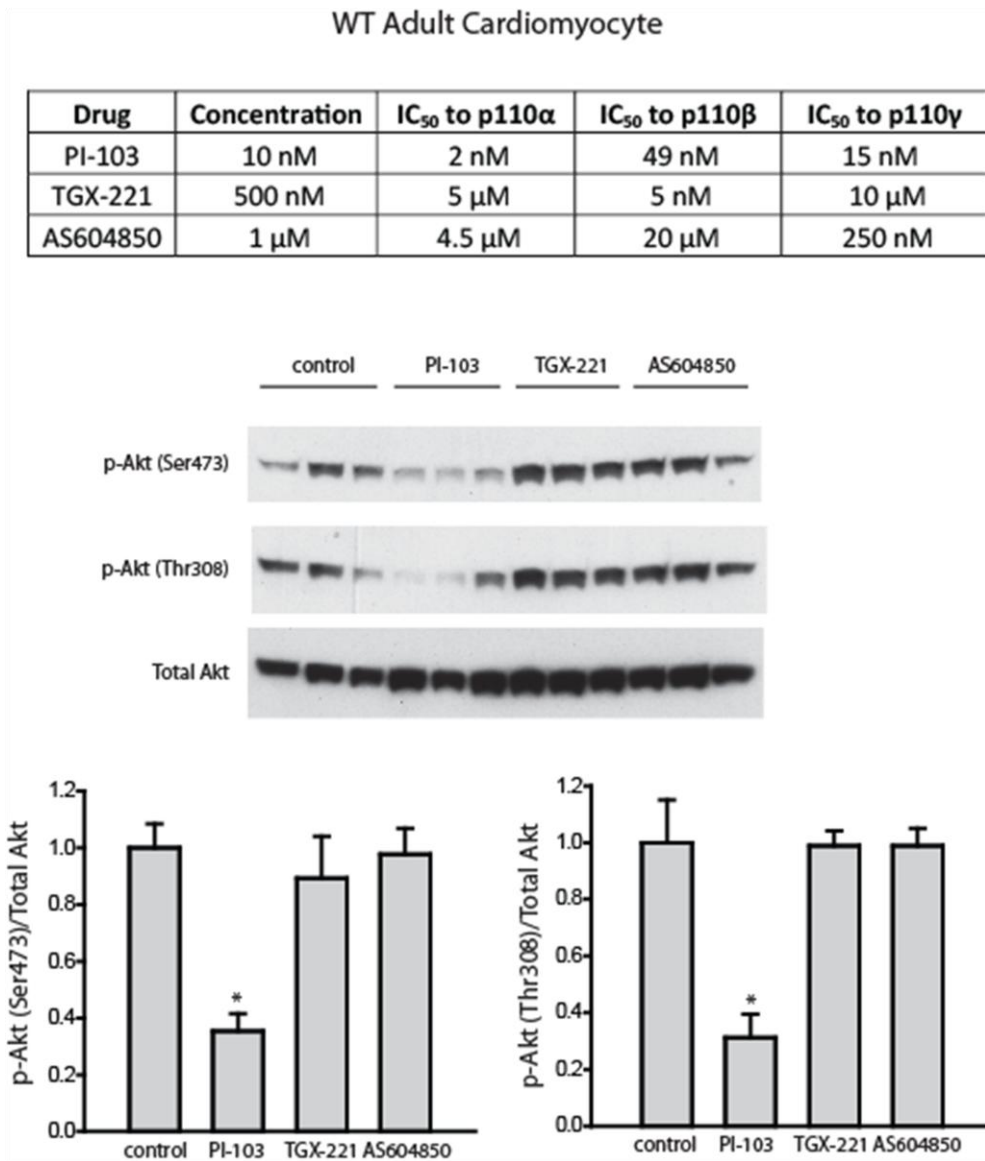


Figure 5.1 PI-103, but not TGX-221 or AS604850, reduces baseline Akt phosphorylation in WT adult cardiomyocytes. WT adult cardiomyocytes were treated with PI-103 (PI3K α inhibitor), TGX-221 (PI3K β inhibitor), or AS604850 (PI3K γ inhibitor) and phospho-(Ser 473) and phospho-(Thr 308) Akt were standardized to total Akt and plotted as bar graphs (n = 8; *p < 0.05 compared to WT group; graphs are plotted as mean \pm SEM).

Figure 5.2

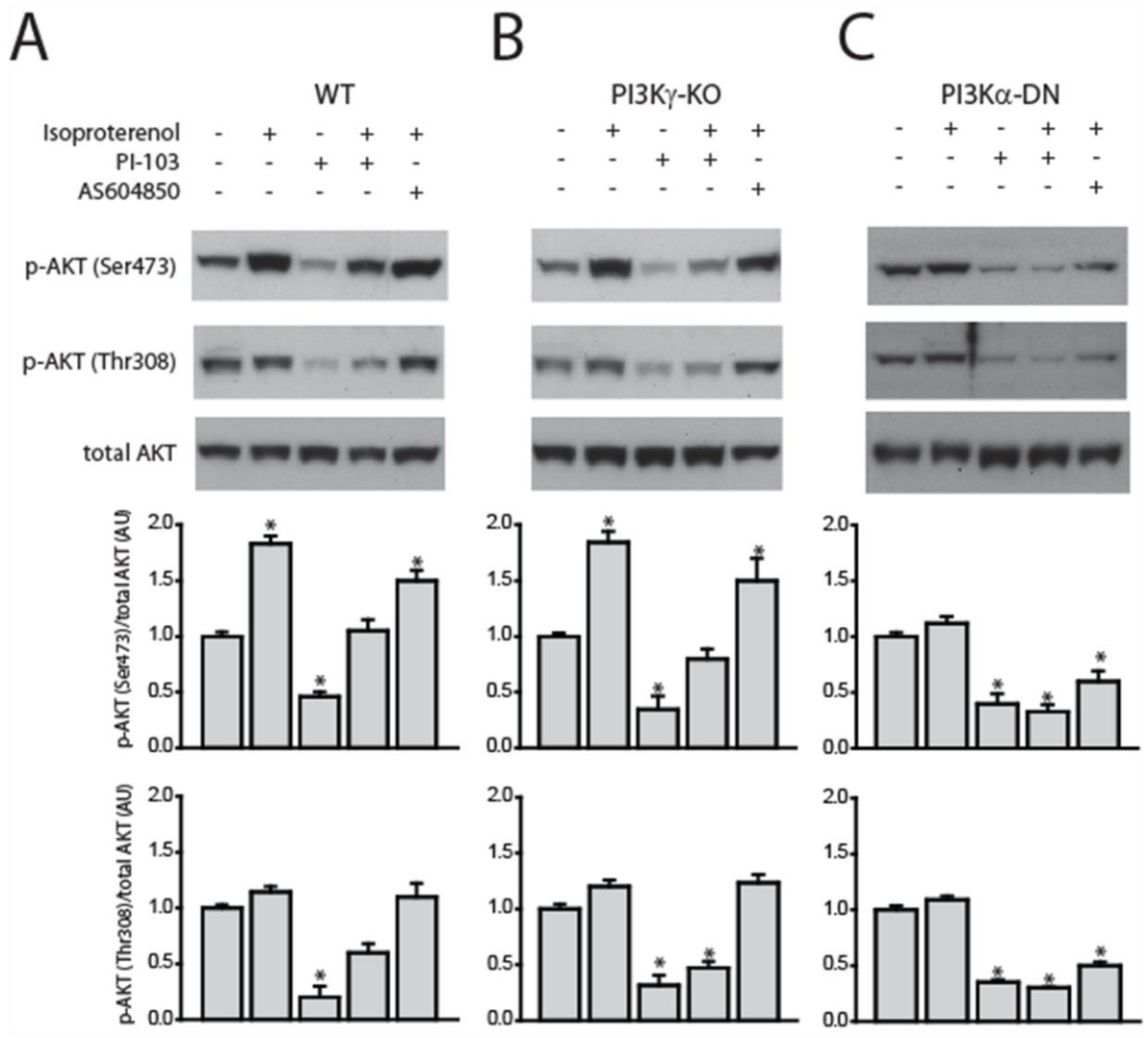


Figure 5.2 Isoproterenol mediated Akt phosphorylation can be blocked by PI-103 and AS604850. Adult cardiomyocyte protein extracts from respective groups were subjected to western blot analysis. The concentration of isoproterenol used was 100 nM and the concentrations of PI-103 and AS604850 were 10 nM and 1 μ M respectively. The western blots shown are representative of Akt (phospho-(Ser 473) Akt, phospho-(Thr 308) Akt, and total Akt). The quantified values of the western blots are displayed in bar graphs (n = 8; *p < 0.05 compared to WT group; graphs are plotted as mean \pm SEM).

Figure 5.3

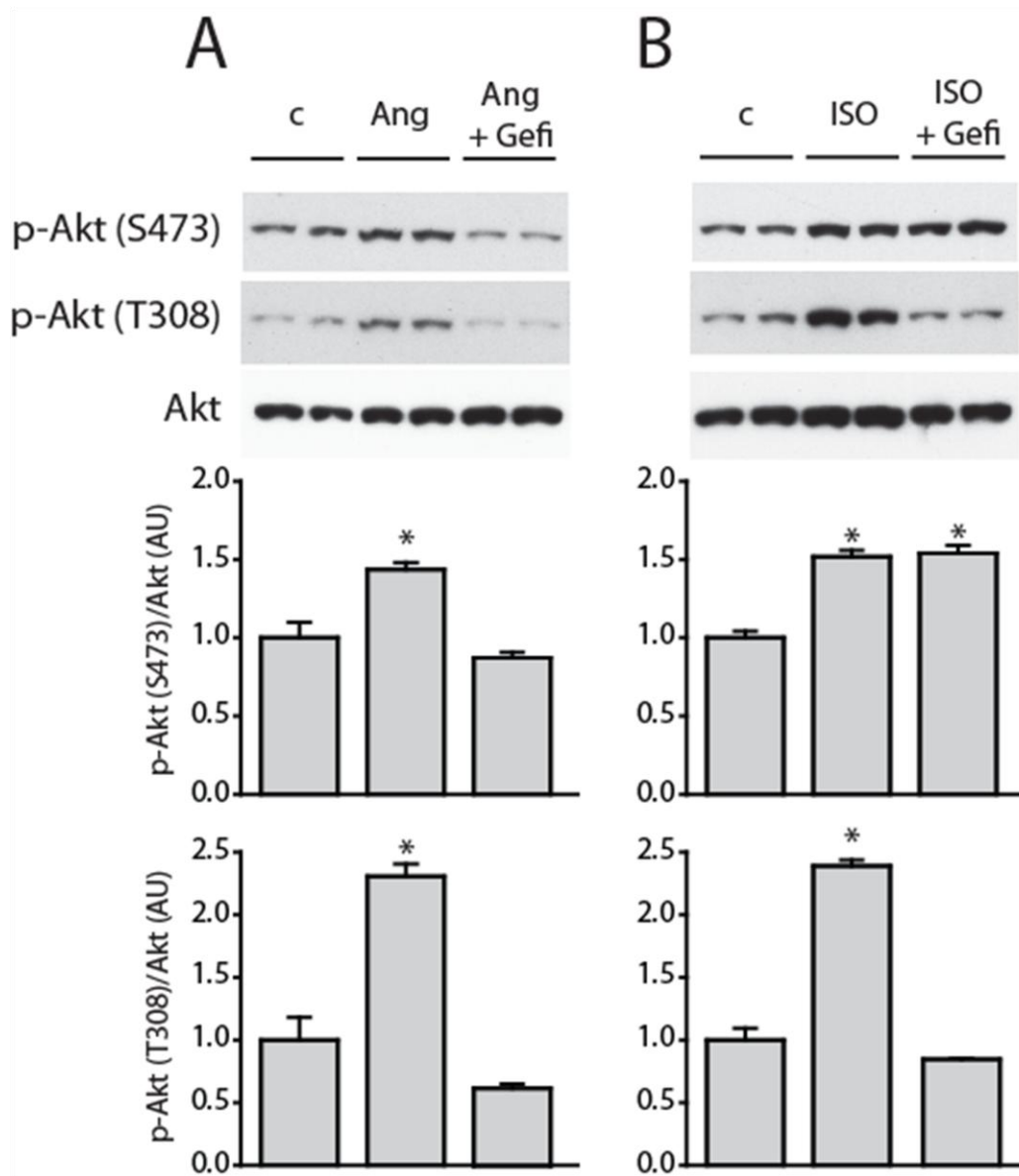


Figure 5.3 Pre-treatment with gefitinib inhibits angiotensin II mediated activation and partially inhibits isoproterenol mediated activation of Akt signaling. Adult cardiomyocyte protein extracts from the treatment groups were subjected to western blot analysis. The concentrations of isoproterenol, angiotensin II and gefitinib used were 100 nM, 100 nM, and 10 μ M respectively (A-B). The western blots shown are representative of Akt (phospho-(Ser 473) Akt, phospho-(Thr 308) Akt, and total Akt). The quantified values of the western blots are displayed in bar graphs (n = 8; *p < 0.05 compared to WT group; graphs are plotted as mean \pm SEM).

5.5 References:

1. Vanhaesebroeck, B. and M.D. Waterfield, *Signaling by distinct classes of phosphoinositide 3-kinases*. Exp Cell Res, 1999. **253**(1): p. 239-54.
2. Vanhaesebroeck, B., S.J. Leever, K. Ahmadi, J. Timms, R. Katso, P.C. Driscoll, R. Woscholski, P.J. Parker, and M.D. Waterfield, *Synthesis and function of 3-phosphorylated inositol lipids*. Annu Rev Biochem, 2001. **70**: p. 535-602.
3. Noma, T., A. Lemaire, S.V. Naga Prasad, L. Barki-Harrington, D.G. Tilley, J. Chen, P. Le Corvoisier, J.D. Violin, H. Wei, R.J. Lefkowitz, and H.A. Rockman, *Beta-arrestin-mediated beta1-adrenergic receptor transactivation of the EGFR confers cardioprotection*. J Clin Invest, 2007. **117**(9): p. 2445-58.
4. Asakura, M., M. Kitakaze, S. Takashima, Y. Liao, F. Ishikura, T. Yoshinaka, H. Ohmoto, K. Node, K. Yoshino, H. Ishiguro, H. Asanuma, S. Sanada, Y. Matsumura, H. Takeda, S. Beppu, M. Tada, M. Hori, and S. Higashiyama, *Cardiac hypertrophy is inhibited by antagonism of ADAM12 processing of HB-EGF: metalloproteinase inhibitors as a new therapy*. Nat Med, 2002. **8**(1): p. 35-40.
5. Nagareddy, P.R., K.M. Macleod, and J.H. McNeill, *GPCR Agonist-Induced Transactivation of the EGFR Upregulates MLC II Expression and Promotes Hypertension in Insulin Resistant Rats*. Cardiovasc Res.
6. Greco, S., A. Muscella, M.G. Elia, P. Salvatore, C. Storelli, A. Mazzotta, C. Manca, and S. Marsigliante, *Angiotensin II activates extracellular signal regulated kinases via protein kinase C and epidermal growth factor receptor in breast cancer cells*. J Cell Physiol, 2003. **196**(2): p. 370-7.

7. Seta, K. and J. Sadoshima, *Phosphorylation of tyrosine 319 of the angiotensin II type 1 receptor mediates angiotensin II-induced trans-activation of the epidermal growth factor receptor*. J Biol Chem, 2003. **278**(11): p. 9019-26.
8. Chen, J., J.K. Chen, E.G. Neilson, and R.C. Harris, *Role of EGF receptor activation in angiotensin II-induced renal epithelial cell hypertrophy*. J Am Soc Nephrol, 2006. **17**(6): p. 1615-23.
9. Laffargue, M., P. Raynal, A. Yart, C. Peres, R. Wetzker, S. Roche, B. Payrastra, and H. Chap, *An epidermal growth factor receptor/Gab1 signaling pathway is required for activation of phosphoinositide 3-kinase by lysophosphatidic acid*. J Biol Chem, 1999. **274**(46): p. 32835-41.
10. Andresen, B.T., J.J. Linnoila, E.K. Jackson, and G.G. Romero, *Role of EGFR transactivation in angiotensin II signaling to extracellular regulated kinase in preglomerular smooth muscle cells*. Hypertension, 2003. **41**(3 Pt 2): p. 781-6.
11. Hart, S., O.M. Fischer, N. Prenzel, E. Zwick-Wallasch, M. Schneider, L. Hennighausen, and A. Ullrich, *GPCR-induced migration of breast carcinoma cells depends on both EGFR signal transactivation and EGFR-independent pathways*. Biol Chem, 2005. **386**(9): p. 845-55.
12. Stabile, L.P., M.E. Rothstein, P. Keohavong, D. Lenzner, S.R. Land, A.L. Gaither-Davis, K.J. Kim, N. Kaminski, and J.M. Siegfried, *Targeting of Both the c-Met and EGFR Pathways Results in Additive Inhibition of Lung Tumorigenesis in Transgenic Mice*. Cancers (Basel), 2010. **2**(4): p. 2153-2170.

Chapter 6

DISCUSSION, LIMITATIONS, FUTURE DIRECTIONS, AND CONCLUSION

6.1 General Discussion:

The PI3K signaling cascade plays an integral role in the heart's morphology and function at both basal and stimulated states. The isoform specific roles of Class I PI3Ks were explored in this thesis, which provided insight into novel aspects to the PI3K's cellular role, modes of activation, and crosstalk pathways.

In this thesis, we have made the following observations:

Chapter 3:

1. PI3K γ KO mice rapidly develop heart failure in response to pressure overload due to excess MMP expression and MMP mediated cleavage of N-cadherin adhesion complexes.
2. The maladaptive remodelling of N-cadherin adhesion complexes in PI3K γ KO mice post AB can be reversed by blocking elevations in cAMP or blocking MMP activity.
3. The maladaptive cardiac remodelling observed in PI3K γ KO mice post AB can be observed in WT mice after 9 weeks of AB.

Chapter 4:

1. PI3K γ KO/ α DN mutants have small hearts at 3 months of age but normalize by 6 months.
2. PI3K γ KO/ α DN mutant hearts are hyper-contractile at 6 months of age due to enhanced cAMP.

3. The dual loss of PI3K α and PI3K γ leads to the paradoxical hyper-activation of Akt and ERK signaling pathways due to inactivation of PTEN.

Chapter 5

1. PI3K α is necessary for isoproterenol mediated phosphorylation of Akt.
2. EGFR is involved in angiotensin II induce transactivation of Akt.

6.1.1 Kinase independent role of PI3K γ in the response to pressure overload induced heart failure.

PI3K γ has a number of cellular functions in cardiomyocytes, including GPCR agonist mediated signaling and contractile functional regulation. In combination with previous studies, which explored PI3K γ 's kinase function in an agonist mediated heart failure mouse model [1], we have shown that PI3K γ has dual protective and pathological functions in heart disease, leading to a controversial role *in vivo*.

Heart disease is comprised of both biochemical and biomechanical features. One of the biochemical aspects of heart disease is the upregulation of angiotensin II and catecholamine pathways. Chronic administration of angiotensin II via mini osmotic pumps generates systemic hypertension in WT mice but not in PI3K γ KO mice, an effect that was observed independent of changes in heart rate [2]. Furthermore, PI3K γ is necessary for angiotensin II mediated vasoconstriction, further exemplifying its role in hypertension mediated pressure overload [2]. Isoproterenol, a β adrenergic agonist, mediates pathological remodeling and fibrosis of the myocardium in a PI3K γ dependent process [1]. Interestingly, phenylephrine, an agonist of the α adrenergic receptor, also mediates a hypertensive response in WT mice as well as PI3K γ KO mice, suggesting

that certain GPCR agonists may stimulate the heart and vasculature independently of PI3K γ [2]. Furthermore, it has also been shown that phenylephrine is capable of transactivation of EGFRs in vascular cells thus suggesting a possible mechanism by which PI3K γ KO mice are not resistant to phenylephrine induced hypertension [3, 4]. It would be interesting to explore whether phenylephrine can mediate a hypertensive response in the absence of PI3K α .

In the case of biochemically mediated pathological response of the cardiovascular system, the loss of PI3K γ is generally protective. However, as discussed in chapter 3, PI3K γ KO mice are very sensitive and highly prone to biomechanical stress, rapidly developing systolic dysfunction and DCM when exposed to pressure overload. This was not observed in PI3K γ KD mice, which retain a loss of function mutant isoform of p110 γ , illustrating that PI3K γ 's interaction with phosphodiesterase (PDE) is key for modulating PI3K γ 's protective effects in cardiomyocytes.

The combination of the current data with previous data suggests that while the loss of PI3K γ 's kinase activity can protect the cardiovascular system from biochemical stressors [1], the loss of p110 γ 's physical interaction with PDE will only exacerbate cardiac damage from mechanical stress. From the pharmacological perspective, the development of drugs to inhibit PI3K γ 's kinase activity can be cardioprotective as long as the inhibitor does not interfere with PDE interaction or activity. Disruption of intracellular concentrations of cAMP may lead to adverse effects downstream as illustrated by the unsuccessful clinical trials involving PDE inhibitors and the animal models involving beta adrenergic receptor transgenic mutants [5-7]. Current drug developments are underway for finding a compound that selectively inhibits PI3K γ in

hope of developing a therapy for inflammatory disorders such as rheumatoid arthritis [8]. Our data suggests that the development of small molecule inhibitors or peptide inhibitors could be useful but PDE activity should be tested. We also demonstrate the potential cardiac toxicity of drugs that target the translation of p110 γ such as RNA interference therapies or antisense oligonucleotides.

6.1.2 Regulation of PI3K signaling cascade by CK2 activity

Chapter 4 indicates the potential linkage between the PI3K/PTEN signaling cascade and Casein Kinase 2 (CK2). Previous efforts to delineate PI3K isoform specific roles in the heart involved the generation of the loss of function PTEN mutant, which exhibited a phenotype exactly opposite to the combined phenotypes of PI3K α DN and PI3K γ KO mutants [9]. This was demonstrated the differential modulation of morphology and contractile function by PI3K α and PI3K γ . Our study aimed at validating this conclusion in adult cardiomyocytes via generating a mouse model that lacked both PI3K α and PI3K γ , the PI3K γ KO/ α DN double mutant (DM) mutant model, but arrived at the surprising conclusion that dual loss of the two primary PI3K isoforms in the heart resulted in hyper-activation of PI3K regulated kinases such as Akt and ERK. We also found that DM mutants had depressed PTEN activity and increased CK2 α ' protein levels suggesting that a potential negative feedback loop may exist to maintain baseline activation of growth and survival pathways. The hyper-activation that we observed can be attributed to an over-compensatory response of this feedback loop. Though CK2 has been previously shown to down-regulated PTEN activity in cancer cells in the same manner discussed in chapter 4, our data remains correlative and a direct causality of PTEN inhibition by CK2 in cardiomyocytes cannot be implied.

Interestingly, while our results suggest a pro-hypertrophic role of CK2 in the heart, another study demonstrated that CK2 activity declines in response to hypertrophic agonists and used this as evidence to argue that CK2 is anti-hypertrophic [10]. Though that argument is plausible, it is also possible that a reduction of CK2's activity in response to agonists such as phenylephrine and TNF α indicates an auto-regulatory mechanism, which cardiac cells could use as a negative feedback loop to prevent exaggerated responses to external stimuli. Nevertheless, our data has provided novel evidence for a potential relationship between PI3K and CK2.

6.1.3 Transactivation of PI3K α by GPCR stressor agonists

The process of transactivation has been extensively investigated in other cell types, including some studies in cardiomyocytes [11, 12]. Our traditional understanding of activation of Class I PI3Ks dictates the exclusive activation of PI3K α and PI3K γ by receptor tyrosine kinases and GPCR agonists, respectively. However, our data suggests that in adult cardiomyocytes, beta adrenergic receptor stimulation activates the Akt pathway only via PI3K α and the absence or presence of PI3K γ makes no significant differences on Akt phosphorylation. On the other hand, a previous study has demonstrated that isoproterenol mediated pathological remodeling of the myocardium and ERK activation are dependent on PI3K γ , suggesting that PI3K γ may activate MAPK instead of the Akt cascade [1]. Patrucco et al (2004) suggested that the loss of PI3K γ prevents the activation of Akt and ERK in response to pressure overload, supporting our results [13]. The difference in our results could be attributed to the complexity of the heart's response to both the biomechanical and biochemical components of pressure overload as well as the differences between an *in vitro* and *in*

vivo model. For instance, it is possible that biomechanical, but not biochemical, activation of Akt depends on PI3K γ . It is also likely that other stressor agonists are released systemically during pressure overload that do not follow the same transactivation pathway as catecholamines.

6.2 Limitations:

There are several limitations to the techniques and mutant models that we used in this study. For instance, isolation and generation of adult cardiomyocytes is an *in vitro* technique that is more representative of cardiomyocytes in a physiological setting than neonatal cardiomyocyte cultures. However, unlike neonatal cardiomyocytes, adult cardiomyocytes are not myogenic and thus lose the chronic biomechanical stimulation that they would normally experience *in vivo*. Because it has previously been demonstrated that mechanical force can stimulate Akt, our adult cardiomyocyte *in vitro* model is not truly representative of cardiomyocytes in a baseline physiological state. Although adult cardiomyocytes have been reported to survive for up to 72 hours post isolation with progressive loss of cellular integrity [14], our lab has only been able to maintain these cells for 48 hours. Such a short length of survival makes it difficult to test for long term effects of chemical agonists thus our results only include acute and short term measurements.

In chapter 3, we used AB as a model of pressure overload. However, the clinical applicability of this model is limited due to its severity and acute nature. AB is an artificial generation of the pressure overload experienced in the left ventricle during conditions such as hypertension and aortic valvular stenosis, both of which are

progressive disorders. Nevertheless, AB is a readily accessible model of pressure overload and has generally been accepted as a useful tool for testing the heart's response to mechanical stress.

The mutant model PI3K α DN is designed to generate a mouse with PI3K α activity deficient cardiomyocytes. This transgenic model requires the over-expression of a dominant negative isoform of p110 α . The over-expression of a protein could introduce unpredicted side-effects due to atypical protein interactions. To reduce this risk, the PI3K α DN is used as a heterozygous mutant where cardiomyocytes retain 1 copy of the WT p110 α gene, retaining roughly 25% of WT PI3K α activity [15]. Ultimately, the PI3K α DN model is imperfect as it does not completely abolish PI3K α activity.

The use of propranolol, PD166793, gefitinib, PI-103, and AS604850 in our studies carries limited clinical relevance as these drugs were all administered prior to the onset of biochemical or biomechanical stress hence their effects do not represent 'rescue' or 'prevention of progression' but instead represent 'prevention prior to onset'. Nevertheless, our purpose for using these drugs was not to generate a clinically applicable scenario but simply to test their respective signaling pathways and thus can still generate valid results. Furthermore, in the cases of PI-103 and AS604850, which are PI3K inhibitors, we confirmed the results with the usage of mutant models thus enhancing the validity of our observations.

In chapter 4, the link between PTEN and CK2 was implied but not directly tested. To overcome this, *in vitro* analysis of PTEN activity using pharmacological or genetic inhibition of CK2 would be necessary. In addition, it was assumed that a reduction of

PTEN lead to the hyper-activation of Akt signaling cascades but was never directly tested. One way to overcome this would be to measure PIP₃ levels in DM mice, though the complications of this measurement process make it difficult to pursue.

6.3 Future directions:

In chapter 3, we have dissected the mechanism for the rapid failure of PI3K γ KO heart when exposed to pressure overload. Izumo's group also showed a rapid failure of PI3K α DN in response to pressure overload [16, 17], but our results indicate that this occurs in a MMP and N-cadherin independent manner, as MMP expression was not altered and N-cadherin levels were retained in PI3K α DN mice post AB [18]. As intercellular adhesion complexes are not jeopardized in PI3K α DN mice post AB, it is possible that the observed failure is due to an intracellular process. Studies have shown that gelsolin, an enzyme that cleaves actin filaments and promotes cytoskeletal remodeling, is regulated by PIP₂/PIP₃ levels [19-21]. A future study could investigate the role of gelsolin in PI3K α DN mice post AB.

Also in chapter 3, we utilized propranolol as our beta blocker in an attempt to rescue the loss of N-cadherin *in vivo*. As propranolol is replaced by newer and more specific beta blockers in the treatment of cardiovascular diseases, it would be interesting and perhaps more appropriate to use other β blockers to obtain more clinical relevance.

In chapter 4, one of the limitations is our correlative conclusion of CK2's regulation of PTEN. If this pathway is correct, then we would have identified an important relationship between the CK2 and PI3K/PTEN pathways in the heart. Future experiments could test ability of TBBz, a CK2 specific inhibitor, in ablating the

augmented activation of Akt and GSK-3 in DM adult cardiomyocytes. The same experiment can also be extended to an *in vivo* model using mini-osmotic pumps for chronic administration of CK2 inhibitors in DM mice.

In chapter 5, we provided evidence for a mechanism of transactivation for angiotensin II and isoproterenol in adult cardiomyocytes *in vitro* by using the EGFR inhibitor gefitinib. As gefitinib is currently being used as a therapy for certain types of cancer, it may be interesting to explore its potential for protecting the heart against angiotensin II or isoproterenol induced pathological remodeling and heart failure. Hence, the use of gefitinib in an *in vivo* mouse model with chronic administration of angiotensin II or isoproterenol by mini-osmotic pumps may help extrapolate the transactivation pathway in a physiological setting.

A fundamental assumption proposed in this thesis is that the GPCR agonist mediated transactivation of RTKs relies on the shedding of membrane bound growth factors by of proteases. This assumption could be tested in future studies by using pharmacological inhibitors of proteases such as MMPs and A Dysintegrin and Metalloproteinases.

6.4 Conclusion:

This thesis explored the isoform specific functions and crosstalk of PI3K γ and PI3K α by utilizing pharmacological agents and mutant models. We identified the kinase independent role of PI3K γ in protecting the heart from mechanical stress and demonstrated the importance of cell-cell adhesion complexes in intercellular force transduction. We also showed evidence that PI3K γ may not be as important as PI3K α in

mediating Akt activation in response to GPCR agonists in adult cardiomyocytes as beta adrenergic stimulation leads to transactivation of PI3K α . We also illustrated that CK2 may have an important role in maintaining Akt signaling via inhibition of PTEN in the absence of both PI3K α and PI3K γ , while this function is not prominent in the absence of only one PI3K isoform.

Since PI3K is a modulator of both cardiac morphology and function, this thesis provides important insight on the isoform specific roles of Class I PI3Ks in the heart and acts as a precedent for future studies in the development of treatments for heart disease.

6.5 References:

1. Oudit, G.Y., M.A. Crackower, U. Eriksson, R. Sarao, I. Kozieradzki, T. Sasaki, J. Irie-Sasaki, D. Gidrewicz, V.O. Rybin, T. Wada, S.F. Steinberg, P.H. Backx, and J.M. Penninger, *Phosphoinositide 3-kinase gamma-deficient mice are protected from isoproterenol-induced heart failure*. *Circulation*, 2003. **108**(17): p. 2147-52.
2. Vecchione, C., E. Patrucco, G. Marino, L. Barberis, R. Poulet, A. Aretini, A. Maffei, M.T. Gentile, M. Storto, O. Azzolino, M. Brancaccio, G.L. Colussi, U. Bettarini, F. Altruda, L. Silengo, G. Tarone, M.P. Wymann, E. Hirsch, and G. Lembo, *Protection from angiotensin II-mediated vasculotoxic and hypertensive response in mice lacking PI3Kgamma*. *J Exp Med*, 2005. **201**(8): p. 1217-28.
3. Ulu, N., H. Gurdal, S.W. Landheer, M. Duin, M.O. Guc, H. Buikema, and R.H. Henning, *alpha1-Adrenoceptor-mediated contraction of rat aorta is partly mediated via transactivation of the epidermal growth factor receptor*. *Br J Pharmacol*. **161**(6): p. 1301-10.
4. Nagareddy, P.R., K.M. Macleod, and J.H. McNeill, *GPCR Agonist-Induced Transactivation of the EGFR Upregulates MLC II Expression and Promotes Hypertension in Insulin Resistant Rats*. *Cardiovasc Res*.
5. Nony, P., J.P. Boissel, M. Lievre, A. Leizorovicz, M.C. Haugh, S. Fareh, and B. de Breyne, *Evaluation of the effect of phosphodiesterase inhibitors on mortality in chronic heart failure patients. A meta-analysis*. *Eur J Clin Pharmacol*, 1994. **46**(3): p. 191-6.

6. Du, X.J., D.J. Autelitano, R.J. Dilley, B. Wang, A.M. Dart, and E.A. Woodcock, *beta(2)-adrenergic receptor overexpression exacerbates development of heart failure after aortic stenosis*. *Circulation*, 2000. **101**(1): p. 71-7.
7. Engelhardt, S., L. Hein, F. Wiesmann, and M.J. Lohse, *Progressive hypertrophy and heart failure in beta1-adrenergic receptor transgenic mice*. *Proc Natl Acad Sci U S A*, 1999. **96**(12): p. 7059-64.
8. Camps, M., T. Ruckle, H. Ji, V. Ardisson, F. Rintelen, J. Shaw, C. Ferrandi, C. Chabert, C. Gillieron, B. Francon, T. Martin, D. Gretener, D. Perrin, D. Leroy, P.A. Vitte, E. Hirsch, M.P. Wymann, R. Cirillo, M.K. Schwarz, and C. Rommel, *Blockade of PI3Kgamma suppresses joint inflammation and damage in mouse models of rheumatoid arthritis*. *Nat Med*, 2005. **11**(9): p. 936-43.
9. Crackower, M.A., G.Y. Oudit, I. Kozieradzki, R. Sarao, H. Sun, T. Sasaki, E. Hirsch, A. Suzuki, T. Shioi, J. Irie-Sasaki, R. Sah, H.Y. Cheng, V.O. Rybin, G. Lembo, L. Fratta, A.J. Oliveira-dos-Santos, J.L. Benovic, C.R. Kahn, S. Izumo, S.F. Steinberg, M.P. Wymann, P.H. Backx, and J.M. Penninger, *Regulation of myocardial contractility and cell size by distinct PI3K-PTEN signaling pathways*. *Cell*, 2002. **110**(6): p. 737-49.
10. Murtaza, I., H.X. Wang, X. Feng, N. Alenina, M. Bader, B.S. Prabhakar, and P.F. Li, *Down-regulation of catalase and oxidative modification of protein kinase CK2 lead to the failure of apoptosis repressor with caspase recruitment domain to inhibit cardiomyocyte hypertrophy*. *J Biol Chem*, 2008. **283**(10): p. 5996-6004.
11. Noma, T., A. Lemaire, S.V. Naga Prasad, L. Barki-Harrington, D.G. Tilley, J. Chen, P. Le Corvoisier, J.D. Violin, H. Wei, R.J. Lefkowitz, and H.A. Rockman,

- Beta-arrestin-mediated beta1-adrenergic receptor transactivation of the EGFR confers cardioprotection.* J Clin Invest, 2007. **117**(9): p. 2445-58.
12. Asakura, M., M. Kitakaze, S. Takashima, Y. Liao, F. Ishikura, T. Yoshinaka, H. Ohmoto, K. Node, K. Yoshino, H. Ishiguro, H. Asanuma, S. Sanada, Y. Matsumura, H. Takeda, S. Beppu, M. Tada, M. Hori, and S. Higashiyama, *Cardiac hypertrophy is inhibited by antagonism of ADAM12 processing of HB-EGF: metalloproteinase inhibitors as a new therapy.* Nat Med, 2002. **8**(1): p. 35-40.
 13. Patrucco, E., A. Notte, L. Barberis, G. Selvetella, A. Maffei, M. Brancaccio, S. Marengo, G. Russo, O. Azzolino, S.D. Rybalkin, L. Silengo, F. Altruda, R. Wetzker, M.P. Wymann, G. Lembo, and E. Hirsch, *PI3Kgamma modulates the cardiac response to chronic pressure overload by distinct kinase-dependent and -independent effects.* Cell, 2004. **118**(3): p. 375-87.
 14. O'Connell, T.D., M.C. Rodrigo, and P.C. Simpson, *Isolation and culture of adult mouse cardiac myocytes.* Methods Mol Biol, 2007. **357**: p. 271-96.
 15. Shioi, T., P.M. Kang, P.S. Douglas, J. Hampe, C.M. Yballe, J. Lawitts, L.C. Cantley, and S. Izumo, *The conserved phosphoinositide 3-kinase pathway determines heart size in mice.* EMBO J, 2000. **19**(11): p. 2537-48.
 16. McMullen, J.R., F. Amirahmadi, E.A. Woodcock, M. Schinke-Braun, R.D. Bouwman, K.A. Hewitt, J.P. Mollica, L. Zhang, Y. Zhang, T. Shioi, A. Buerger, S. Izumo, P.Y. Jay, and G.L. Jennings, *Protective effects of exercise and phosphoinositide 3-kinase(p110alpha) signaling in dilated and hypertrophic cardiomyopathy.* Proc Natl Acad Sci U S A, 2007. **104**(2): p. 612-7.

17. McMullen, J.R., T. Shioi, L. Zhang, O. Tarnavski, M.C. Sherwood, P.M. Kang, and S. Izumo, *Phosphoinositide 3-kinase(p110alpha) plays a critical role for the induction of physiological, but not pathological, cardiac hypertrophy*. Proc Natl Acad Sci U S A, 2003. **100**(21): p. 12355-60.
18. Guo, D., Z. Kassiri, R. Basu, F.L. Chow, V. Kandalam, F. Damilano, W. Liang, S. Izumo, E. Hirsch, J.M. Penninger, P.H. Backx, and G.Y. Oudit, *Loss of PI3Kgamma enhances cAMP-dependent MMP remodeling of the myocardial N-cadherin adhesion complexes and extracellular matrix in response to early biomechanical stress*. Circ Res. **107**(10): p. 1275-89.
19. Azuma, T., K. Kohts, L. Flanagan, and D. Kwiatkowski, *Gelsolin in complex with phosphatidylinositol 4,5-bisphosphate inhibits caspase-3 and -9 to retard apoptotic progression*. J Biol Chem, 2000. **275**(6): p. 3761-6.
20. El Sayegh, T.Y., P.D. Arora, K. Ling, C. Laschinger, P.A. Janmey, R.A. Anderson, and C.A. McCulloch, *Phosphatidylinositol-4,5 bisphosphate produced by PIP5Kgamma regulates gelsolin, actin assembly, and adhesion strength of N-cadherin junctions*. Mol Biol Cell, 2007. **18**(8): p. 3026-38.
21. Chellaiah, M.A., R.S. Biswas, D. Yuen, U.M. Alvarez, and K.A. Hruska, *Phosphatidylinositol 3,4,5-trisphosphate directs association of Src homology 2-containing signaling proteins with gelsolin*. J Biol Chem, 2001. **276**(50): p. 47434-44.